Programmed cell death-ligand 1 (PD-L1) expression in HIV-associated Diffuse Large B-cell Lymphoma – role and regulation

Zahra Latib

Thesis Presented for the Degree of

DOCTOR OF PHILOSOPHY

In the Division of Haematology

Department of Pathology

Faculty of Health Sciences

University of Cape Town

Supervisor: A/Prof Shaheen Mowla

Co-supervisors: A/Prof Estelle Verburgh & Dr Dharshnee Chetty

July 2024

Declaration

I, Zahra Latib, hereby declare that the work on which this Doctoral thesis is based is my original work (except where acknowledgements indicate otherwise) and that neither the whole work nor any part of it has been, is being, or is to be submitted for another degree in this or any other University.

I empower the University to reproduce for the purpose of research either the whole or any portion of the contents in any manner whatsoever.

Signature: _____

July 2024

Dedication

To my late mother

Acknowledgements

First and foremost, all thanks and praise are to my creator, Allah (SWT), for granting me the opportunity to complete my PhD. I am humbled by the abundance of blessings in my life.

To my father, thank you for your motivation which has given me strength to pursue my dreams. Your ability to make the impossible seem possible is the driving force behind all my endeavours, and I am evermore grateful to have you by my side at every step. To my brother and step-mom, thank you for your support, love and compassion, especially during the last stretch of this journey. I am blessed to have such a strong support system in each of you.

To my fellow lab members, Leo, Beatrice, Aaliyah, Lungile, Babalwa, Thando and Lincoln, thank you for all the good memories, laughs and support, and making the long hours in the lab so much more bearable. I have no doubt that you will all go on to have fruitful careers. To the Division of Haematology staff, A/Prof Jessica Opie, A/Prof Karen Shires, Jolene, Cylene, Zhaheed and ex-staff members (Jean and Coleen) thank you for your support and assistance over these last few years.

Thanks are due to the following individuals for their contribution throughout this PhD:

- Dr Dharshnee Chetty, Dr Zainab Mohamed, A/Prof Estelle Verburgh and the Clinical Haematology staff (in E5, GSH), for their assistance in recruiting patients and collecting samples for our study.
- Tim Reid and Prof Glenda Davidson for their help and training on the flow cytometer.
- Jenna Oosthuizen and Karryn Brown, for assisting with statistical measures and access to clinical data.
- Dr Musalula Sinkala, for his assistance with the Bioinformatic analysis.
- Dr Ashwin Isaacs, for providing training, guidance and access to his laboratory.
- The National Health Laboratory Sciences (NHLS), Anatomical Pathology Department, at UCT, especially Nafiesa Allie, for providing training and assistance.
- Muneeb Adonis, for his assistance with the digital scanning of glass slides.
- Dr Zenda Woodman and Bianca Abrahams for their assistance with generating HIV-1 pseudoviruses.
- Prof Bjoern Chapuy and Dr Jens Loeber for hosting me in their laboratory at Charité – Universitätsmedizin Berlin, in Germany.

I would also like to thank the study participants and their families for their valuable contribution to this research.

I wish to express my sincere gratitude to the following funders: The National Research Foundation and the German Academic Exchange Service (NRF-DAAD), the University of Cape Town, and the Fogarty International Centre of the National Institutes of Health – Fogarty Research Training Program.

Last but most certainly not least, I would like to thank my supervisor, A/Prof Shaheen Mowla. Shaheen, your invaluable knowledge, positivity, kindness and graceful nature has kept me motivated over the years. I consider myself exceptionally privileged to have not only been working on a project that I am passionate about, but also doing so under your guidance. You have been a fundamental part of this degree, as a primary contributor to my scientific growth and development, and one of my biggest inspirations. I am immensely grateful to have learnt so much from you, both professionally and personally.

Table of Contents

List of Figures

Chapter 4

List of Tables

Abbreivations

°C	Degrees Celsius
µL	Microlitre
µM	Micromolar
ABC	Activated B Cell
AICDA	Activation-Induced Cytidine Deaminase
AIDS	Acquired immunodeficiency syndrome
AMC	AIDS Malignancy Consortium
ANOVA	Analysis of Variance
APC	Allophycocyanin
APCs	Antigen-presenting cells
ART	Antiretroviral therapy
ASCT	Autologous Stem Cell Transplantation
AT-2 HIV-1	Attenuated HIV-1
BCL2	B-cell Lymphoma 2
BCL6	B-cell Lymphoma 6
BL	Burkitt Lymphoma
BRAF	B-Raf Proto-Oncogene
Bregs	Regulatory B cells
BSA	Bovine Serum Albumin
cART	Combination ART
CD	Cluster of Differentiation
CD79B	Cluster of Differentiation 79B
CDKN2A	Cyclin Dependent Kinase Inhibitor 2A
cHL	Classical Hodgkin Lymphoma
COO	Cell-Of-Origin
CRISPR	Clustered Regularly Interspaced Short Palindromic Repeats
DCs	Dendritic cells
DEL	Double-expressor Lymphoma
DEPC	Diethylpyrocarbonate
DFS	Disease-free survival
dH_2O	Distilled water
DHL	Double-hit Lymphoma
DLBCL	Diffuse Large B cell Lymphoma
DMEM	Dulbecco's Modified Eagle Medium
DTT	Dithiothreitol
EBF-1	Early B-Cell Factor 1.
EBNA2	Epstein-Barr virus Nuclear Antigen 2
EBV	Epstein-Barr virus
ECM	Extracellular matrix

ECOG	Eastern Cooperative Oncology Group
EDTA	Ethylenediaminetetraacetic acid
EPOCH	Etoposide, Prednisone, Oncovin, Cyclophosphamide, Hydroxydaunorubicin
ER β	Estrogen Receptor β
EZH2	Enhancer of zeste homolog 2
FACS	Fluorescence-Activated Cell Sorting
FBS	Fetal Bovine Serum
FDA	Food and Drug Approved
FFPE	Formalin-Fixed Paraffin-Embedded
FITC	Fluorescein isothiocyanate
FSC	Forward scatter
GC	Germinal Centre
GCB	Germinal Centre B Cell
GEP	Gene Expression Profiling
GM-CSF	Granulocyte-Macrophage Colony-Stimulating Factor
GSH	Groote Schuur Hospital
HAART	Highly Active Antiretroviral Therapy
HIV	Human Immunodeficiency Virus
HPV	Human Papillomavirus
HRS	Hodgkin and Reed Sternberg
IFN-γ	Interferon-gamma
IGH	Immunoglobulin H
IL-10	Interleukin-10
IMDM	Iscove's Modified Dulbecco's Medium
ITSM	Immunotyrosine Switch Motif
JAK	Janus Kinase
LMP1	Latent Membrane Protein 1
LTR	Long terminal repeat
mABs	Monoclonal antibodies
MDSCs	Myeloid-Derived Suppressor Cells
MHC	Major Histocompatibility Complex
miRNA	Micro-RNA
moDCs	Monocyte-Derived Dendritic Cells
MUC1-C	Mucin 1 -C
MV	Microvessicle
MYD88	Myeloid Differentiation Primary Response 88
Nef	Negative Factor
NF-kB	Nuclear Factor-Kappa B
NHL	Non-Hodgkin Lymphoma
NHLS	National Health Laboratory Services
NIH	National Institutes of Health

NK	Natural Kiler
NOTCH2	Neurogenic Locus Notch Homolog Protein 2
NR4A2	Nuclear Receptor 4A2
OS	Overall survival
P/S	Penicillin/treptomycin
PBMCs	Peripheral blood mononuclear cells
PBS	Phosphate-buffered saline
PC	Peridinin-Chlorophyll-Protein
PC5	Peridinin-Chlorophyll-Protein (PerCP) - cyanine (Cy) 5
PC5.5	Peridinin-Chlorophyll-Protein (PerCP) - cyanine (Cy) 5.5
PC7	Peridinin-Chlorophyll-Protein (PerCP) - cyanine (Cy) 7
PD-1	Programmed Death-1 receptor
PD-L1	Programmed Death-Ligand 1
PD-L2	Programmed Death-Ligand 2
PE	Phycoerythrin
PFS	Progression-free survival
PI3K	Phosphoinositide 3-kinase
PIP3	Phosphatidylinositol 3,4,5-Trisphosphate
PKC-β 2	Protein Kinase C - β 2
PLWH	People Living With HIV
PTEN	Phosphatase and tensin homolog (PTEN)
pvHIV-1	Pseudovirus HIV-1
QC	Quality control
R-CHOP	Rituximab, Cyclophosphamide, Doxorubicin, Vincristine, and Prednisone
RNases	Ribonucleases
Rpm	Revolutions per minute
RPMI	Roswell Park Memorial Institute
SCNAs	Somatic copy number alterations
SDS-PAGE	Sodium Dodecyl Sulphate-Polyacrylamide Gel Electrophoresis
SGK1	Serum/Glucocorticoid Regulated Kinase
SHM	Somatic hypermutation
SHP-2	Src homology region 2
sPD-L1	Soluble PD-L1
SSC	Side scatter
STAT	Signal transducers and activators of transcription
SVs	Structural variants
TAMs	Tumour-associated macrophages
Tat	Transactivator of transcription
TBE	Tris/Borate/EDTA
TBS	Tris-buffered saline
TCGA	The Cancer Genome Atlas

TCR	T cell receptor
TET2	Ten-Eleven Translocation-2
TFG-β	Transforming Growth Factor β
THL	Triple-hit Lymphoma
TILs	Tumour-infiltrating lymphocytes
TLR4	Toll-like receptor 4
TME	Tumour microenvironment
TNF-α	Tumour Necrosis Factor α
TSS	Transcription start site
TYK2	Tyrosine Kinase 2
UC	Unclassified
UCT	University of Cape Town
VL	Viral Load
WES	Whole-exome sequencing

Abstract

Diffuse Large B cell Lymphoma (DLBCL) is an aggressive disease that displays striking heterogeneity at both the molecular and clinical levels; and as a result, up to 40% of patients relapse or are refractory to standard first-line therapy. DLBCL is the most common subtype of lymphoma affecting people living with HIV (approximately 50% of all lymphomas seen in this group), and while the introduction of Highly Active Antiretroviral Therapy (HAART) has improved patient outcome, the incidence of DLBCL in this group remains disproportionately high, especially in resource-limited settings. Emerging data indicate that HIV-associated DLBCL, although highly heterogeneous, has distinct clinical, morphological and molecular features from non-HIV-related DLBCL. The complex biology that underpins HIV-associated DLBCL remains largely undefined, necessitating clinical and molecular investigations to identify biomarkers which can be targeted for therapy, specifically within those populations most affected, such as in Sub-Saharan Africa.

The programmed death-1/programmed death-ligand 1 (PD-1/PD-L1) signalling pathway is an important immunoregulatory mechanism that dampens the immune response by inhibiting T cell activity, playing a central role in controlling and maintaining tolerance to self-antigens. However, cancer cells have hijacked this mechanism by overexpressing PD-L1 to impair T cell functioning and ultimately escape immune recognition and destruction. Additionally, impairment of this pathway impacts the broader tumour microenvironment (TME), for instance through inhibition of T cell function, creating favourable conditions for tumour progression. In a previous report, PD-L1 levels were shown to be elevated in HIV-positive patients prior to a lymphoma diagnosis, with those harbouring the highest levels of PD-L1 progressing to develop malignancies, suggesting that PD-L1 is a key factor in the onset of lymphoma among HIV-infected individuals.

While blockade of the PD-1/PD-L1 pathway with monoclonal antibodies has achieved considerable success in several cancer types, the results remain suboptimal in DLBCL, where the status and relevance of the deregulation of the pathway, and particularly the role and status of PD-L1, remains unclear, and even more so, within an HIV-positive background. This warrants a deeper exploration into the significance of PD-L1 overexpression, as well as the mechanisms influencing PD-L1 expression, in HIV-associated DLBCL.

In the current study, three approaches were taken to explore this. Firstly, PD-L1 levels were evaluated and compared within the peripheral blood cell populations of a cohort of newly diagnosed, treatment naïve, HIV-positive and HIV-negative DLBCL patients, using flow cytometry. As per previous observations, HIV-positive DLBCL patients were typically diagnosed at a younger age (64% below the

age of 50 years) compared to their HIV-negative counterparts (36% under the age of 50 years). The GCB subtype was the major DLBCL subtype (64%) within the HIV-positive DLBCL group, and a striking 82% of cases had extranodal involvement, reflecting an aggressive/advanced-stage disease. Flow cytometric analysis revealed a significantly higher proportion of PD-L1-positivity overall ($CD274^+$; median: 0.44%; $p \leq 0.01$), as well as PD-L1-positive B cells ($CD19^+$ $CD274^+$; median: 6.62%; $p \leq 0.001$), in DLBCL patients (irrespective of HIV status), compared to healthy controls. When comparing within the DLBCL patient groups based on HIV status, the HIV-positive cohort displayed a significantly higher proportion of PD-L1-positive cells overall ($CD274^+$; median: 0.65%; $p \leq 0.05$), and PD-L1-positive B cells ($CD19^+$ $CD274^+$; median: 10.9%; $p \leq 0.05$). No noticeable differences were observed regarding the population of regulatory B cells ($CD19^+$ $CD24^+$ $CD38^+$; median: 57.5% vs 61.2%; $p = 0.5344$) and PD-L1-positivity within this subset of B cells ($CD19^+$ $CD24^+$ $CD38^+$ $CD274^+$; median: 1.74% vs 0.83%; $p = 0.3551$) between HIV-negative and HIV-positive DLBCL patients.

In the second approach, the status of PD-L1, and T cells and macrophages were evaluated in the TME of HIV-positive and HIV-negative DLBCL tissues, using immunohistochemistry. In concordance with what was observed in the peripheral blood, a higher proportion of PD-$L1^+$ cells were present in the TMEs of HIV-positive DLBCL patients, relative to HIV-negative ones (HIV-positive vs HIV-negative; median: 0.47% vs 0.09%; $p \leq 0.0.5$). This was accompanied by reduced $CD8^+$ cytotoxic T cell infiltration (HIV-positive vs HIV-negative; median: 1.25% vs 2.12%; $p \leq 0.0.5$), and enhanced $CD68^+$ tumour-associated macrophage infiltration (HIV-positive vs HIV-negative; median: 2.69% vs 1.56%; $p \leq 0.0.5$), suggesting differential impairment of the TME in these two groups, and representing a heightened immunosuppressive environment in DLBCL patients infected with HIV.

The third approach in this study attempted to delineate the complex relationship between PD-L1, c-MYC, EBNA2 and HIV, using a combination of in silico tools, as well as in vitro analyses using established DLBCL cell lines and models. Using DLBCL gene expression data publicly available on The Cancer Genome Atlas, we found highest expression of *PD-L1* to be associated with the ABC subtype. Additionally, an inverse (negative) correlation between *PD-L1* and *c-MYC* expression was observed in patients with this specific subtype of DLBCL. The regulation of PD-L1 by c-MYC was assessed in DLBCL cell lines through an experimental approach, taking HIV and EBV infections into account. In vitro analyses using qPCR and western blotting experiments confirmed this inverse correlation within ABC-derived DLBCL cell lines, as well as within a c-MYC knock-down DLBCL cell model.

To investigate the effect of HIV-1 on PD-L1 expression in DLBCL cells, two independent experimental laboratory HIV-1 variants were used, namely aldrithiol-2 inactivated HIV-1, and HIV-1 pseudovirus. Exposure to the virus led to reduced expression of both PD-L1 and c-MYC protein levels, even in the

presence of EBNA2, a result which contrasts with our observations using patient derived blood, and tumours. This indicated the importance of studying complex interactions using the appropriate experimental systems.

Overall, this study provided novel insights into the status, role and regulation of PD-L1 in DLBCL, specifically within the context of HIV-infection. These findings further confirm that HIV-associated lymphomas harbour unique pathobiological features and provides directions for future basic and clinical research aimed at improving therapeutic approaches specifically tailored for this patient group.

Chapter 1

Literature Review

1.1 Introduction

Lymphomas comprise of a diverse group of malignancies of the haematopoietic system, originating from lymphocytes (1). Lymphomas can be classified into two groups, namely Hodgkin Lymphoma and Non-Hodgkin Lymphoma (NHL) (2). NHL, a highly heterogenous disease, accounts for up to 90% of all malignant lymphomas and arises from B cells, T cells, or Natural Killer (NK) cells (3, 4). Approximately 85% of NHL cases are of B cell origin (5). NHLs can emerge during various stages of cellular maturation, with the biological features of these malignant cells resembling that of their normal state (6). NHL tumour cells generally infiltrate both lymphoid and haematopoietic tissues and are also capable of spreading to other organs (7). The major mechanisms behind the pathogenesis of NHL involves immunosuppression and chronic antigen stimulation. The latter increases B cell proliferation which not only increases the likelihood of genetic errors occurring but also leads to the downregulation of T cell responses due to T cell exhaustion, resulting in an immunosuppressive state (8). Infectious agents such as Human immunodeficiency virus (HIV), Epstein-Barr virus (EBV), *Helicobacter pylori*, and hepatitis C virus, have been associated with certain subtypes of NHL (9).

The primary target cells of HIV are $CD4^+$ T cells (10), which are essential for B cell maturation and differentiation into memory or antibody-producing B cells (11). In the context of HIV-infection, a reduced number of $CD4^+$ T cells impacts B cell functioning and increases vulnerability to opportunistic infections, such as human papillomavirus (HPV) and EBV (12, 13). Due to the compromised state of the immune system, individuals infected with HIV are at a higher risk of developing several types of malignancies, with the most common being Kaposi sarcoma, cervical cancer and NHLs (14). HIV-infected patients are reported to be up to 23-fold more at risk of developing a NHL, compared to the HIV-uninfected population, due to of the immunosuppressive role of HIV (15) and it is reported that up to 20% of HIV-infected individuals develop an NHL in their life-time (16). While HIV does not directly lead to the development of an NHL, co-infections with oncogenic viruses, such as EBV, are frequent in HIV-positive individuals, thereby promoting lymphomagenesis (17). Additionally, HIV-infection is associated with chronic antigen stimulation, chronic B cell activation as well as an overproduction of B-cell activating cytokines (18). The oncogenic role of HIV itself is also gaining attention with recent studies reporting that HIV viral proteins can directly promote oncogenic events and tumour development (19). For instance, studies emanating from our own laboratory as well as others show

that HIV proteins Transactivator of transcription (Tat) and Negative regulatory factor (Nef) promote the expression of oncogenic factors in Burkitt Lymphoma (BL), another NHL subtype of high prevalence among HIV-infected individuals (20, 21).

There are over 30 subtypes of NHLs classified according to "morphology, immunophenotype, cytogenetic features, molecular features, clinical behaviour, aetiology and pathogenesis" (22). Based on the speed of disease progression, NHLs are grouped into either indolent or aggressive lymphomas. Diffuse Large B Cell Lymphoma (DLBCL) is classified as highly aggressive and is the most commonly diagnosed NHL (23).

1.2 Diffuse Large B Cell Lymphoma

DLBCL is a highly heterogenous disease, arising from mature B-cells in the germinal centre (GC), and accounts for up to 40% of all NHL cases (24, 25). Translocations of *B-cell Lymphoma 6 (BCL6), B-cell Lymphoma 2 (BCL2) and MYC* are molecular characteristics of DLBCLs and are present in up to 40%, 30% and 15% of cases, respectively (26, 27). GCs are formed in secondary lymphoid organs and represent the site where antibody-secreting B cells and memory B cells are produced (28). Within the GC, two distinct zones are present (Figure 1.1). The dark zone represents the site for B cell proliferation and somatic hypermutation (SHM), whereas the light zone consists of high-affinity B cells that are preferentially selected (29). Gene expression profiling (GEP) has resulted in the identification of two main subtypes of DLBCL based on the cell of origin (COO), namely the germinal centre B cell (GCB)-like subtype and the activated B cell (ABC)-like subtype (30). These subtypes are defined by (i) their difference in clinical outcomes, where the ABC-DLBCL subtype is associated with a poor survival outcome, and (ii) disease biology (30, 31).

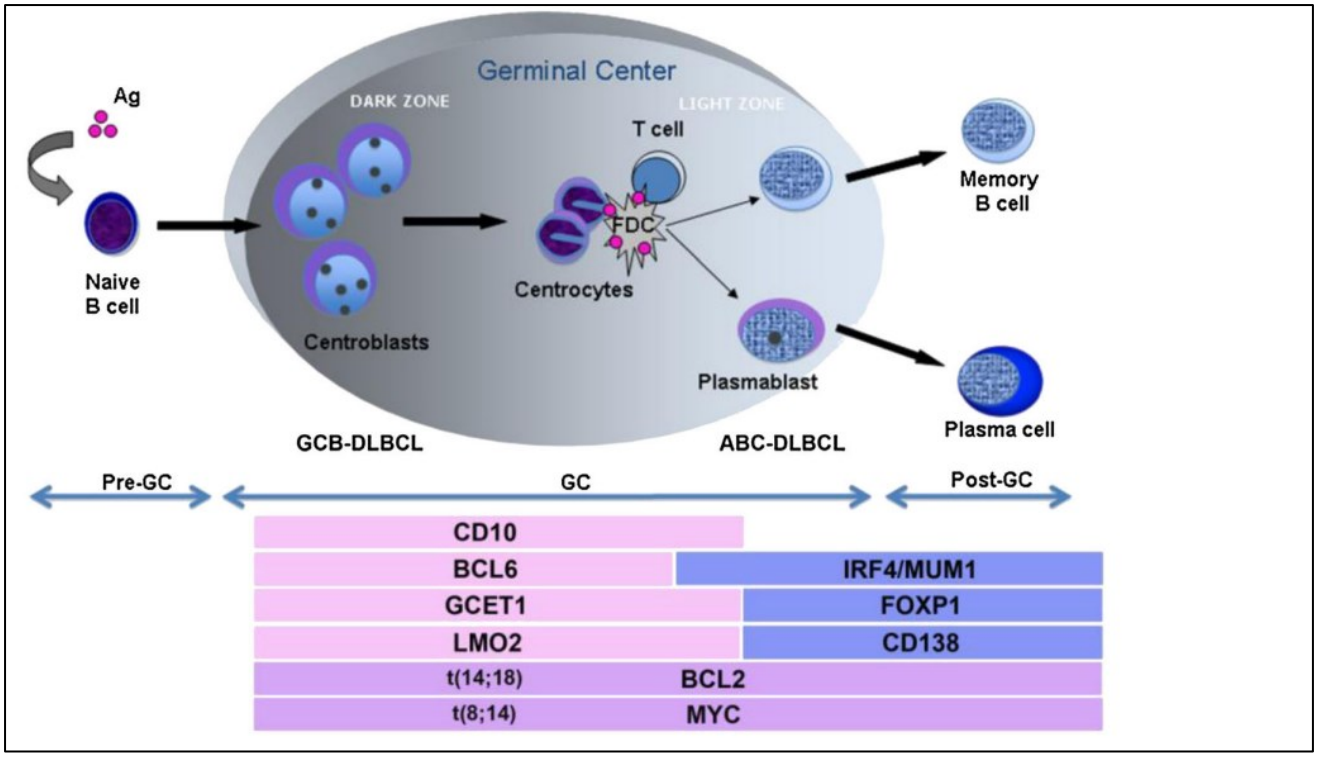

Figure 1.1: Overview of the GC reaction and the two main molecular subtypes of DLBCL. Schematic diagram illustrating the GC reaction and its relationship with the two main subtypes of DLBCL. The lower table indicates markers associated with the GCB- and ABC-DLBCL subtypes. which are depicted in pink and blue, respectively. Depicted in purple are prognostic factors in DLBCL. Ag, antigen; GC, Germinal Centre; GCB-DLBCL, germinal centre B-cell diffuse large B cell lymphoma; ABC, activated B cell; FDC, follicular dendritic cell (from Quintanilla-Martinez, 2015) (32).

Similarly to normal GC B cells, GCB-DLBCL cells also exhibit continual SHM of the variable immunoglobulin heavy chain gene which is governed by activation-induced cytidine deaminase (AICDA), an enzyme that is highly expressed in GC B cells (33). A number of oncogenic pathways are dysregulated in GCB-DLBCL, all contributing to the pathogenesis of this disease. Common in this subtype is a t(14;18) translocation which induces the activation of BCL2, an anti-apoptotic protein. A proportion of GCB-DLBCLs also harbour a *PTEN* deletion, which results in dysregulation of the Phosphatase and tensin homolog - Phosphoinositide 3-kinase (PTEN-PI3K) signalling pathway. Loss of PTEN leads to the accumulation of phosphatidylinositol 3,4,5-trisphosphate (PIP_3) which, ultimately further stimulates cell survival and proliferation (33). Because PTEN loss is not encountered in the ABC subtype, it has been noted that this aberration is a specific feature of GCB-DLBCLs (34).

ABC-DLBCL resembles the GEP of normal Activated B cells that have progressed through the GC and are about to differentiate into plasma cells (35). Most of the genes expressed by normal GC B cells are typically downregulated in this subtype, with the genes generally expressed in plasma cells being upregulated (33). Common genetic abnormalities in ABC-DLBCL include trisomy 3, gains of 3q and 18q21-q22, losses of 6q21-q22, and alterations in genes controlling the Nuclear factor-kappa B (NF-

kB) pathway (26). EBV-positivity is also commonly seen in this subtype of DLBCL (36). Following standard treatment, the ABC subtype is associated with an adverse outcome when compared to GCB-DLBCL outcomes (35).

Due to the heterogeneity of DLBCL, several classification techniques have been developed in order to (i) improve diagnostic accuracy, (ii) detect appropriate molecular subtypes, (iii) develop prognostic models, and (iv) classify patients for disease management (37). Advancements in next generation sequencing (NGS) has allowed for the genomic characterization of DLBCL, thus resulting in newer classifications of this disease (38).

In 2018, Schmitz et al. uncovered four distinct molecular subtypes of DLBCL by performing "a multiplatform analysis of structural genomic abnormalities and gene expression in DLBCL biopsy samples". Samples from GCB-, ABC- and unclassified-DLBCL cases were subtyped into MCD, BN2, N1 and EZB groups according to four seed classes, namely (1) *Cluster of Differentiation 79B* (*CD79B)* and *Myeloid differentiation primary response 88* (*MYD88)* ^{L265P} mutations (MCD), (2) *Neurogenic locus notch homolog protein 2 (NOTCH2)* mutation or *BCL6* fusion (BN2), (3) *NOTCH1* mutations (N1), and (4) *Enhancer of zeste homolog 2* (*EZH2)* mutation or *BCL2* translocation (EZB). While MCD and N1 subtypes comprised of mainly ABC cases, the EZB subtype was dominated by GCB cases. The BN2 subtype was reported to contain a mix of ABC, GCB and unclassified cases. These subtypes also differed in their response to immunotherapy, with poorer outcomes observed in the MCD and N1 subtypes and improved outcomes associated with the BN2 and EZB subtypes (39). A subsequent study by Wright and colleagues added another two subtypes, namely the A53 and ST2 groups. The A53 subtype is associated with inactivation of *TP53* and comprises of more ABC cases, whereas the ST2 group is characterized by mutations in *Serum/Glucocorticoid Regulated Kinase 1 (SGK1)* and *Ten-Eleven Translocation -2* (*TET2)* and is made up by majority of GCB cases (40).

Additionally, another independent study conducted by Chapuy et al. in 2018 identified five DLBCL clusters with outcome-associated distinct genetic signatures. In this approach, whole exome sequencing (WES) was performed and mutations, somatic copy number alterations (SCNAs), and structural variants (SVs) were detected (41). Cluster 5 (C5) was strongly associated with the ABC subtype and contained *BCL2* amplifications as well as recurrent mutations in *CD79B* and *MYD88*. Also associated with the ABC subtype was cluster 1 (C1), which displayed *BCL6* SVs along with *NOTCH2* alterations. Cluster 3 (C3) comprised of primarily GCB-DLBCLs and harboured mutations in *BCL2* and chromatin modifiers, including *EZH2*. Majority of cluster 4 (C4) was also comprised of GCB-DLBCLs, with discrete alterations in B Cell Receptor (BCR)/PI3K, Janus of protein tyrosine kinases/signal transducer and activator of transcription (JAK/STAT) and B-Raf Proto-Oncogene (BRAF) pathway

components. Cluster 2 (C2) included both ABC- and GCB-DLBCLs and harboured tumours with biallelic inactivation of *TP53*, copy loss of 9p21.3/*Cyclin Dependent Kinase Inhibitor 2A* (*CDKN2A*) and genomic instability (37). While C1 and C4 DLBCL patients had a more favourable outcome, patients with C3 and C5 exhibited less favourable outcomes. C2 DLBCL patients had a stable progression rate over time (41).

The studies by Schmitz et al. and Chapuy et al. were conducted independently and involved different approaches, yet similar genetic features can be observed between certain subtypes identified. More importantly, these studies showcased that the conventional subclassification of DLBCL into GCB-, ABC- or unclassifiable has limitations in terms of patient treatment and management, and that the classification of DLBCL into these newly reported molecular subtypes has both biological and clinical relevance (42).

Rearrangements in MYC is a feature typically seen in several types of B cell lymphomas, including DLBCL (43). MYC is a crucial transcription factor with roles in proliferation, cell cycle growth, apoptosis and differentiation (44), and its aberrant activation has implicated in several cancers, including DLBCL (45). In DLBCL, translocations involving *MYC* and either *BCL2* or *BCL6* are present in up to 10% of cases (46) and have been termed as double-hit lymphomas (DHL), with *MYC* and *BCL2* rearrangements typically being of GCB origin while *MYC* and *BCL6* rearrangements are of ABC origin (31). In addition, DLBCLs with concurrent *MYC*, *BCL2* and *BCL6* rearrangements are less common and referred to triple-hit lymphomas (THL) (47). Moreover, approximately 30% of DLBCLs overexpress both MYC and BCL2 at the protein level, termed as double-expressor lymphoma (DEL) (45). Aberrant MYC expression promotes many tumorigenic processes in DLBCL, and also has an impact on the clinical outcomes of patients (48).

1.3 Clinical outcomes of DLBCL

Currently, the standard treatment for patients with DLBCL is a chemotherapeutic regimen consisting of cyclophosphamide, doxorubicin, vincristine and prednisone, with the addition of the anti-CD20 monoclonal antibody, Rituximab, (R-CHOP) (49). Despite the aggressive nature of DLBCL, up to 70% of patients achieve complete remission with R-CHOP, but a remaining 30-40% relapse or are refractory to the treatment (50).

Prior to the addition of rituximab to chemotherapy, the overall 5-year survival rate for ABC and GCB DLBCL was 35% and 60% respectively. Once rituximab was included (R-CHOP), the 3-year survival rates for ABC- and GCB-DLBCL improved to approximately 45% and 80%, respectively (51). Rituximab is a chimeric monoclonal antibody with specific affinity for CD20, a B cell transmembrane protein. CD20 is expressed on healthy B cells and most malignant B cells (52), and plays a role in regulating the early stages of cell-cycle activation and differentiation. Three in vitro modes of action have been reported

for rituximab: (i) antibody-dependant cellular cytotoxicity, (ii) complement-dependant cytotoxicity and (iii) direct activation of apoptosis (53).

Although the addition of rituximab to chemotherapy has significantly improved therapeutic outcomes in both ABC and GCB DLBCL patients, it doesn't reduce the disadvantage of presenting with ABC-DLBCL. Furthermore, in DLBCL, alterations in MYC are linked to a more aggressive disease and inferior clinical outcomes (54). DLBCL patients with DHL and THL subsets have been linked to a poor chemotherapy response, with low chances of complete remission being attained (31), and similarly, patients with the DEL subset are associated with advanced stage disease and poor prognosis after treatment with R-CHOP (45).

Since DLBCL subgroups differ in genetic aberrations and disrupted signalling pathways, it is crucial to identify novel therapeutic targets with the aims of improving therapeutic outcomes (55).

1.4 HIV-associated DLBCL

As mentioned, HIV-infection is associated with a compromised immune surveillance, viral infections, chronic antigenic stimulation and cytokine imbalance, which increases the risk of NHL development (56). DLBCL is 17-times more likely to arise in HIV-infected individuals, compared to the general population (57) and is considered to be an AIDS-defining cancer, as it arises at the advanced stages of HIV-infection, when the immune system is highly compromised and vulnerable (58, 59). EBV-infection is reported to be driver of several malignancies and is observed in up to 15% of all diagnosed DLBCL tumours (60, 61). In an HIV-positive setting, the association of EBV-infection with DLBCL is increased to up to approximately 50% of cases (62, 63). EBV primarily infects B lymphocytes and by remaining in its latent form, EBV is capable of avoiding the host immune response (36).

As depicted in Figure 1.2, HIV-positive DLBCLs are associated with a younger age at DLBCL diagnosis, a higher frequency of B-symptoms, advanced clinical staging and an Eastern Cooperative Oncology Group (ECOG) score of more than 2, which indicates poor performance status and worse survival, compared to DLBCLs arising in the general population (64, 65). Compared to HIV-uninfected patients, HIV-positive DLBCL patients also frequently present with an advanced disease stage and extranodal involvement, indicative of an aggressive disease, at the time of diagnosis (17); and in low socio-economic settings where the prevalence of HIV is high, such as sub-Saharan Africa, the outcomes of these patients are poor compared to those in well-resourced settings (66, 67).

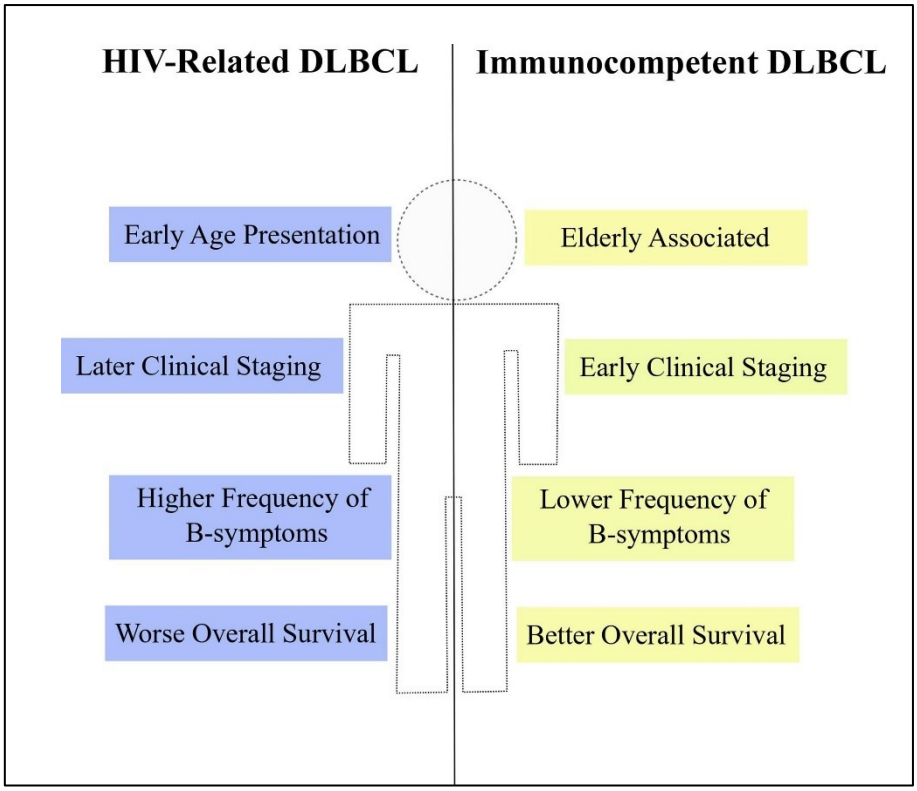

Figure 1.2: Clinical features of HIV-associated DLBCL. HIV-positive DLBCLs display worse clinical features and outcomes (blue), compared to HIV-negative DLBCLs (yellow) (from de Carvalho et al., 2021) (64).

Despite the introduction of combination antiretroviral therapy (cART), the incidence of DLBCL remains high in HIV-infected individuals and HIV-associated DLBCL continues to display more aggressive traits when compared to DLBCLs arising in the general population (65, 68). Compared to HIV-uninfected DLBCL patients, those with HIV-associated DLBCL were reported to having a worse overall survival (OS), regardless of showing a similar disease-free survival (DFS) (65). In a recent study conducted in Malawi by Coelho et al., HIV-positive DLBCL patients who were on antiretroviral therapy (ART) for less than 6 months had improved survival outcomes compared to HIV-negative DLBCL patients, while no difference in outcomes was observed between HIV-positive DLBCL patients on ART for more than 6 months and HIV-negative DLBCL patients (69). All DLBCL patients enrolled into the study by Coelho et al. were newly diagnosed and received chemotherapy during the study period. These finding suggest that that the initiation of ART alongside chemotherapy is of therapeutic benefit (69). Similarly, another study carried out in Malawi by Kimani et al. reported no difference in the survival outcomes of HIV-positive DLBCL patients, of which a majority were receiving ART, and HIV-negative DLBCL patients (70). While these findings are generalized to HIV-positive DLBCL patients who were receiving concurrent ART (69, 70), they do not align with studies emanating from South Africa, which demonstrated a lower survival rate in DLBCL patients infected with HIV, despite being on HAART (71, 72).

Since a study conducted in 2003 by the US National Cancer Institute (NCI) demonstrated a 79% complete remission rate, a dose-adjusted regimen of etoposide, prednisone, vincristine, cyclophosphamide, doxorubicin and cyclophosphamide (EPOCH) has been the predominant approach in the treatment of HIV-associated DLBCL (73, 74). In 2010, a trial conducted by the AIDS Malignancy Consortium (AMC) found that the addition of Rituximab to EPOCH (R-EPOCH) resulted in an improved complete response rate (75).

While current therapeutic regimens have prolonged the survival of HIV-positive DLBCL patients, there remains a difference in survival between HIV-infected and HIV-uninfected groups, therefore highlighting the need for an improved therapeutic strategy (76). Due to the difference in disease biology, clinical features and therapeutic outcomes between DLBCLs occurring in the HIV-positive and HIV-negative populations, a deeper molecular understanding of this disease is required (64).

The clinical heterogeneity of HIV-positive DLBCL compared to HIV-negative DLBCL is a reflection of distinct molecular differences in the presence of HIV-infection. Recently, Peng and colleagues analysed HIV-positive and -negative DLBCL tissues to identify and compare high-frequency mutated genes. Among the mutated genes identified, mutation in *MYC* and *tyrosine kinase 2* (*TYK2*) were associated with the HIV-positive group and additionally were associated with a higher mutation probability (57). As mentioned earlier, MYC is a powerful oncogenic transcription factor that is frequently dysregulated in DLBCL and is associated with aggressive disease and an inferior prognosis (77). TYK2 is a member of the of the JAK family, which consists of proteins involved in survival, growth, and differentiation of various cell types, especially immune and haematopoietic cells (78). Studies have shown that overexpression of TYK2 leads to constitutive activation of the STAT3 (79), an especially interesting finding since constitutive activation of STAT3 is associated with cell proliferation and survival of ABC-DLBCL cells (80). Overall, the study by Peng and colleagues provides insight into molecular alterations associated with HIV-positive DLBCL, potentially contributing to the aggressive nature of this disease. In 2015, Chao and colleagues identified expression of c-MYC, protein kinase C - β 2 (PKC-β2), BCL6 along with other markers as being increased in HIV-positive DLBCLs compared to HIV-negative cases, and suggested that c-MYC-mediated dysregulation may be a partial contributor to the aggressive clinical course observed in HIV-positive DLBCL patients (81). Another study conducted within our local setting in South Africa reported that a high Ki-67 proliferation index was more common in HIV-positive DLBCL patients, than their HIV-negative counterparts (82). Ki-67 is a marker of proliferation, and a high index correlates with inferior survival outcomes in DLBCL (83). Collectively, the studies above demonstrate that HIV-associated DLBCL is a distinct disease, both molecularly and clinically, from DLBCLs diagnosed in immunocompetent individuals (63), although the molecular studies are limited

due to the fact that in high-income countries, HIV-positive DLBCLs are not very common and affects marginalized populations (69). This warrants comprehensive investigations into the unique pathobiology of HIV-associated DLBCL as well the genetic mechanisms underlying this disease.

1.5 The PD-1/PD-L pathway

The programmed death-1/programmed death-ligand 1 (PD-1/PD-L1) signalling pathway plays a crucial role in maintaining immune cell tolerance and limiting tissue damage by negatively regulating T cell activity (84). PD-1 is expressed on many activated immune cell types including $CD4^+$, $CD8^+$ and natural killer (NK) T cell subsets as well as B cells and monocytes, and serves as an inhibitor of both adaptive and innate immune responses (85, 86). PD-1 is involved in immune tolerance by interacting with its ligands, namely PD-L1 and PD-L2, located on chromosome 9p24.1 (87). While PD-L1 is broadly expressed on a variety of cells, including T and B lymphocytes, dendritic cells (DCs), macrophages and non-haematopoietic cells, PD-L2 has more of a restricted expression in that it is only expressed on haematopoietic cells such as DCs, macrophages and some B cells. A key role of the PD-1/PD-L pathway is to inhibit T cell function to maintain balance in the immune system, and this occurs via an interaction between the PD-1 receptor on T cells and PD-L1/PD-L2 on antigen presenting cells (APCs) (88, 89). While the binding affinity of PD-L2 to PD-1 is higher, PD-L1 acts as the primary ligand (90).

Figure 1.3 depicts the interaction between PD-1 and PD-L1 on T cells and APCs, respectively, which ultimately inhibits T cell functioning. Briefly, the activation of T cells is dependent on two signals: (i) the interaction between major histocompatibility complexes (MHC), presenting foreign antigens, and the T cell receptor (TCR) which stimulates positive signalling, and (ii) co-stimulatory and -inhibitory signals, which regulate TCR signalling, and ultimately T cell activation (91). Engagement of PD-1 by PD-L1, recruits the phosphatase Src homology region 2 domain-containing phosphatase-2 (SHP-2) to the to the immunoreceptor tyrosine-based switch motif (ITSM) in the cytoplasmic domain of PD-1. This results in the dephosphorylation of ZAP70, a tyrosine kinase necessary for the initiation of T cell responses, and negates the positive signalling stimulated by the TCR, ultimately inhibiting downstream signalling pathways and promoting T cell anergy (92, 93).

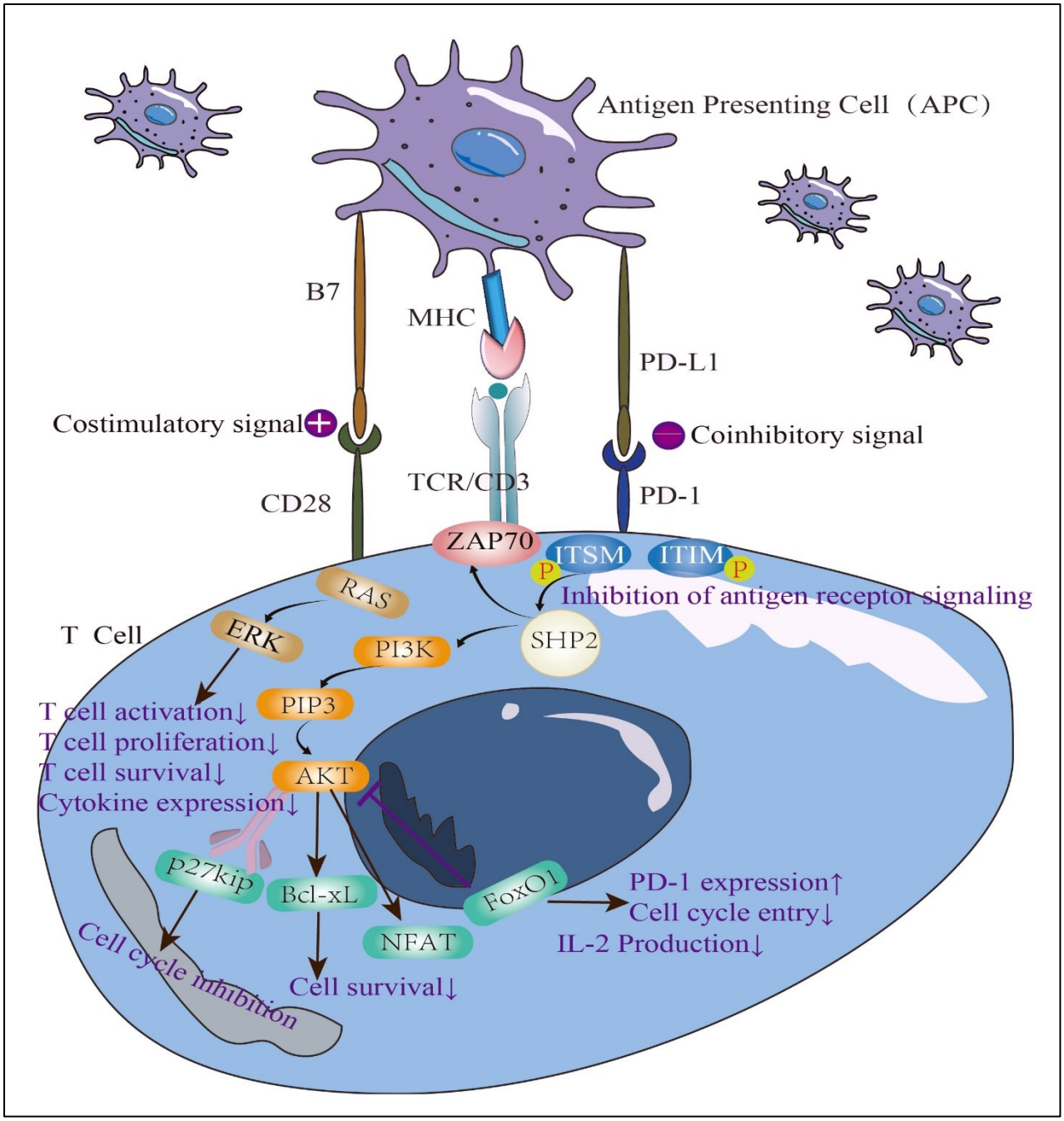

Figure 1.3: T cell inhibition through the PD-1/PD-L1 pathway. Graphical illustration showing the immunosuppressive interaction between PD-1 and PD-L1, which negatively affects T cell activation, proliferation and survival (adapted from Wang et al., 2023) (93).

In addition to the membrane-bound form, PD-L1 can also exist in soluble form (sPD-L1). sPD-L1 originates predominantly via cleavage of the membrane form, however it can also derive from the release of exosome-associated PD-L1 and spliced transcripts that are deficient in the exon that encodes the PD-L1 transmembrane domain (94). Whether or not sPD-L1 affects T cell activation remains debatable. Some studies have reported that sPD-L1 inhibits T cell activation while others have

noted that it may act as a “decoy receptor” that retains PD-1 binding activity but does not inhibit T cell activation (94).

While PD-1 mediated T cell inhibition is a crucial mechanism in preventing autoimmunity, it also represents an immune resistance mechanism by diseased cells, allowing the latter to evade immune destruction (95).

1.5.1 PD-L1 expression in an HIV-positive context

In an HIV-positive setting, where immune activation is chronic, PD-L1 is known to be upregulated in an attempt to mitigate the ongoing inflammation (96). Several studies have demonstrated the increase in PD-L1 expression in HIV-positive patients, relative to healthy individuals (97, 98). PD-L1 was found to be elevated specifically on B cells, dendritic cells and monocytes (97). The precise mechanism on PD-L1 upregulation by HIV is not fully elucidated and various studies have explored the potential involvement of HIV-1 viral proteins.

HIV-1 Tat is a 14 kDa protein that acts as a strong transcriptional transactivator of key viral genes necessary for infection, replication, and transmission (99, 100). Tat is produced at an early stage of the virus life cycle and several studies have shown that the Tat protein disrupts normal functioning of the immune system (101, 102, 103). By treating monocyte-derived dendritic cells (MoDCs) with the HIV-1 Tat protein followed by Fluorescence-Activated Cell Sorting (FACS) to assess cell-surface expression of PD-L1, Planès and colleagues reported upregulation of PD-L1 which affected the ability of these cells to promote T cell proliferation. PD-L1 upregulation by HIV-1 Tat was demonstrated to occur through indirect mechanisms involving the tumour necrosis factor alpha (TNF-α) and Toll-like receptor 4 (TLR4) pathways (100).

In 2022, an article published by Munoz and colleagues revealed that HIV virions incorporated PD-L1 into their envelop, affecting follicular T helper cell functioning, through involvement of the HIV matrix protein p17 (104). P17 is a structural protein which acts as a viral cytokine by promoting viral replication (105, 106). The study by Munoz et al. showed that the p17 protein interacts with the intracytoplasmic tail of the PD-L1 protein on host cells, to achieve incorporation onto virions. The aforementioned study served as evidence on the exploitation of PD-L1 by HIV to promote immune suppression during infection (104).

1.5.2 PD-L1 in cancer

The PD1-1/PD-L1 signalling axis can be hijacked by tumour cells to evade immune recognition. By expressing PD-1 ligands, tumour cells avoid immune recognition (107), and while cancer cells can express both PD-L1 and PD-L2, the former has been shown to be more frequently expressed (89). As

depicted in Figure 1.4, the interaction between PD-1 and PD-L1/2 on T cells and tumour cells, respectively, inhibits T cell activation, proliferation, survival, and cytokine production (85).

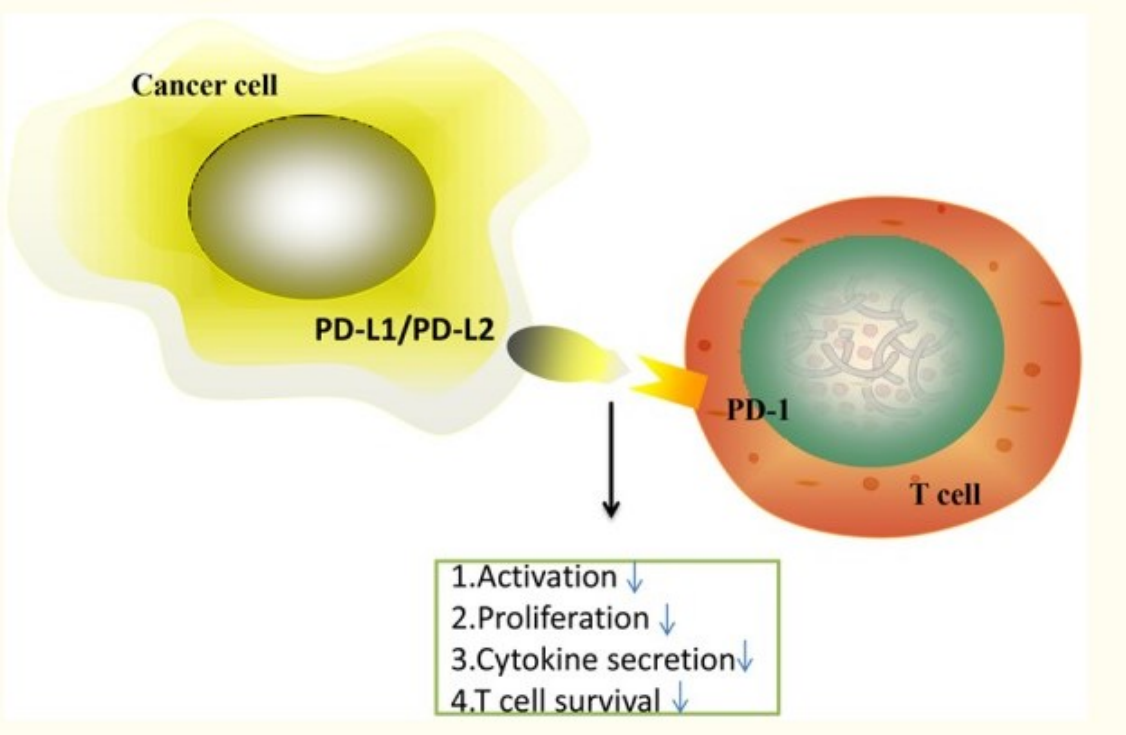

Figure 1.4: Tumour cells inhibit T cell function via the PD-1/PD-L interaction (from Han et al., 2020) (85).

In addition to being expressed on tumour cells, PD-L1 can also be expressed on several non-malignant cell types within the tumour microenvironment (TME) to support an immunosuppressive state that promotes tumour growth (108). In the TME, PD-L1 interacts with PD-1 on tumour-infiltrating lymphocytes (TILs) to negate TCR-signalling and ultimately escape immune surveillance (109). In classical Hodgkin Lymphoma (cHL), PD-L1 expression on Hodgkin Reed-Sternberg cells (HRS) is a defining feature with up to 75% of cases harbouring copy number alterations or amplifications of chromosome 9p24.1 (110). Genomic alteration at this locus not only increases PD-L1 expression but also its neighbouring gene, JAK2 (111). Increased expression of JAK2 also promotes PD-L1 expression through phosphorylation of STAT3 and STAT5 (112).

Blockade of PD-1/PD-L1 signalling using antibodies against PD-1 and/or PD-L1 has had varying successes in several cancers, including colorectal cancer, renal cancer, breast cancer and certain subtypes of lymphomas (113). To date, a total of seven monoclonal antibodies (mAbs) against the PD-1/PD-L1 pathway have been Food and Drug Administration (FDA) approved for use in the treatment of several cancers (Table 1.1).

Table 1.1: FDA approved PD-1/PD-L1-based immunotherapies

Inhibitor name	Target	Year of first approval
Nivolumab	PD-1	2014
Pembrolizumab	PD-1	2014
Cemiplimab	PD-1	2018
Dostarlimab	PD-1	2023
Avelumab	PD-L1	2015
Atezolizumab	PD-L1	2016
Durvalumab	PD-L1	2016

PD-1 – programmed death-1; PD-L1 – programmed death-ligand 1

In cHL specifically, PD-1/PD-L1 blockade is proven to be extremely effective, with an overall response rate of over 80.4% (114). The success of PD-1 blockade in this disease is attributed to its unique biology, including the fact that up to 30% of cHL cases are associated with EBV-infection, a known up-regulator of PD-L1 (115, 116). Additionally, recent studies revealed that PD-1 blockade leads to activation of PD-1-positive T helper (T_H) 1 effector cells within the TME of HL, which in turn promotes the activation of cytotoxic T cells (117, 118).

While PD-1/PD-L1 blockade has revolutionized treatment of HL, the outcome of clinical trials shows that the same is not the case for other cancers, and thus it is important to adequately identify patient groups that are likely to respond well to this type of therapy. Molecular and clinical studies aimed at evaluating PD-1/PD-L1 as a reliable biomarker are thus necessary (119).

1.5.3 The status of PD-L1 in DLBCL

In contrast to cHL, blockade of the PD-1/PD-L1 pathway in DLBCL is suboptimal, and this was initially attributed to the lower frequency of alterations at the *PD-L1* locus (120).

In 2016, Georgiou and colleagues performed whole genome sequencing, RNA sequencing, and cytogenetic analysis using samples from Chinese, American and Swedish DLBCL patients which revealed that approximately 12%, 3% and 4% of DLBCL cases were affected by gains, amplifications and translocations, respectively, at the *PD-L1* locus, and these directly correlated with increased *PD-L1* expression. The study also reported that the *PD-L1* locus is a recurrent *immunoglobulin heavy-chain locus* (*IGH*) translocation partner in DLBCL - translocations involving *IGH* and a proto-oncogene, such as *BCL2*, *BCL6* and *c-MYC*, are frequently observed in DLBCL (121). Similarly to the study by Georgiou et al., a later report published in 2019 by Wang and colleagues revealed that 6.5% and 3.5% of DLBCL cases were affected by gains and amplifications, respectively, at the *PD-L1* locus, 9p24.1 (122). In yet

another study, 16%, 7% and 2% of DLBCL cases were found to harbour copy gains, amplifications, and translocations, respectively, at the *PD-L1* locus (120). Additionally, the study reported high PD-L1 expression to be most commonly associated with the non-GCB subtype of DLBCL (120). Collectively these studies indicate that, while the frequency of PD-L1 alterations is much lower in DLBCL relative to cHL, the use of PD-1 inhibitors may be useful for a subset of DLBCL patients.

As mentioned earlier, infection with EBV is associated with increased PD-L1 expression, particularly via the activities of EBV proteins Epstein-Barr virus nuclear antigen 2 (EBNA2) and latent membrane protein 1 (LMP1), (123, 124). Indeed, enhanced expression of PD-L1 expression has been demonstrated in EBNA2-expressing DLBCL and BL cell lines, via repression of PD-L1 suppressor miR-34a (125).

Interestingly, PD-L1 expression was found to be elevated on the B cells of HIV-positive patients who went on to develop NHL, relative to those who did not develop the malignancy (126), suggesting its role in lymphomagenesis and that HIV promotes an immunosuppressive environment through expression of PD-L1. This will be further discussed in Chapter 2.

Because approximately 30-40% of DLBCL patients fail standard therapy and suffer from relapsed or refractory disease (127), it is quite clear that an improved therapeutic approach is required. In 2019, the results of a clinical trial which assessed the safety and efficacy of PD-1 inhibitor, Nivolumab, as a monotherapy for patients with Relapsed/Refractory (R/R) DLBCL, demonstrated a low overall response rate (128). Another trial using the PD-1 inhibitor in patients with R/R DLBCL following autologous stem cell transplantation (ASCT) concluded that while pembrolizumab can be administered safely to R/R DLBCL patients, the progression-free survival (PFS) rate did not meet the primary objective specified in the protocol and therefore did not warrant further investigations on a larger scale (129). In yet another study assessing the safety and efficacy of adding PD-L1 inhibitor, atezolizumab, with R-CHOP, the data found that the safety profile was acceptable, and that while the addition of atezolizumab improved complete response (CR) rates, it was not enough to warrant further investigations (130). There have been several other trials involving PD-L1 blockade in DLBCL, all of which demonstrating marginal response rates. However, taken together, the data indicate that PD-L1 blockade may benefit a subset of DLBCL patients, and particularly, there is strong indication that DLBCL patients who are HIV positive will benefit from this additional monotherapy.

While there has been more recent focus on the pathobiology and genetics of DLBCL within the context of HIV, the status of PD-L1 within this patient category remains largely undefined. The current study sought to evaluate the status of PD-L1 in newly diagnosed, treatment naïve DLBCL patients, and

compare by HIV status. Additionally, the regulation of PD-L1 in DLBCL was investigated, in the context of HIV. The approaches taken are outlined in the section which follow.

1.6 Research Aims

This study sought to assess the status and regulation of PD-L1 in DLBCL, within the context of HIV infection through the following three key objectives:

1. To evaluate and compare PD-L1-positivity within the peripheral blood cell populations of a cohort of newly diagnosed HIV-positive and HIV-negative DLBCL patients, using flow cytometry.

The results are presented and discussed in Chapter 2.

2. To perform a small-scale study, to assess and compare PD-L1 expression, T cell and macrophage populations within the TME of HIV-positive and HIV-negative DLBCL tumours, using immunohistochemical staining.

The results are presented and discussed in Chapter 3.

3. To investigate the impact of HIV, as well as key role-players, EBV and c-MYC, on PD-L1 expression within DLBCL cells, using a combination of in silico and in vitro approaches.

The results are presented and discussed in Chapter 4.

The overall findings and conclusion of the study as well as future directions are discussed in Chapter 5.

Chapter 2

Assessing the status of PD-L1-positivity within the peripheral blood cells of HIV-positive and HIV-negative DLBCL patients

2.1 Introduction

B cells are essential in regulating the immune system by secreting antibodies and acting as APCs (131). Because of their ability to generate antibodies, B cells were generally considered to be positive regulators of immune responses; however, in the last few decades data has revealed that B cells are also capable of exerting a negative immunoregulatory effect, primarily by producing interleukin-10 (IL-10) (132, 133). This newly designated subset of B cells are termed regulatory B cells (Bregs) and have received significant attention in recent years. While the level of Bregs remain low in a normal and healthy state, the level increases in response to inflammation with their function being to maintain immune tolerance, by limiting ongoing immune responses and ensuring homeostasis (131, 134).

The immunoregulatory function of Bregs has been linked to cancer progression, with several lines of evidence implicating Bregs in dampening the anti-tumour response, ultimately promoting tumour growth and metastasis (131, 135).

In 2019, a study by Epeldegui and colleagues reported on the status of Bregs and PD-L1-expressing B cells in HIV-positive patients over a period of 1 – 4 years prior to receiving an NHL diagnosis (126). The expression of PD-L1 on B cells, within the peripheral blood of HIV-positive patients and healthy controls were monitored over the 4-year period, and it was found that PD-L1-expressing B cells were elevated in HIV-positive patients compared to healthy individuals, and even further elevated in those HIV positive patients who went on to develop NHL. In addition, the majority of the PD-L1-expressing B cells were within the Bregs subpopulation. The authors further found that, when compared to BL, PD-L1 expression was significantly higher in those patients who developed DLBCL. It is noteworthy that several other studies have shown a positive correlation between Bregs and HIV viral load, and inverse correlation with CD4 counts, suggesting that Bregs is associated with HIV disease progression (136, 137).

The study by Epeldegui and colleagues offered insight into the mechanism by which Bregs and PD-L1-expressing B cells may be induced by HIV-infection. By exposing resting B cells from healthy donors to HIV virions containing the CD40L, the authors found an increase in Bregs and PD-L1 expression on B cells, and that this was brought about due to HIV particles inserting the CD40L on their surface when

budding from activated T cells (126). In so doing, these CD40L-positive HIV particles could directly induce B cell activation and transformation. Overall, while studies are limited, the current available data suggests that the induction of PD-L1 by HIV could be an early oncogenic driving event in HIV-positive individuals, driving lymphomagenesis, and attenuating the immune response (126).

To the best of our knowledge, there have been no other reports on the status of Bregs and PD-L1-positivity within the context of HIV, with a focus of the development of lymphoma, and DLBCL in particular. This emphasizes the need for additional investigations to provide insight and understanding into the molecular events in DLBCL driven by HIV, a disease of significant burden within our context.

In the study reported here, the objective was to assess and compare, by HIV status, the expression of PD-L1, B cells and Bregs, as well as PD-L1-positivity within these sub-populations, in a cohort of newly diagnosed DLBCL patients.

2.2 Methods

2.2.1. Study design and inclusion and exclusion criteria

This cross-sectional study involved HIV-positive and HIV-negative newly diagnosed DLBCL patients referred to Groote Schuur Hospital (GSH). Once ethical clearance was approved by the UCT Human Research Ethics Committee (HREC Ref: 716/2019), patients were recruited from two sites, namely the E5 Haematology and LE32 Radiation Oncology clinics. The study was carried out according to the code of Ethics of the Helsinki declaration, as recommended by the World Medical Association (138). A convenience sampling approach was taken and written informed consent (Appendix A) was obtained from all participating patients. Blood samples were collected in vacutainer Ethylene Diamine Tetra Acetic Acid (EDTA) blood collection tubes (BD Biosciences, USA) by a qualified clinician, and the patients' clinical data was accessed via the National Health Laboratory Service (NHLS) LabTrak database. To preserve patient confidentiality, de-identifying numbers were assigned to each case. All included participants were over 18 years old with a confirmed DLBCL diagnosis, known HIV status and had not yet received chemotherapy. Patients were excluded if they were pregnant, had co-existing chronic illnesses, or had relapsed-refractory disease. A small number of healthy donors were included as a reference point and recruited via convenience sampling. To determine the absolute B cell counts, thirteen healthy controls were included, with consent, as described above. Of the thirteen healthy controls, six controls were included for flow cytometric analysis to assess the specific cell populations listed in Table 2.2 below and allow for comparison to the DLBCL patients.

2.2.2 Biochemical measurements

Routine tests were conducted at the NHLS (GSH), a service accredited by the South African National Accreditation Systems (SANAS). Routine tests included (i) haematological tests, to obtain full blood counts (FBCs) and differential counts, (ii) histological testing, to determine EBER status and the DLBCL COO subtype, and (iii) virology testing to determine HIV status. Once testing was complete, results and medical records were available on the NHLS LabTrak database.

2.2.3 Sample collection and processing

Venous blood, collected in EDTA vacutainer tubes (BD Biosciences, USA), was kept at room temperature during transportation to the laboratory. Blood samples were processed for flow cytometry analysis, as well as plasma and peripheral blood mononuclear cells (PBMCs) isolation and storage, within 24 hours of collection.

Two BD flow cytometers were used during the study period: (i) BD Fluorescence-activated cell sorting (FACS) Calibur™ flow cytometer (BD Biosciences, USA), and (ii) BD FACSymphony™ A5 Cell Analyzer (BD Biosciences, USA). Antibody titrations were conducted to determine the optimal antibody concentration to use for the assay. The whole blood was stained to measure specific cluster of differentiation (CD) cell surface markers using fluorescent labelled antibodies. Details of all antibodies used are shown in Table 2.1.

Table 2.1: Fluorochrome-conjugated antibodies included for flow cytometric analysis.

Antibody	Catalogue number	Antibody clone	Supplier
CD45 APC	340910	2D1	BD Biosciences, USA
CD19 PC5.5	B49211	J3-119	Beckman Coulter, USA
CD24 PE	B92425	ALB9	Beckman Coulter, USA
CD38 FITC	A07778	T16	Beckman Coulter, USA
CD274 APC	563741	MIH1	BD Biosciences, USA

CD - cluster of Differentiation; APC - Allophycocyanin; PC - Peridinin-Chlorophyll-Protein (PerCP) - cyanine (Cy); PE - Phycoerythrin; FITC - Fluorescein isothiocyanate.

Using Falcon™ Polystyrene tubes (BD Biosciences, USA), a maximum of 4 antibodies were added to 100 µL of whole blood to measure specific cell populations of interest. These cell populations are listed in Table 2.2. After the blood was mixed with the specific panel of antibodies, the tubes were incubated for 30 minutes, in the dark. Thereafter, red blood cells were lysed by adding FACS™ lysis solution (BD Biosciences, USA) (Appendix B) and samples were centrifuged at 2000 revolutions per minute (rpm) for 10 minutes. Pelleted cells were washed twice by resuspending in cold 1X Phosphate-buffered saline (PBS) (Appendix B) and centrifuging for 5 minutes. Labelled cells were resuspended in 100 µL of

cold 1X PBS and analysed on either the FACS Calibur™ flow cytometer (BD Biosciences, USA) or the BD FACSymphony™ A5 Cell Analyzer (BD Biosciences, USA).

Table 2.2: Cell populations analysed using flow cytometry.

Tube	Cell population of interest	Antibodies used
1	PD-L1$^+$ immune cells	CD274 APC
2	B cells	CD45 APC, CD19 PC5.5
3	PD-L1$^+$ B cells	CD19 PC5.5, CD274 APC
4	Bregs	CD45 APC, CD19 PC5.5, CD24 PE, CD38 FITC
5	PD-L1$^+$ Bregs	CD19 PC5.5, CD24 PE, CD38 FITC, CD274 APC

Bregs – Regulatory B cells; PD-L1 – Programmed Death-Ligand 1; CD - cluster of Differentiation; APC - Allophycocyanin; PC - Peridinin-Chlorophyll-Protein (PerCP) - cyanine (Cy); PE - Phycoerythrin; FITC - Fluorescein isothiocyanate.

2.2.4 Flow cytometric analysis

The BD FACS™ Calibur flow cytometer (BD Biosciences, USA) runs on the BD FACStation™ software and uses the CellQuest Pro 5.1 software (BD Biosciences, USA) for data acquisition and analysis. Performance was assessed using the BD calibration beads (BD CaliBRITE™ beads 3-colour kit and APC beads, BD Biosciences, USA) for each fluorophore and run using the BD FACSComp software (BD Biosciences, USA). Instrument settings were adjusted for quality control and standardization. Details of the instrument configuration are provided in Appendix D.

The BD FACSymphony™ A5 Cell Analyzer (BD Biosciences, USA) runs on FACSDiva™ software and FlowJo 10.9 (BD Biosciences, USA) is used for data analysis. For each sample analysed on this specific flow cytometer, daily quality control (QC) settings were applied and compensation beads (Anti-Mouse Ig κ/Negative Control Compensation Particles Set, BD Biosciences, USA) were run to obtain accurate fluorescence signal. The compensation matrix was then applied and used for the sample.

2.2.4.1 Gating strategy and optimization

For the BD FACS™ Calibur flow cytometer (BD Biosciences, USA), a minimum of 10 000 total events were counted for each cell population of interest. Regarding patient samples assessed on the FACSymphony™ A5 Cell Analyzer (BD Biosciences, USA), 20 000 lymphocytes were counted prior to counting 10 000 cells of each population of interest.

Overall PD-L1-positivity was assessed by gating on all immune cells with high CD274 expression based on side scatter versus CD274 (SSC vs CD274). To analyse B cells and Bregs, a sequential gating strategy was implemented where cells were initially gated based on the forward versus side scatter (FSC vs SSC) plot to specify lymphocytes and exclude cell debris. Figure 2.1 illustrates the sequential gating strategy implemented. Lymphocytes were selected as cells with high CD45 expression, and from there

B cells were identified and gated on as $CD45^+ CD19^+$. From B cells, PD-$L1^+$ B cells as $CD19^+ CD274^+$ and Bregs as $CD45^+ CD19^+ CD24^+ CD38^+$ were identified, and finally using the Bregs plot, PD-$L1^+$ Bregs were identified as $CD19^+ CD24^+ CD38^+ CD274^+$.

(A)

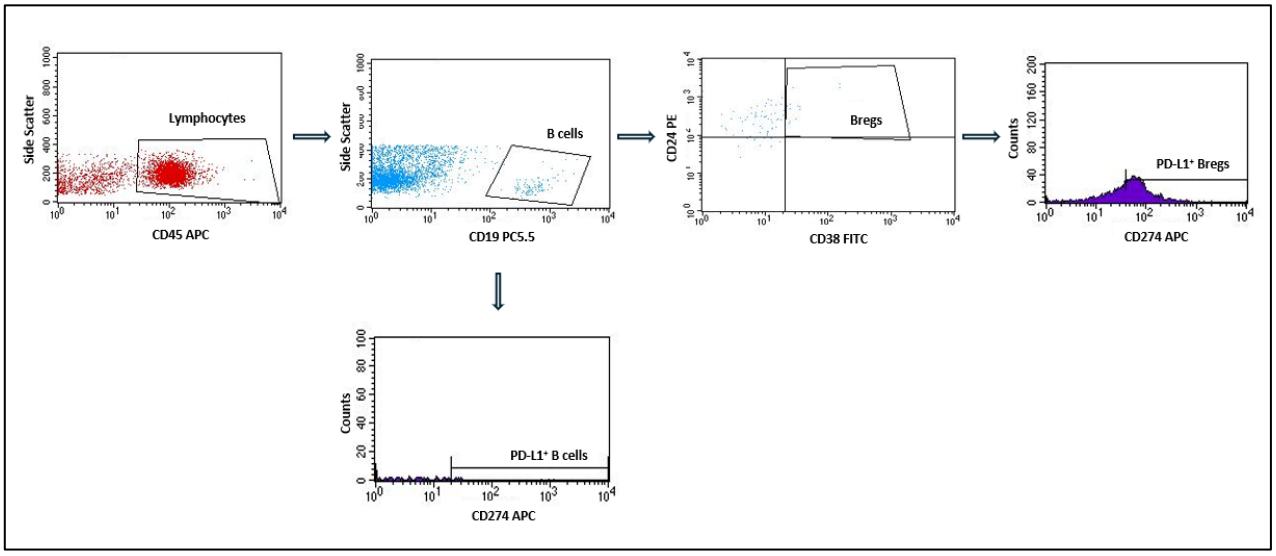

(B)

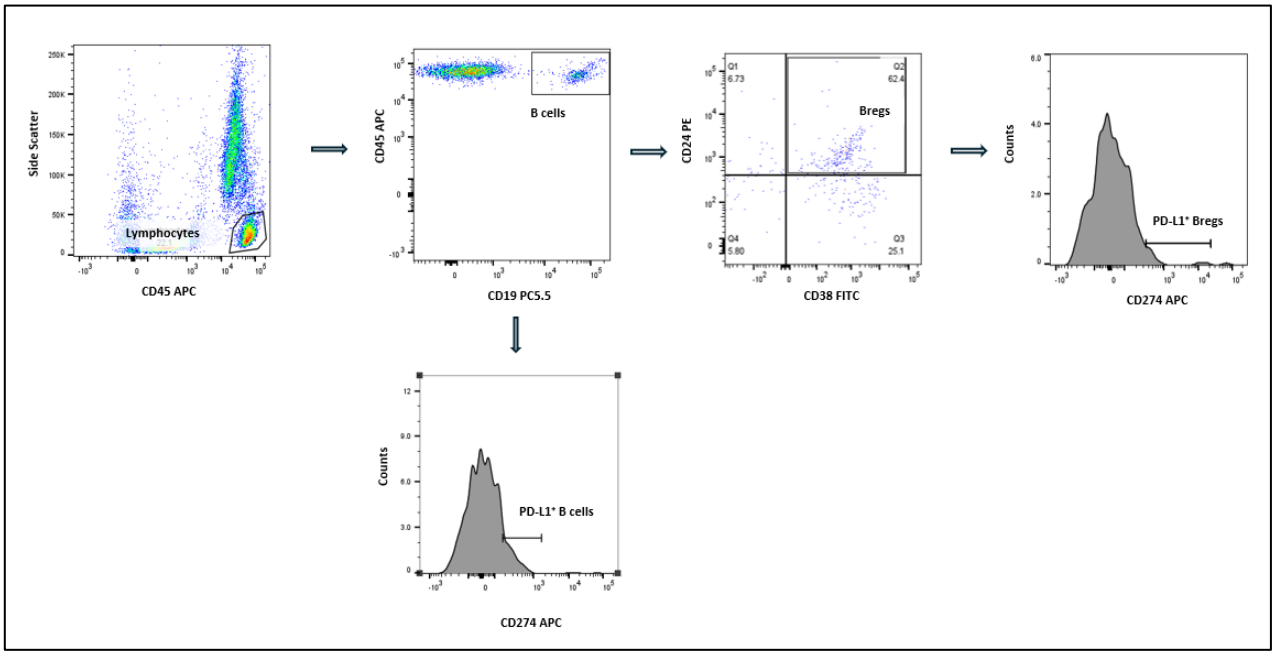

Figure 2.1: Sequential gating strategy implemented on the (A) BD FACS™ Calibur flow cytometer and (B) the BD FACSymphony™ A5 Cell Analyzer

Fluorescence Minus One (FMO) controls were used, where samples were stained with each fluorophore minus one, to determine the boundary for background signal and allow for accurate gating of positive populations. These controls were used to set gates, excluding negative populations.

2.2.5 Statistical analyses

To identify baseline characteristics that were significantly different between patient groups, Fishers exact tests were performed. Since this specific test only analyses two categories of data, p-values for COO and EBV status were calculated by only comparing GCB to non-GCB and EBV-positive to EBV-negative, respectively. Data was recorded in a Microsoft Excel Spreadsheet and statistical analyses was performed using GraphPad Prism version 9 (GraphPad Software, USA). Cell populations were analysed within the program suited for the FACS system used and the data was recorded in a Microsoft Excel Spreadsheet and GraphPad Prism version 9 (GraphPad Software, USA) was used to generate graphs and perform statistical tests. The Kruskal-Wallis test was used to compare the absolute B cell counts between three data groups, i.e. heathy controls, HIV-positive DLBCL and HIV-negative DLBCL. Mann-Whitney U non-parametric test was used to compare the data between two data groups, i.e. healthy controls to DLBCL patients, and HIV-positive DLBCL to HIV-negative DLBCL. Data was presented as individual points, with the median being marked. The p-value for statistical significance was set at $p \leq 0.05$, with a 95% confidence interval.

2.3 Results

2.3.1 Patient characteristics

A total of 33 patients were recruited into this study and a summary of the clinical characteristics are shown in Table 2.3 below. Of the 33 participants, approximately two thirds were HIV-negative (67%; n=22). Within the HIV-negative group, 59% was males (n=13), while in the HIV-positive group 45% was male (n=5). At the time of DLBCL diagnosis, the majority of HIV-negative patients were above the age of 50 (64%; n=14), whereas in the HIV-positive group the majority of the patients were under the age of 50 (64%; n= 7).

There was significant difference in DLBCL subtypes according to HIV status. The majority of HIV-negative patients were of the non-GCB subtype (73%; n=16), while the GCB subtype was most common among the HIV-positive DLBCL patients (64%; n=7) ($p \leq 0.05$). There was notable extranodal involvement within the HIV-positive group (82%; n=9) relatively to the HIV-negative group (50%; n=11). In both cases, tumours tested negative for EBV in the majority of cases (73% and 86% for HIV-positive and HIV-negative respectively).

Table 2.3: Clinical characteristics of study participants.

	HIV-positive	HIV-negative	*P-value*
Patients	11 (33%)	22 (67%)	
Gender			*0.4875*
Male	5 (45%)	13 (59%)	
Female	6 (55%)	9 (41%)	
Age (n; range; median)			*0.163*
<50	64% (n=7; 23-48; 34)	36% (n=8; 24-49; 36)	
>50	36% (n=4; 51-61; 55)	64% (n=14; 50-74; 60)	
Subtype			*0.0214**
GCB	7 (64%)	5 (23%)	
Non-GCB	3 (27%)	16 (73%)	
Other	1 (plasmablastic) (9%)		
Unknown		1 (4%)	
Biopsy site			*0.1322*
Nodal	2 (18%)	11 (50%)	
Extranodal	9 (82%)	11 (50%)	
Tumour EBV status			*0.3098*
Positive	3 (27%)	2 (9%)	
Negative	8 (73%)	19 (86%)	
Unknown		1 (5%)	

GCB – Germinal Center B-Cell (GCB); EBV – Epstein-Barr virus. Fishers exact test *$p \leq 0.05$ = statistically significant. P-values were calculated for COO and EBV status by only taking GCB vs non-GCB and EBV-positive vs EBV-negative into account, respectively.

2.3.2 Difference in cell counts between HIV-negative and HIV-positive DLBCL patients

Routine full and differential blood counts were performed for each patient on sample collection day. This data was accessed, with consent, from the NHLS patient database LabTrak portal, and is displayed in Table 2.4 below, grouped and analysed based on HIV status.

Table 2.4: Full blood and differential lymphocyte counts of study participants.

	Normal range	HIV-positive (n=11) Median (range)	HIV-negative (n=22) Median (range)	*P-value*
White cell count ($x10^9$/L)	3.9-12.6	6.28 (3.03-11.01)	8.1 (1.13-22.53)	*0.0633*
Lymphocyte differential count ($x10^9$/L)	1.4-4.5	1.24 (0.47-3.24)	1.675 (0.3-6.55)	*0.3907*
Neutrophils ($x10^9$/L)	1.6-8.3	3.29 (1.94-9.46)	5.075 (0.39-14.58)	*0.0894*
Monocytes ($x10^9$/L)	0.2-0.8	0.59 (0.06-0.81)	0.875 (0.17-5.43)	*0.0027***
Eosinophils ($x10^9$/L)	0-0.04	0.05 (0-0.43)	0.04 (0-0.32)	*0.5893*
Basophils ($x10^9$/L)	0-0.1	0.02 (0-0.05)	0.045 (0.02-0.19)	*0.0093***
Red cell count ($x10^{12}$/L)	3.8-4.8	4.33 (2.17-5.27)	4.44 (2.76-5.64)	*0.3961*
Platelet count ($x10^9$/L)	186-454	325 (210-718)	367 (175-1048)	*0.453*

Mann-Whitney U test, p-value ≤0.05 = statistically significant (**p ≤ 0.01).

HIV-positive DLBCL patients had significantly lower monocyte and basophil counts compared to the HIV-negative DLBCL group. In addition, white cell counts were generally lower within the HIV-positive cohort, as well as the neutrophil counts.

2.3.3 Analysis of cell populations

PD-L1-positivity on peripheral immune cells present in the peripheral blood was determined by gating on cells with high CD274 expression. A sequential gating strategy on CD45 was implemented to assess B cells and its subpopulations. An initial CD45 gating allows for exclusion of cellular debris and other "noise" within the sample, which was followed by sequential gating within this population (139). The methodology and antibody panels used are outlined in section 2.2.3 above.

2.3.3.1 Overall PD-L1 positivity

The overall status of PD-L1 positivity across peripheral immune cells within the peripheral blood (lymphocytes, granulocytes and monocytes) was evaluated in DLBCL patients and compared to six healthy controls. The findings are represented in Figure 2.2A and demonstrate a statistically significant difference in overall PD-L1 status ($CD274^+$) between healthy individuals and DLBCL patients, with the latter group displaying elevated numbers of $PD\text{-}L1^+$ cells (healthy controls vs DLBCL patients; median: 0.14% vs 0.44%; $p \leq 0.01$). DLBCL patients were then stratified according to HIV status and PD-L1-positivity was assessed in each patient group. Despite the number of HIV-positive patients being half the number of HIV-negative patients, a significant difference was observed between the groups (Figure 2.2B), whereby increased PD-L1-positivity was observed in the HIV-positive group (HIV-negative vs HIV-positive; median: 0.37% vs 0.65%; $p \leq 0.05$).

(A)

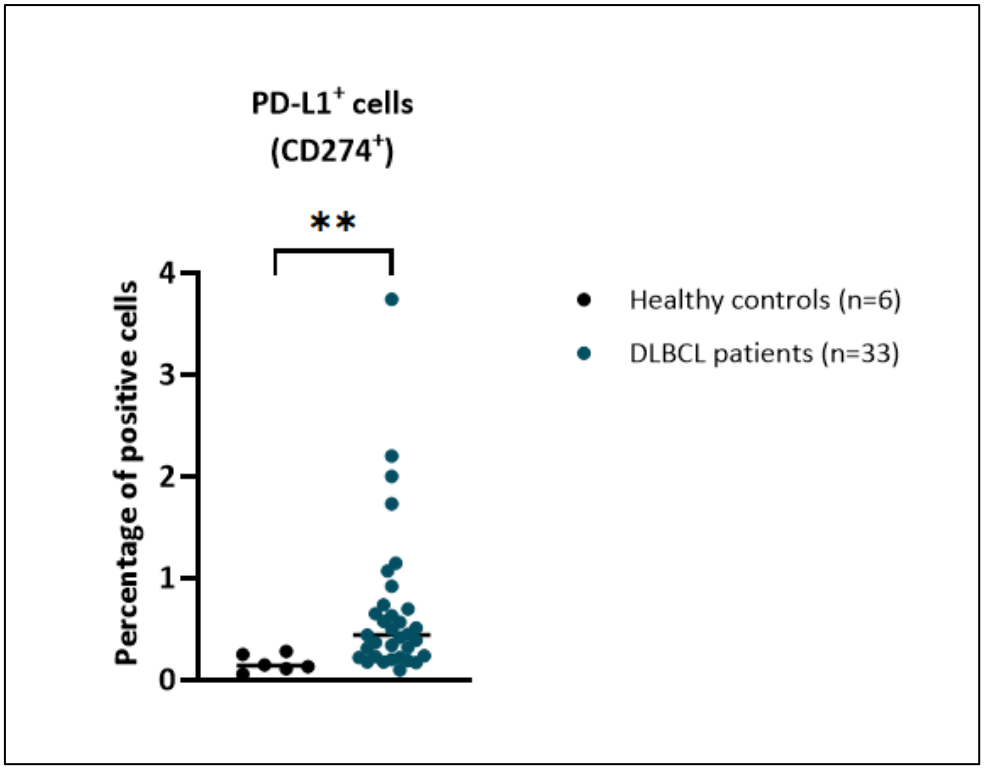

(B)

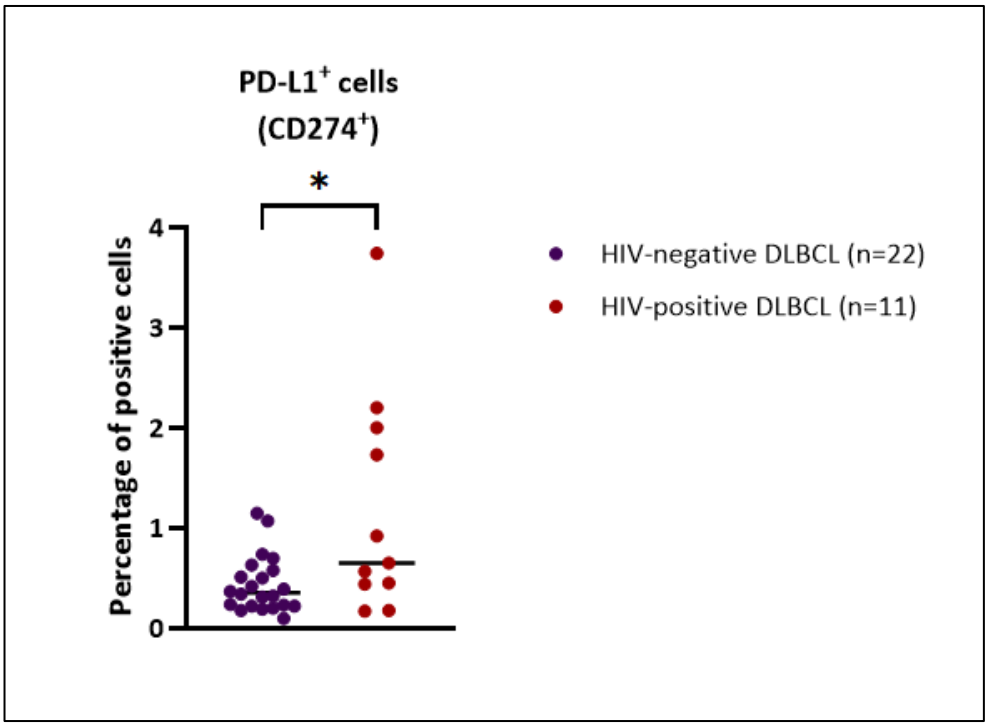

Figure 2.2: Percentage of PD-L1$^+$ cells (CD274$^+$) in DLBCL patients. Blood samples were incubated with fluorochrome-conjugated antibodies to assess PD-L1-positivity. (A) PD-L1 status in healthy controls and DLBCL patients. (B) PD-L1$^+$ cells in DLBCL patients stratified according to HIV status. Individual data points are represented above, with the centre line indicating the median. Statistical analysis was performed using GraphPad Prism version 9 (Mann-Whitney U test, *p ≤ 0.05; **p ≤ 0.01).

2.3.3.2 PD-L1 expression within B lymphocytes

B cells were analysed through sequential gating using antibodies against CD45 and CD19. CD19 is recognized as a pan B cell marker expressed by most B cells from the early stages of development until differentiation to plasma cells and recognised as a reliable B lymphocyte marker (140). Thirteen healthy controls were included to compare the absolute count to that of the two DLBCL groups. As shown in Figure 2.3, the absolute count of $CD19^+$ B cells was significantly higher in healthy individuals compared to both DLBCL patients groups (control vs HIV-negative, $p \leq 0.01$; control vs HIV-positive, $p \leq 0.01$), while no significant difference was observed between HIV-positive and HIV-negative DLBCL patients, although a general trend of a slightly lower B cell count was observed in the HIV-positive DLBCL group (HIV-negative vs HIV-positive, $p > 0.9999$).

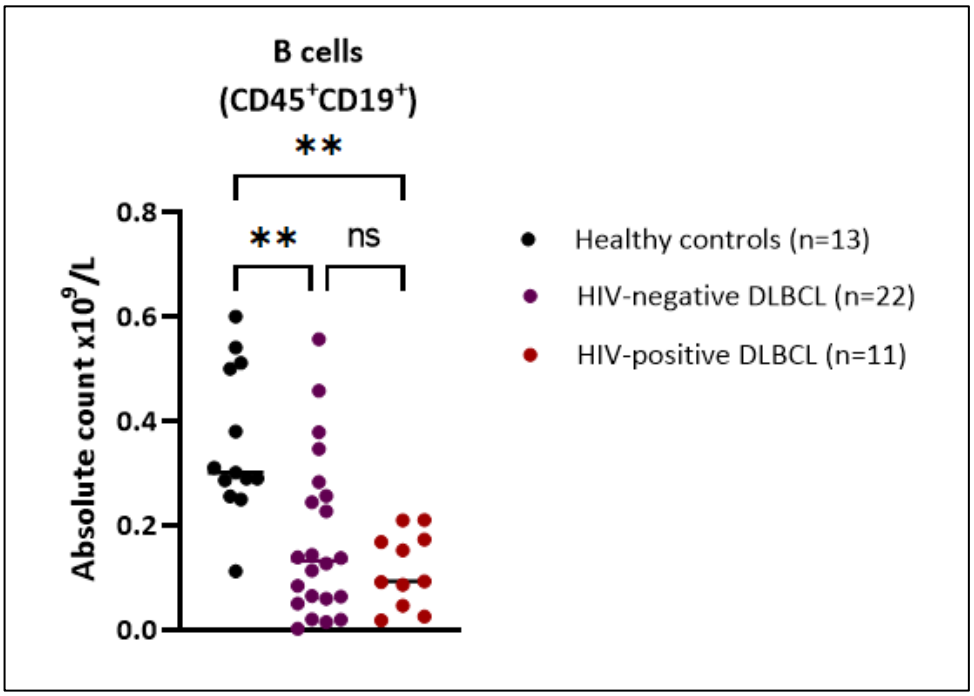

Figure 2.3: Absolute count of B cells ($CD45^+$ $CD19^+$) in healthy individuals and HIV-negative and -positive DLBCL patients. Blood specimens, collected in EDTA tubes, were stained with fluorochrome-conjugated antibodies, and analysed using flow cytometry. Absolute $CD19^+$ B cell counts were determined for each patient by multiplying the percentage of $CD45^+$ $CD19^+$ B cells with their respective lymphocyte count (retrieved from NHLS LabTrak) and dividing by 100. Individual data points in all groups are represented above, with the centre line indicating the median. Statistical analysis was performed using GraphPad Prism version 9 (Kruskal-Wallis test, **$p \leq 0.01$).

The B cell population was then further subtyped to assess PD-$L1^+$ B cells ($CD19^+$ $CD274^+$) between healthy controls and all DLBCL participants included in this study. We found B cells to be significantly higher expressors of PD-L1 in DLBCL patients, compared to healthy individuals (Figure 2.4A; healthy controls vs DLBCL patients; median: 1.97% vs 6.62%; $p \leq 0.001$). DLBCL patients were then stratified according to HIV status, which revealed that B cells in HIV-positive DLBCL patients expressed higher

levels of the immune regulatory ligand relative to the HIV-uninfected patient group (Figure 2.4B; HIV-negative vs HIV-positive; median: 5.66% vs 10.9%; $p \leq 0.05$).

(A)

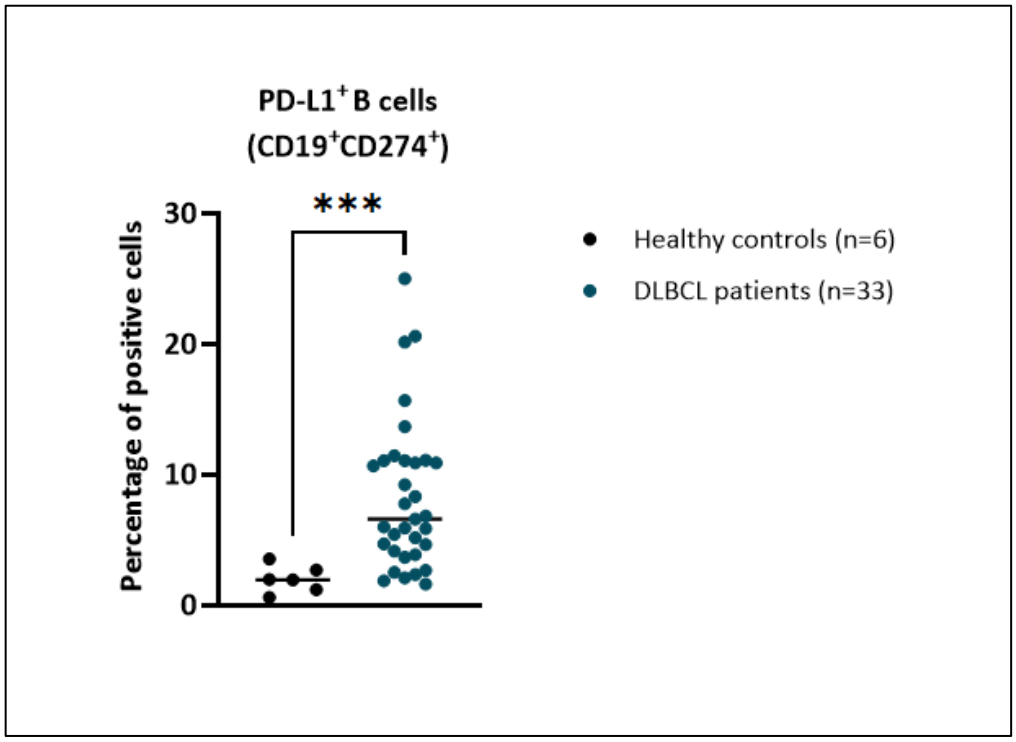

(B)

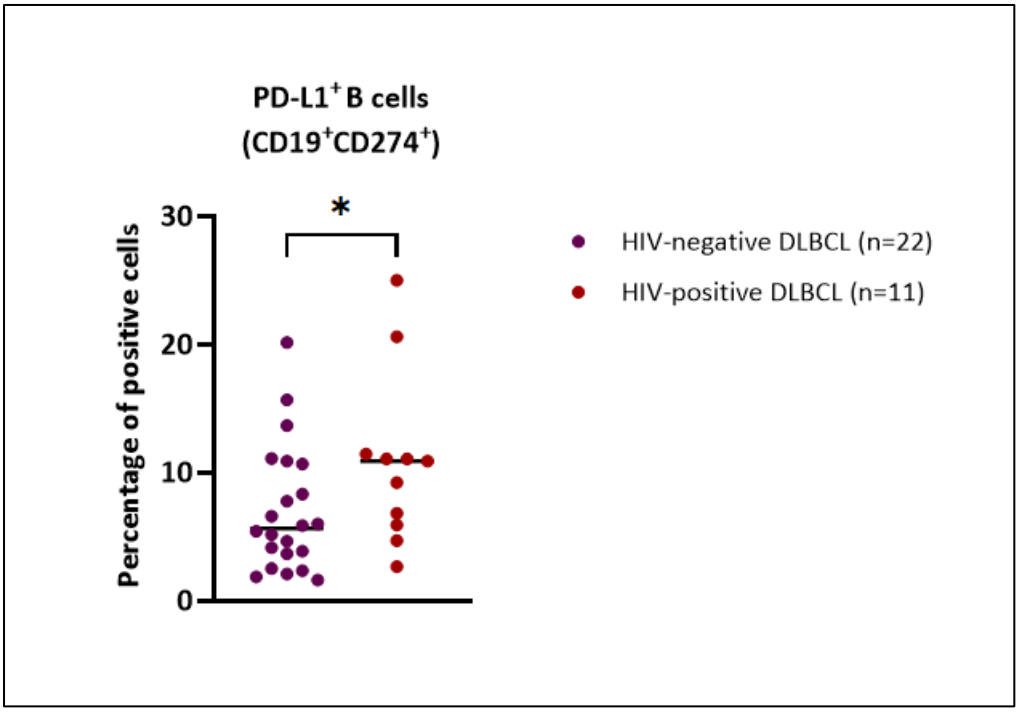

Figure 2.4: Comparison of PD-L1$^+$ B cells (CD19$^+$ CD274$^+$) in DLBCL patients. Blood specimens, collected in EDTA tubes, were stained with fluorochrome-conjugated antibodies, and analysed using flow cytometry. (A) Percentage of CD19$^+$ CD274$^+$ PD-L1-positive B cells in healthy controls and DLBCL patients. (B) Percentage of CD19$^+$ CD274$^+$ PD-L1-positive B cells in HIV-negative and HIV-positive DLBCL patients. Statistical analysis was performed using GraphPad Prism version 9 (Mann-Whitney U test, *$p \leq 0.05$; ***$p \leq 0.001$). Individual data points in all 01groups are represented above, with the centre line indicating the median.

2.3.3.3 Regulatory B cells and PD-L1 expression

Bregs ($CD19^+$ $CD24^+$ $CD38^+$) were sequentially identified from the B cell population and as shown in Figure 2.5A, there was no significant difference between the proportion of Bregs in healthy controls and DLBCL patients; although a high degree of variability was observed within the DLBCL patient group, with a much higher median (Healthy controls vs DLBCL patients; 26.55% vs 58.3%; p = 0.0524). When comparing Bregs in DLBCL patients according to HIV status, no major differences were observed (Figure 2.5B; HIV-negative vs HIV-positive; median: 57.5% vs 61.2%; p = 0.5344).

(A)

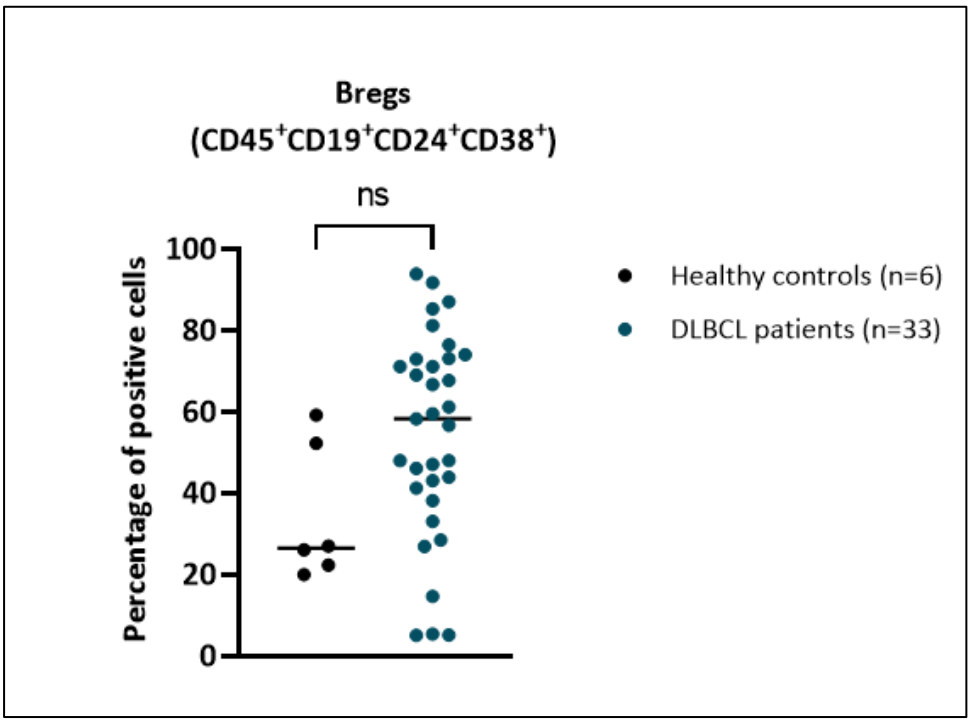

(B)

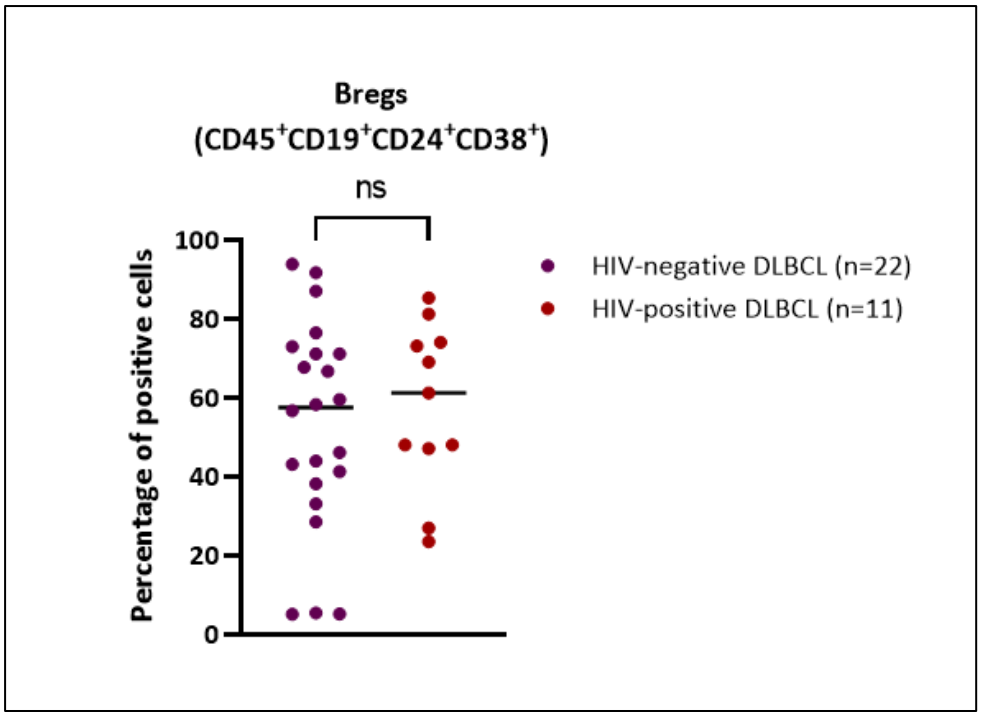

Figure 2.5: Comparison of Bregs ($CD45^+$ $CD19^+$ $CD24^+$ $CD38^+$) in DLBCL patients. Blood samples were incubated with fluorochrome-conjugated antibodies to assess the Breg population. A Fluorescence Minus One (FMO) control was used to identify cells positive for CD24 and CD38. (A) Percentage of Bregs in healthy individuals and DLBCL patients. (B) Percentage of Bregs in DLBCL patients segregated based on HIV status. Individual data points are represented above, with the centre line indicating the median.

PD-L1-positivity within the Breg subpopulation ($CD24^+$ $CD38^+$ $CD274^+$) was assessed in DLBCL patients and compared to healthy controls (Figure 2.6A). While not statistically significant, less than 2% of Bregs in the healthy controls were positive for PD-L1 expression, whereas DLBCL patients demonstrated high variability in their proportion of $PD\text{-}L1^+$ Bregs, with up to ~35% of Bregs being $PD\text{-}L1^+$ (healthy controls vs DLBCL patients; median: 0.54% vs 1.43%; p = 0.1730). When stratified according to HIV status, no noticeable difference in the proportion of $PD\text{-}L1^+$ Bregs was observed between groups (Figure 2.6B; HIV-negative vs HIV-positive; median: 1.74% vs 0.83%; p = 0.3551).

(A)

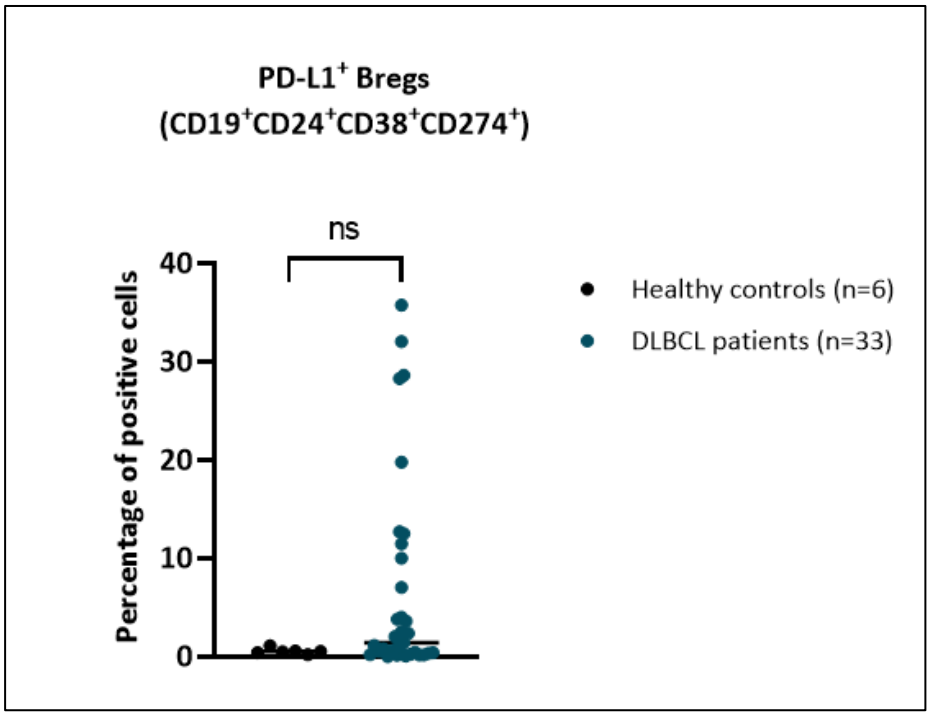

(B)

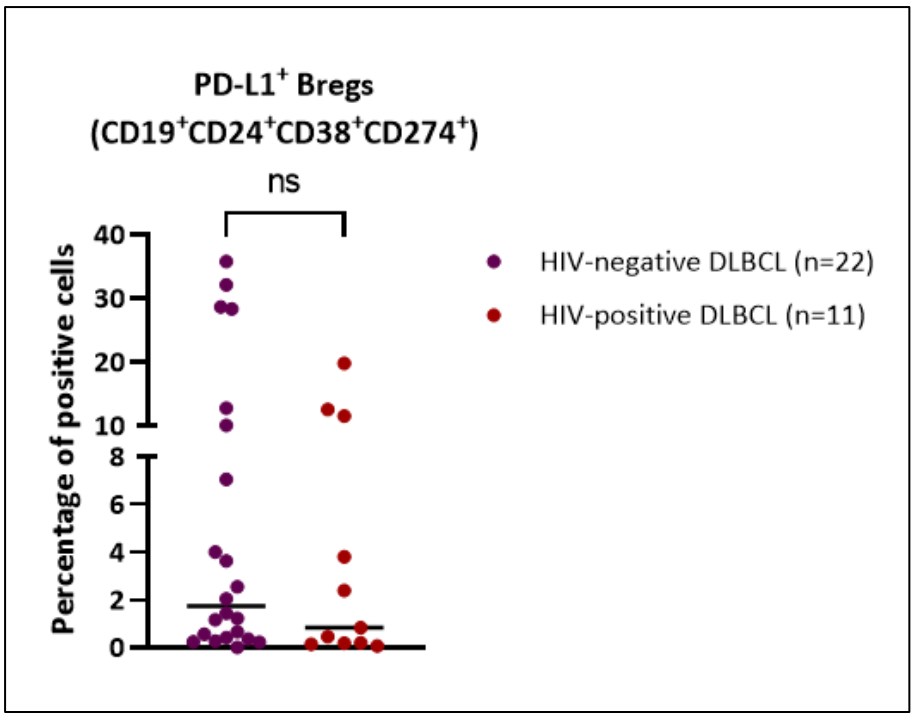

Figure 2.6: Comparison of PD-L1-positivity within the Breg population ($CD19^+$ $CD24^+$ $CD38^+$ $CD274^+$) in DLBCL patients. Blood samples were incubated with fluorochrome-conjugated antibodies to assess PD-$L1^+$ Bregs. A Fluorescence Minus One (FMO) control was used to identify cells positive for CD274. (A) Percentage of PD-$L1^+$ Bregs in healthy individuals and DLBCL patients. (B) Percentage of PD-$L1^+$ Bregs in DLBCL patients segregated based on HIV status. Individual data points are represented above, with the centre line indicating the median.

2.4 Discussion

This study sought to assess and compare the overall status of PD-L1 as well as B cells, Bregs and PD-L1-positivity within the peripheral blood of newly diagnosed, treatment naïve, DLBCL patients based on their HIV status. Over the period of August 2021 to March 2024, 33 newly diagnosed DLBCL patients were recruited into the study and their blood samples were used for flow cytometric analysis. The cohort consisted of a higher proportion of HIV-negative cases (67%), which is in line with previous reports recruiting patients from the same site (82, 141).

Of the total participants recruited in this study, 55% were males. Several reports note that DLBCL is slightly more common in males as opposed to females (142, 143). In line with those reports, we observed slightly more males (59%; n=13) than females (41%; n=9) in the HIV-negative group. However, this finding could be biased due to the small sample size. Although there is no clear explanation behind the difference in DLBCL incidence rates between genders, multiple studies have attributed this to estrogen signalling (144, 145). Yakimchuk and colleagues demonstrated, in a mouse model, that the presence of the estrogen receptor (ER)β on lymphoid cells, conferred an anti-proliferative effect on lymphoma tumours (146). Interestingly, a recent report revealed that *nuclear receptor 4A2 (NR4A2)*, a tumour suppressor in lymphoma, is regulated by estrogen and that females

with the ABC subtype of DLBCL and high *NR4A2* expression exhibited better survival outcomes compared to those with low expression of *NR4A2 (143)*. Additionally, pregnancy, natural birth as well as the use of oral contraceptives have been associated with lowering the risk of DLBCL in females (144, 145, 147). With regards to the HIV-positive group, while our cohort is small, we noted almost equal number of males (45%; n=5) and females (55%; n=6). Studies assessing the South African DLBCL population in an HIV-positive setting, have revealed that there is a slightly higher female to male ratio in the HIV-positive DLBCL group (72, 148), and while this trend is not explicitly clear in our findings, the sample size of the current study is relatively small. In South Africa, women are considered to be a high-risk population for contracting HIV, primarily due to age-disparate relationships with older men who are HIV-positive and unaware of or do not disclose their status (149), resulting in a higher number of HIV-positive females, who are at risk for DLBCL development. An investigation on a larger scale may reveal interesting trends on the frequency of DLBCL in males and females, taking HIV-infection into account, in a South African context.

EBV-infection was detected in 27% of HIV-positive samples (n=3), as opposed to 9% in the HIV-negative group (n=2). Of the total participants included, only five were EBV-positive, of which three were HIV-positive. While the results from this study show that EBV-infection is more common in HIV-positive DLBCLs, the frequency is lower than that reported in other studies. Retrospective studies conducted in the USA revealed that between 31% and 44% of HIV-positive DLBCLs were EBV-positive (63, 150), and some reports indicate up to 50% of HIV-positive DLBCLs being EBV-positive (62). Despite the low sample size, the number of EBV-positive cases among HIV-positive DLBCL patients reported in the current study is slightly higher than that reported by Cassim and colleagues, which involved participants from the same recruitment site. Cassim et al. revealed that only 16% of HIV-positive DLBCLs were EBV-positive; but nonetheless, EBV-infection was still detected more frequently in HIV-positive cases (82). Since infection with EBV in DLBCL is associated with an aggressive disease (151)even more so in South Africa where co-infection with HIV and Tuberculosis (TB) is prevalent (152); it is plausible that most of these patients may have already succumbed to their disease prior to reporting to the hospital and receiving their diagnosis, ultimately resulting in a lower frequency of EBV-positive HIV-associated DLBCL cases being reported within our local setting.

HIV-positive DLBCL patients generally presented at an earlier age compared to the DLBCL patients who were HIV-negative. This observation is well documented in the literature (72, 153, 154), and has been linked to several factors, such as (a) impaired immune defence and specific molecular events driven by HIV-infection, as well as co-infection with other oncogenic viruses such as EBV, and (b) the possibility that HIV-infected patients frequent ARV clinics, and thus are typically closely monitored at

these clinics and hospitals upon receiving their HIV-positive status, allowing for an earlier DLBCL diagnosis to be made (155). Additionally, in South Africa, the incidence of HIV is higher in younger individuals, between 20 - 24 years for women and 25 – 29 years for men (156), and ultimately, acquiring HIV at an earlier age would lead to an earlier onset of DLBCL, given the high risk of DLBCL development that is associated with HIV-infection.

Within our cohort, a statistically significant difference in subtypes was observed between groups where 64% of HIV-positive DLBCLs were of GCB-origin, and 84% of HIV-negative DLBCLs were assigned to the non-GCB subtype ($p < 0.05$). This is an unexpected finding, given that ABC-DLBCL is associated with a worse outcome and so are HIV-associated DLBCLs, and thus one may expect that ABC-DLBCLs would be more prevalent within this patient group (65, 157). In the literature, there appears to be conflicting data on which DLBCL subtype is more commonly observed in HIV-infected individuals. For instance, in 2014, a study conducted by Morton and colleagues evaluated and compared the molecular traits and prognosis in DLBCL patients who were HIV-negative and HIV-positive. In that particular study, it was reported that in the HIV-infected group, 83% of tumours were of ABC-origin, compared to 54% in the HIV-negative group (158). Contrasting to that, a later study reported that GCB-DLBCLs are more frequent in HIV-positive cases, while a more even distribution of subtypes is observed in the HIV-negative group (159). It is important to note that the two studies mentioned above were performed on different patient populations. In a recent retrospective study involving an American cohort of patients, GCB-DLBCLs arising in the HIV-infected population were reported to be molecularly distinct from GCB-DLBCLs arising in HIV-uninfected individuals, suggesting that HIV-positive GCB-DLBCLs is a distinct entity of DLBCL (160). It is also highly plausible that since ABC-DLBCL is more aggressive, HIV-positive patients with this subtype of DLBCL may have already succumbed to their disease before reporting to the hospital for treatment, and thus, this could be a spurious correlation.

In the current study, 50% of HIV-negative DLBCL patients (n=11) presented with extranodal involvement, whereas a striking 82% of HIV-positive patients (n=9) were diagnosed with DLBCL from extranodal sites. This is in line with other studies reporting that HIV-associated lymphomas, including DLBCL, tend to involve extranodal sites (161, 162). Extranodal involvement relates to sites, other than the lymph nodes and tonsils, from which DLBCL can arise, and this is associated with a worse prognostic outcome (163). Additionally, DLBCL can also spread to extranodal organs, which would be indicative of advanced stage disease (164). Since we have reported a higher frequency of extranodal involvement in the HIV-positive cohort, this emphasizes the aggressive nature of HIV-associated DLBCL (165).

While not statistically significant, a slightly lower white blood cell count is observed for the HIV-positive group compared to the HIV-negative group. Cytopenia is indeed a frequent observation in HIV-infected individuals. Cytopenia results from the effect of HIV on lymphocytes, monocytes and other immune cell populations which ultimately impacts haematopoiesis (166). Interestingly, our study noted a significantly lower count of monocytes (monocytopenia) observed in the HIV-positive group ($p \leq 0.01$). Monocytes are involved in the first line of defence against pathogens, including HIV, and may become infected with HIV due to the presence of CD4 receptors and CCR5 coreceptors (167, 168). In a recent investigation, the monocyte count in people living with HIV (PLWH) was compared to healthy controls and a slightly lower monocyte count was noted in HIV-infected individuals (168); however, a separate study revealed that in the context of HIV-positive DLBCL, the monocyte count did not offer any prognostic value (169).

A significantly lower basophil count was also noted among our HIV-positive DLBCL patients ($p \leq 0.01$). Basophils migrate to sites of inflammation to mediate allergy response and hypersensitivity reactions (170). It has been reported that circulating basophils are capable of capturing HIV-1 particles on their cell surface and mediate trans-infection of $CD4^+$ T cells by forming viral synapses (171). Jiang and colleagues co-cultured basophils, bound with HIV-1, with $CD4^+$ T cells and discovered that basophils can transfer HIV-1 to $CD4^+$ T cells resulting in the infection of these cells (172). Certain strains of HIV utilize CCR3, present on basophils, as a co-receptor for HIV-infection (171). The HIV-1 Tat and Nef proteins are said to be strong chemo-attractants for basophils through interaction with CCR3 and CXCR4, respectively (173, 174). The findings from these studies highlight basophils as an important population of cells that are involved in the spread and persistence of HIV-infection. With that being said, it is not evidently clear how HIV-infection impacts the basophil count. This warrants further investigation into whether HIV has an impact on the number of basophils in infected patients, or if the count is lower in HIV-positive individuals but the basophils that are present, are utilized by HIV to reach $CD4^+$ target cells. Since $CD4^+$ T cells are the primary targets for HIV, most of the immune dysregulation caused by HIV-infection is a result of the indirect effects associated with the virus (175).

While not statistically significant, our findings suggested a lower neutrophil count in the HIV-positive group compared to HIV-negative patients. Abnormalities resulting in a lower neutrophil count (neutropenia) have been previously described in HIV-infection (176, 177). Neutrophils are generally considered to act in defence against invading pathogens and neutropenia critically affects patients, especially with the immune system already being compromised by HIV (178). There is currently no evidence that HIV directly infects neutrophils, but several potential causes for neutropenia observed in the presence of HIV-infection have been described (176). For example, the development of

neutropenia is said to be closely associated with HIV viral load which implies that HIV may exert toxicity to haematopoietic cells, including neutrophil precursors (178). In addition, HIV also negatively affects T cell production of Granulocyte-macrophage colony-stimulating factor (GM-CSF), a cytokine that stimulates neutrophils (179). Taken together, in addition to the direct targeting of $CD4^+$ T cells, it is clear that HIV-infection also influences several other types of immune cells, whether it be by direct or indirect mechanisms.

With regards to the status of PD-L1, compared to healthy controls, where PD-L1 levels were relatively low, DLBCL patients displayed significantly higher PD-L1 positivity in their peripheral blood. To date, there has been few studies evaluating overall PD-L1-positivity in the peripheral blood of DLBCL patients compared to healthy individuals. In a recently published study, increased levels of PD-1-positive cells and soluble PD-L1 (sPD-L1) were reported in the blood samples from DLBCL patients relative to healthy controls, and the level of PD-1 expression within DLBCL patients was significantly correlated with advanced disease staging (180). In addition to the membrane-form of PD-L1, the soluble form of PD-L1 is also present within fluids, and originates predominantly via cleavage of the membrane form, however there is no clear correlation between PD-L1 and sPD-L1 (94, 181). Nonetheless, our result clearly indicates that PD-L1 expression is likely a significant player in DLBCL pathogenesis due to its high expression, relative to healthy controls.

In the presence of HIV, certain cell subsets are reported to express upregulated levels of PD-L1 (98, 182), but there are limited studies describing the status of PD-L1 in the peripheral blood of HIV-positive DLBCL patients. When comparing DLBCL patients based exclusively on HIV status, this study observed a noticeable trend of increased PD-L1-positive cells in the HIV infected group, thus confirming that HIV-infection is associated with increased PD-L1 levels. This association could be made despite the fact that the HIV-positive cohort was 50% smaller in numbers than the HIV-negative cohort. As mentioned, limited studies exist on the status of PD-L1 in the peripheral blood of HIV-positive DLBCL patients. In the context of HIV-infection solely, Bowers and colleagues (2014) reported that in the blood of HIV-positive individuals, neutrophils express high levels of PD-L1 (183). Additionally, PD-1 expression was reported to be increased on monocytes in the PBMCs of HIV-positive patients, and the interaction between $PD\text{-}1^+$ monocytes and cells expressing high levels of PD-L1, resulted in the dampening of T cell functions (184). There are only a few reports assessing immune cell counts in HIV-positive DLBCL as an entity, thus emphasizing the importance of understanding this disease at the cellular level, as trends may differ to what is described in the context of HIV-infection alone. Furthermore, identifying cell-specific PD-L1 expression contributing to the overall elevated status of PD-L1 observed in HIV-positive DLBCLs, and how that may differ from PD-L1-expressing cells

in HIV-negative DLBCL, is important to unmask the specific cells involved in establishing a favourable environment for tumours.

The absolute count of $CD19^+$ B cells was significantly lower in the DLBCL patient group, compared to the healthy controls, and this is in line with what has been previously reported (141). An even lower B cell count was observed in the HIV-positive group, relative to the HIV uninfected DLBCL cohort of patients. While HIV does not infect B cells, studies have shown that HIV-infection leads to B cells dysfunction and a reduced number of B cells (185, 186). In an HIV setting, impaired B cell functioning has been suggested to be related to the low levels of $CD4^+$ T cells, which are essential in initiating B cell activation and proliferation (187, 188). In addition, during HIV-replication and progression the complement receptor CD21, which forms a complex with CD19 to enhance BCR signalling, is reported to be absent or expressed at very low levels on B cells ($CD21^{-/low}$ B cells) (185, 189), which results in a decreased proliferation rate upon receiving B cell stimuli (190).

When comparing PD-L1 expression on B cells within patient groups, our findings revealed a significantly higher proportion of PD-$L1^+$ B cells in DLBCL patients compared to healthy controls. This demonstrates that B cells are a contributor to the elevated PD-L1 expression in DLBCL observed earlier. Upon stratifying DLBCL patients according to HIV status, this study noted a significant trend of increased PD-L1-expressing B cells in the HIV-positive group, despite the number of HIV-positive DLBCL patients being 50% less than the number of patients in the HIV-negative group. As stated by Epeldegui and colleagues, who also revealed elevated PD-L1 expression on B cells in the presence of HIV-infection (126), it is highly plausible that increased PD-L1-expressing B cells may contribute to the impairment of $CD4^+$ and $CD8^+$ T cells by interacting with PD-1, ultimately impacting the anti-tumour response. The wide range of PD-$L1^+$ B cells observed in our HIV-positive group (percentages range from 2.69% to 25%) may be explained by variations in the viral load (VL) and CD4 counts among the patients (although no correlation could be made, due to high variability in our data). While a negative correlation between CD4 count and VL would be expected, this feature is not always demonstrated (191), reflecting variation between patients with the same disease. A recent study by Rafael and colleagues showed that PD-L1 expression on B cells was increased in HIV-infected participants with a detectable VL, compared to both healthy individuals and HIV-infected patients who received ARTs and displayed undetectable VLs; thus confirming that PD-L1 was upregulated on B cells during HIV replication (192). While the data on ART status of our patient cohort was not available, it should be noted that, in our local setting, the majority of our HIV-positive patients discover their HIV status during their cancer diagnosis, and thus would not have been on ARTs, and a small number would have defaulted on their ART. Additional studies assessing the potential impact of ARTs on PD-L1 expression

in our local setting may prove to be useful in providing further insight. Overall, these finding suggest that HIV promotes an immunosuppressive environment in newly diagnosed DLBCL patients, partly through PD-L1$^+$ B cells.

Regarding the assessment of Bregs and PD-L1$^+$ Bregs, our findings show no significant difference between healthy individuals and DLBCL patients. Of note was that the proportion of Bregs and PD-L1$^+$ Bregs was highly variable in DLBCL patients relative to healthy controls, which indicates that this population of cell is affected/abnormal within this patient group, with some patients harbouring relatively high Bregs/PD-L1$^+$ Bregs, with the p-value approaching significance (Bregs, $p = 0.0524$). Additionally, in healthy controls, a very small percentage of Bregs expressed PD-L1 (less than 2%), whereas the percentage of PD-L1$^+$ Bregs was variable in DLBCL patients, ranging from 0% to 35.76%. Upon segregating DLBCL patients based on their HIV status, no apparent difference in the percentage of Bregs or PD-L1$^+$ Bregs was observed between HIV-positive and HIV-negative patients. Both patient groups presented with a similar trend of these cell populations, thus indicating that infection with HIV did not significantly impact PD-L1-positivity on Bregs in our cohort of DLBCL patients. This contrasts with what was reported by Epeldegui and colleagues, although these two studies were different in several aspects. For instance, our study compared DLBCL patients who were HIV-positive and HIV-negative, whereas Epeldegui and colleagues compared HIV-positive patients who developed DLBCL and those who did not. More importantly, a key difference is the population of patients included in our study, compared to the study conducted by Epeldegui et al. In South Africa, HIV-positive individuals present more frequently with co-morbidities, such as TB, as well as opportunistic infections, which are associated with a more aggressive disease (148). Furthermore, Epeldegui and colleagues also included a larger number of patient specimens. Our study comprised of a small number of healthy controls and twice as many HIV-negative patients relative to the HIV-positive group. Therefore, including a larger number of healthy controls along with more DLBCL patients, both HIV-positive and -negative, may prove to be worthwhile in establishing the relevance of these cell populations within our patients in South Africa. Other than the study conducted by Epeldegui and colleagues, there is a dearth of information around the status of Bregs and PD-L1$^+$ Bregs in HIV-positive DLBCL. In the context of HIV-infection alone, Bregs were reported to contribute to T cell impairment through IL-10 and PD-L1 (193). Additionally, in treatment-naïve HIV-positive patients, the frequency of Bregs were reported to be higher when compared to healthy controls, and significantly less in in those who received treatment (194). To our knowledge, there are limited studies assessing the proportion of Bregs solely in the context of DLBCL. Recently, Mishina et al. reporting on the characteristics of DLBCLs positive for markers of Bregs, such as IL-10 and transforming growth factor

β (TFG-β). They found that these "Breg-type DLBCLs" were associated with the ABC-like cell of origin as well as poor prognosis (195).

The proportions of Bregs and PD-L1$^+$ Bregs were further stratified, using the median of each cell population, to determine if there was any relationship between the expression levels of these cells and the DLBCL subtype, EBV-status, or site of diagnosis (Supplementary Tables 2.1 and 2.2). In the HIV-positive cohort, two out of the three non-GCB cases (67%) expressed a percentage of Bregs above the median, while four out of the seven GCB cases (57%) expressed a percentage of Bregs below the median. In the HIV-negative cohort, there was no major difference or trend in the DLBCL subtypes of Bregs expressed below or the above the median. Similarly, for the PD-L1$^+$ Bregs, there is an equal proportion of non-GCB subtypes below and above the median in the HIV-negative cohort. In the HIV-negative group, the majority of the cases who had Bregs and PD-L1$^+$ Bregs expressed at a percentage above their respective medians, were DLBCLs diagnosed from extranodal sites, while the majority of the nodal cases had a low percentage of these cells present, i.e. below the median. In the HIV-positive group, the distribution of both cell populations followed no definitive trend based on their site of diagnosis (nodal or extranodal).

Another study conducted within our laboratory by Dr Ramorola, recruiting patients from the same site, revealed that in addition to HIV-positive DLBCL patients presenting with significantly less CD4$^+$ T cells compared to the HIV-negative DLBCL patients, a higher proportion of CD8$^+$ cytotoxic T cells was also uncovered in the peripheral blood of the HIV-positive cohort (141). Chronic activation of CD8$^+$ T cells occur as a result of continuous antigen stimulation, associated with HIV-infection, ultimately leading to the dysfunction of these cells. There is a scarcity of studies evaluating and comparing immune cell populations in HIV-positive and HIV-negative DLBCL patients, which ultimately provide valuable insight into the immune dysregulation driven by HIV.

Overall, the data from this study provided significant insight into the status of PD-L1 in HIV-positive DLBCL patients, which has not been described before in a South African cohort of patients. We have demonstrated that HIV-positive DLBCL patients have significantly increased levels of PD-L1-positive cells in their peripheral blood, of which CD19$^+$ B cells are a contributor, signifying that immune evasion through PD-L1 is a mechanism associated with HIV-infection in DLBCL. This may also, in part, explain the aggressive phenotype of HIV-associated DLBCL. Increasing the sample size is a future endeavour of this project. Additional studies assessing the status of PD-L1 on other cell types in DLBCL, in the context of HIV-infection, may uncover interesting trends and provide more insight into the regulation of PD-L1 by HIV.

Chapter 3

Evaluation of PD-L1 expression, T lymphocyte and macrophage populations in the TME of HIV-positive and HIV-negative DLBCL tumours

---

3.1 Introduction

The function of PD-L1 as an important component of the tumour immunosuppression was discussed in section 1.5.2 (Chapter 1), and evidence to date suggests that the status of this factor within the TME is one of the major elements affecting therapeutic efficiency (196). The TME is not only composed of malignant cells, but also includes a large number of non-transformed cells, some of which are recruited by the malignant cells. Together, they constitute a highly complex state that sustains the TME's internal signalling network which influences tumour progression, metastasis, immune evasion and therapeutic response (197, 198). While the composition of the TME differs between cancer types, the key components include stromal cells, fibroblasts, fat cells, endothelial cells, immune cells (T and B lymphocytes, NK cells, tumour-associated macrophages, dendritic cells, etc), blood vessels, and the extracellular matrix (ECM) (Figure 3.1).

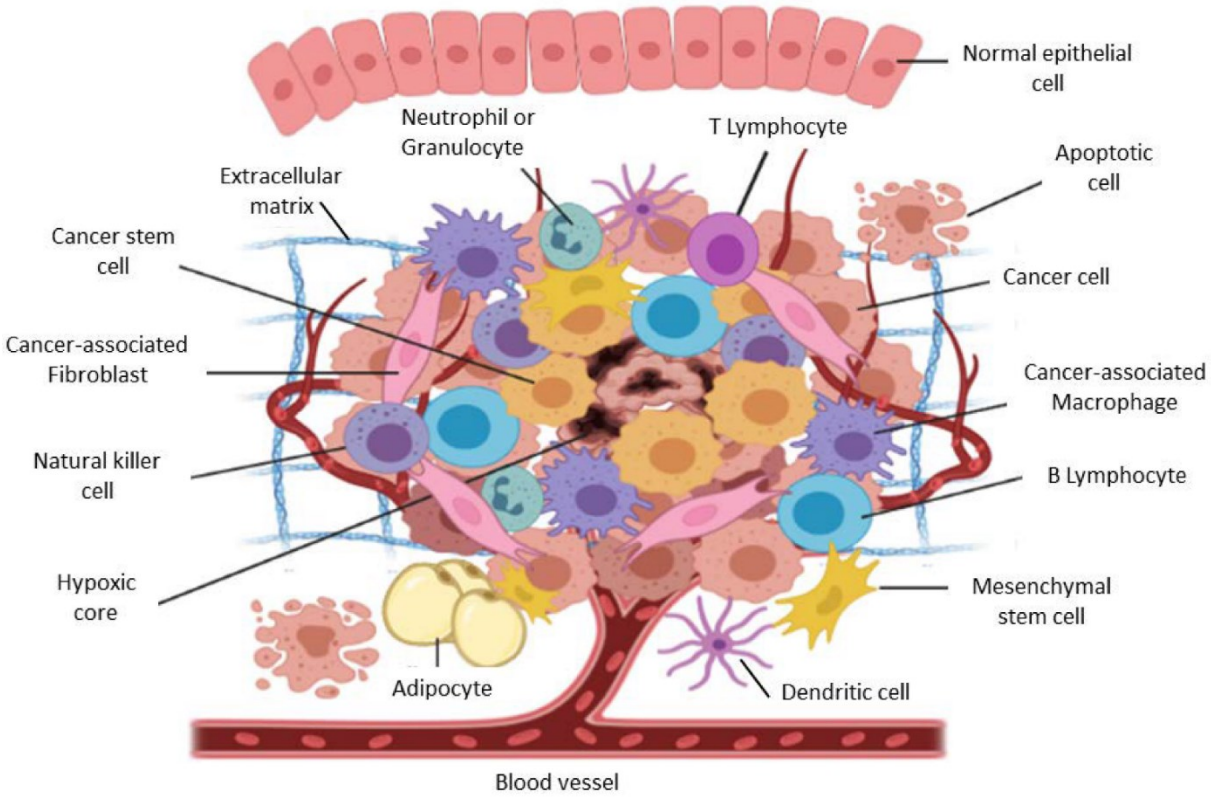

Figure 3.1: Main components of the TME. Graphical illustration of the various cellular and non-cellular components present in the TME, contributing to tumour progression (from Dzobo et al., 2023) (199).

The relationship between the TME and infiltrating immune cells can either promote or hinder tumour growth (200). Innate immune cells, such as macrophages, and adaptive immune cells, including B and T cells, are important components of the TME (201). Cytotoxic T cells ($CD8^+$) identify abnormal tumour antigens and exhibit cytotoxic activity against them; therefore, their presence in the TME is correlated to a favourable prognosis in cancer patients (202, 203). Helper T cells ($CD4^+$) can differentiate into various subsets, and thus regulates a broad range of immune responses within the TME (204). Macrophages are key regulators in maintaining tissue homeostasis and can be classified as either pro-inflammatory macrophages (M1) or immune-suppressive macrophages (M2) (205). While both types may be found in the TME, M2 macrophages are generally favoured by tumour cells since they promote growth and progression of the tumour (206). An inferior prognosis is often seen in cancer patients with high macrophage infiltration (207). Within the TME, PD-L1 can be widely expressed on the surface of multiple cell types, including B and T lymphocytes, dendritic cells and macrophages, as well as on the surface of the tumour cells, leading to T cell exhaustion and immune tolerance/escape.

In DLBCL, as is the case for many other cancers, the cross-talk between tumour cells and the microenvironment has been shown to be dysregulated to avoid immune detection by the host, and several mechanisms have been described (208). MHCs are essential molecules for the presentation of self and non-self antigens to T cells (209), and are frequently dysregulated in DLBCL to reduce recognition by T cells, thus promoting an immunosuppressive TME (210). Additionally, impaired immune response by PD-L1 overexpression has been reported on both DLBCL tumour cells and TME components (211, 212, 213, 214). PD-L1 expression was also demonstrated to positively correlate with the number of PD-1^+ TILs (215). Roussel and colleagues demonstrated that PD-L1 expression was elevated in DLBCL and even more so in the ABC subtype, which also showed increased levels of PD-1^+TIM3^+ TILs (216). Similarly to PD-1, TIM3 is an inhibitory receptor that is often co-expressed with other inhibitory receptors to regulate T cell exhaustion (217), and co-expression of PD-1 and TIM3 is said to exert a greater level of T cell exhaustion (218). Interestingly, Roussel and colleagues reported that while PD-1^+TIM3^+ TILs displayed an impaired cytokine production in DLBCL, they retain high expression of cytotoxic molecules, and their functions could be restored upon PD-1 blockade (216).

While the dynamics of the TME has been well studied, much less work has been done on the impact of HIV-infection on the TME, within the context of HIV-associated cancers, such as DLBCL. Immunohistochemical studies to examine prognostic markers in DLBCL found that the latter had much reduced predictability within an HIV positive context, which indicate differences in the pathophysiology of the tumours (219). Indeed, an enhanced angiogenic state has been associated with HIV-related malignancies, and a few studies have reported on differences in the immune cell composition of the TME in patients with or without HIV infection (220). With regards to DLBCL, a study

published in 2013 reported increased microvessel density in the TME of HIV-positive DLBCL cases, but no changes in macrophage density, compared to HIV-negative DLBCL cases (221). However, a slightly later study published in 2015 reported increased density of macrophages in HIV-positive DLBCLs, keeping in mind that macrophages with a proinflammatory phenotypes have been reported to stimulate angiogenesis (222). Exposure to ART has also been shown to impact the TME composition of HIV-positive DLBCLs, where a recent report revealed an enrichment of exhausted $CD8^+$ cytotoxic cells in ART-naïve tumours, compared to the ART-experienced group (69).

There remains a dearth of information on how HIV infection may be impacting the physiology of the TME in DLBCL patients, accounting for the more aggressive phenotype of the disease observed in this patient group. Particularly, studies related to the status of PD-L1, a factor which has been reported to promote aggressive tumours, including via enhanced angiogenesis, within the TME, has, to the best of our knowledge, not yet been described. Here, using immunohistochemistry (IHC), a small-scale study was conducted, whereby the TME of 10 HIV-positive and 10 HIV-negative DLBCL tumours were evaluated and compared, assessing T cell status ($CD4^+$ and $CD8^+$), TAM infiltration, and overall PD-L1 expression.

3.2 Methods

3.2.1 Antibodies

The following antibodies were used in the immunohistochemical assay: anti-CD4 ([EPR6855] ab133616, (Abcam), anti-CD8 ([C8/144B] ab17147, Abcam), anti-PD-L1 (CD274) ([E1L3N] 13684, Cell Signalling) and anti-CD68 ([PG-M1] ab783, Abcam).

Optimizations for each antibody were carried out using lymph node, appendix and tonsil formalin-fixed paraffin-embedded (FFPE) tissue sections to ensure specificity and to maximize signal detection.

3.2.2 Patient identification for inclusion

Based on the University of California, San Francisco (UCSF) sample size calculator, it was estimated that 44 patients in each group is required in this study. Due to the large number of samples required, this study served as a pilot study by first assessing 10 FFPE tissue samples in each patient group.

The cases included in this study (10 HIV-positive and 10 HIV-negative DLBCL) were retrieved through a convenience sampling approach from the UCT Anatomical Pathology FFPE archive and assessed by an expert Anatomical Pathologist to confirm diagnosis, as well as to assess tissue quality and quantity. Specimens from newly diagnosed DLBCL patients who presented at GSH were included for analysis.

3.2.3 Sample preparation, antigen retrieval and staining.

Following a period of extensive optimization, two distinct IHC procedures were employed as outlined below.

3.2.3.1 IHC staining procedure for $CD4^+$ and $CD68^+$ cells.

Glass slides containing tissue sections were heated on a heating block for 15 minutes at 60˚ C and thereafter dewaxed for two 20-minute cycles in xylene, followed by rehydration for two 20-minute cycles in 100% ethanol and then two 20-minute cycles in 96% ethanol. CD68 staining required an antigen retrieval step in Proteinase K (20 µg/ml) (Appendix B) at 37˚ C for 20 minutes. The EnVision FLEX Mini, High pH (Dako, Denmark) kit was used - the supplied peroxidase-blocking reagent, EnVision/HRP, DAB chromogen, substrate buffer and wash buffer (20X) were used across all staining procedures. To minimise false-positive staining, endogenous peroxidase activity was blocked for 5 minutes using peroxidase supplied with the EnVision kit (Dako, Denmark). Slides were washed with wash buffer (Dako, Denmark) for 20 minutes. Non-specific binding was minimised by incubating slides in blocking buffer containing 3% BSA in 1X TBS/0.1% Triton X-100 (Appendix B) for 30 minutes. Thereafter, the sections were incubated with the primary antibodies diluted in 3% BSA in 1X TBS/0.1% Triton X-100, at 4˚ C overnight. CD4 and CD68 were incubated at a dilution of 1:500 and 1:80, respectively.

Following primary antibody incubation, slides were washed in the supplied wash buffer (Dako, Denmark) for 10 minutes, and thereafter incubated with EnVision/HRP (Dako, Denmark) for 1 hour at room temperature. Thereafter, the slides were washed as before, and a solution mix of DAB chromogen and substrate buffer (Dako, Denmark) was added to each specimen for 10 minutes. Slides were then washed in running tap water, followed by counterstaining in haematoxylin for 2 minutes, and immersion in Scott's tap water for 30 seconds. The slides were then washed in water for 3 minutes, dehydrated for two 5-minute cycles in 96% alcohol followed by two 5-minute cycles in 100% alcohol, cleared with xylene and mounted with rapid mounting medium.

Negative controls were included, which involved staining with secondary antibodies only, as well as positive controls, which included tissue known to express the antigens of interest.

3.2.3.2 IHC staining procedure for $CD8^+$cells and $CD274^+$ (PD-L1) cells.

All IHC experiments included an additional DLBCL specimen to serve as a negative control, and lymph node and tonsil sections to serve as positive controls for CD8 and CD274, respectively. Glass slides containing tissue sections were heated on a heating block for 15 minutes at 60˚ C and thereafter dewaxed for two 5-minute cycles in xylene, followed by rehydration for two 5-minute cycles in 100%

ethanol and then two 5-minute cycles in 96% ethanol. CD8 and CD274 staining required an antigen retrieval step of 2 minutes in 1X TBE (appendix B), at high pressure in a pressure cooker. The EnVision FLEX Mini, High pH (Dako, Denmark) kit was used - the supplied peroxidase-blocking reagent, EnVision/HRP, DAB chromogen, substrate buffer and wash buffer (20X) were used across all staining procedures. To minimise false-positive staining, endogenous peroxidase activity was blocked for 5 minutes using peroxidase supplied with the EnVision kit (Dako, Denmark). Slides were rinsed briefly with wash buffer (Dako, Denmark). Sections were incubated with the primary antibodies diluted in 3% BSA in 1X TBS/0.1% Triton X-100, for 45 minutes. CD8 and CD274 were incubated at a dilution of 1:50 and 1:400, respectively.

Following primary antibody incubation, slides were washed briefly in wash buffer (Dako, Denmark), and thereafter incubated with EnVision/HRP (Dako, Denmark) for 30 minutes at room temperature. Thereafter, the slides were washed as before, and a solution mix of DAB chromogen and substrate buffer (Dako, Denmark) was added to each specimen for 10 minutes. Slides were submerged in 1% copper sulphate (Appendix B) for 5 minutes. Slides were then washed in running tap water, followed by counterstaining in haematoxylin for 30-45 seconds, and immersion in Scott's tap water for 10 seconds. The slides were then dehydrated for 10 seconds in 96% alcohol followed by two 10-second cycles in 100% alcohol, cleared with xylene and mounted with rapid mounting medium.

3.2.4 Visualization, image capture and analysis.

All stained slides were scanned using the Olympus vs120 Virtual Slide Scanner (Olympus Corporation, Japan) at the Pathology Learning Centre at UCT. Scanned slides were visualized using QuPath version 0.5.1 (University of Edinburgh, United Kingdom) and analysis of staining for all four antibodies was performed at 20X magnification within the same tumour area in each sample, using the ImageJ software version 1.54 (National Institute of Health, USA).

Results are reported as the percentage of positively stained cells within the region analysed. Statistical analysis was performed using GraphPad Prism version 9 (GraphPad Software, USA), where the Mann-Whitney U test was implemented.

3.3 Results

3.3.1 Clinical characteristics of study participants.

The clinical characteristics of the 20 patients included in this small-scale study are shown in Table 3.1. The cases were selected based on convenience sampling, as described in section 3.2.2. A majority of the cases (70%, n=7 for HIV-positive and 60%, n=6 for HIV-negative) were of the GCB subtype. Similarly, most of the cases (80% overall, n=16) were negative for tumour EBV status. At the time of

diagnosis, the median CD4 count of our HIV-positive group was 288 cells/mm^3, below the normal range of CD4 count typically observed in HIV-uninfected individuals (500 – 1500 cells/mm^3) (223). Regarding the HIV viral load at presentation, 20% of cases (n=2) displayed an undetectable level, and low-level viremia ranging from 21 to 1000 IU/mL was also observed for 20% of HIV-positive cases (n=2). A higher viral load of 1000 IU/mL was observed in 40% of cases (n=4), and in this cohort of HIV-positive patients, a slight majority were on ARTs (60%, n=6).

Table 3.1: Clinical characteristics of cases included.

	HIV-positive	**HIV-negative**
Cases (n)	10 (50%)	10 (50%)
Subtype		
GCB	7 (70%)	6 (60%)
Non-GCB	3 (30%)	2 (20%)
Unknown		2 (20)
Tumour EBV status		
Positive	2 (20%)	
Negative	8 (80%)	8 (80%)
Unknown		2 (20%)
CD4 count at diagnosis (cells/mm^3)		
Median (IQR)	288 (177,75-376)	
HIV viral load (IU/mL)		
0-20	2 (20%)	
20-1000	2 (20%)	
>1000	4 (40%)	
Unknown	2 (20%)	
Receiving ART		
Yes	6 (60%)	
No	4 (40%)	

GCB – Germinal Center B-Cell (GCB); EBV – Epstein-Barr virus. ART – Antiretroviral therapy.

3.3.2 Visualization, quantification and analysis of stained cells

As mentioned in section 3.2.4, image visualization was performed by a virtual slide scanning system and quantification was performed using ImageJ software version 1.54 (National Institute of Health, USA). Representative images of each antibody stain in one HIV-positive DLBCL and one HIV-negative DLBCL case, at 20X magnification, are shown in Figure 3.1. These images were used to quantify the

staining of each antibody used, for each of the 20 patient samples (data shown in Supplemental Figure 1, Appendix C). Thereafter, the dataset for each antibody stain was segregated based on HIV status, and percentage positivity compared. These results are shown in the sections which follow.

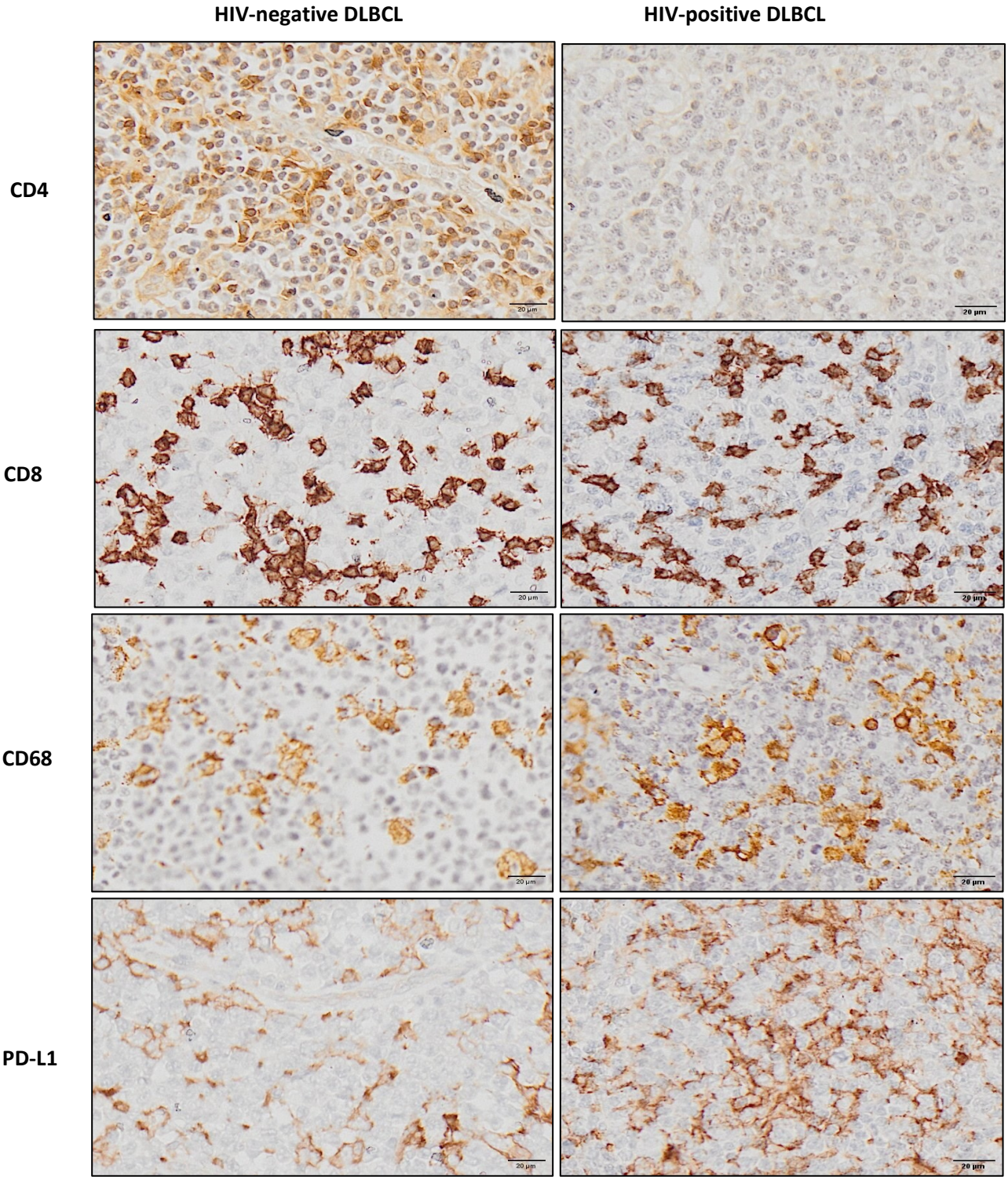

Figure 3.1: Representative images of CD4, CD8, CD68 and PD-L1 immunohistochemical staining in HIV-negative and HIV-positive DLBCL FFPE tissues. Slides were scanned and visualized at 20X magnification (scale bar 20µm), using QuPath version 0.5.1 (University of Edinburgh, Edinburgh, United Kingdom).

3.3.2.1 T cell infiltration

TILs are important players in the anti-tumour response, and their composition within the TME is crucial in driving the immune response. $CD4^+$ T cells are involved in anti-tumour activity; however, this is dependent on recognition of MHC-II on other cells (224). Since most cancer cells do not express MHC-II, this anti-tumour response can be via cross-presentation of antigens by other cell types, such as stromal cells, which may take up components of tumour cells (for example, secreted vesicle by tumour cells, or necrotic components of tumour cells). Normal B cells, which are the cell of origin of DLBCL tumour cells, do express MHC-II and serve as antigen-presenting cells for $CD4^+$ T cells. However, studies have shown that DLBCL tumours display decreased MHC-II expression, which correlates with poor outcomes (225, 226). In the present context, since $CD4^+$ T cells are the primary hosts of HIV, it was expected that a significant difference would be seen between the two groups. Indeed, as can be seen in Figure 3.2, the difference was highly significant (HIV-negative vs HIV-positive; median: 1.56% vs 0.0005%; $p \leq 0.0001$). This finding is in line with the low CD4 count displayed in Table 3.1 for the HIV-positive group.

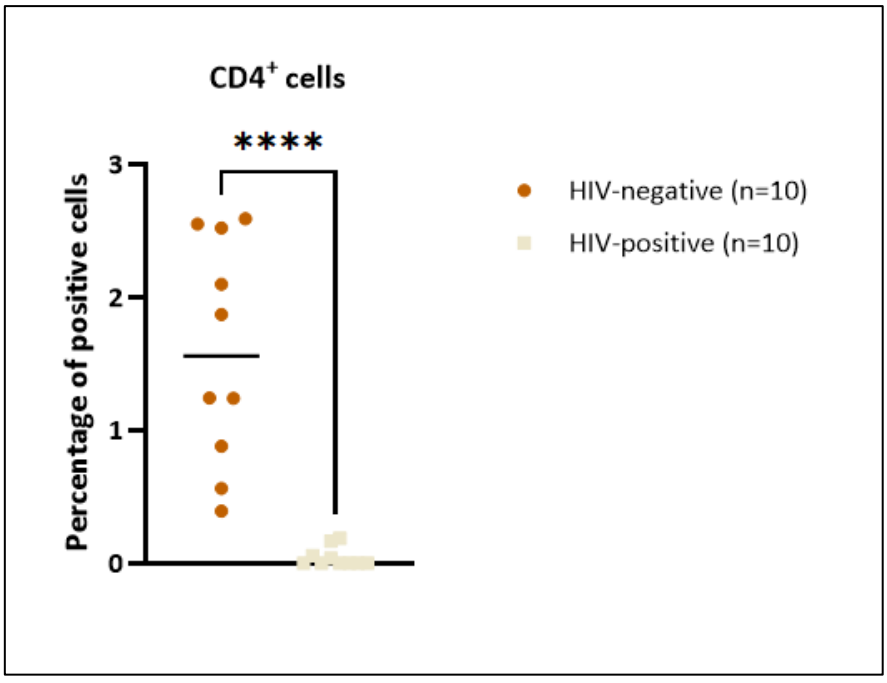

Figure 3.2: Percentage of CD4-positive cells in HIV-negative and HIV-positive DLBCL tissues. FFPE tissues were stained using a CD4 antibody to detect helper T cells. Individual data points represent the percentage of positively stained cells in each case, with the centre line indicating the median. Statistical analysis was performed using GraphPad Prism version 9 (Mann-Whitney U test; ****$p \leq 0.0001$).

$CD8^+$ T cells are an important subpopulation of T cells involved in the anti-tumour response and are reported to be the "backbone of current successful cancer immunotherapies" (227). By differentiating into cytotoxic T cells, $CD8^+$ T cells infiltrate into the TME and exert cytotoxic activity against tumour cells. This involves recognition through the TCR of specific antigens on the surface of tumour cells,

presented by MHC-I complexes (228). Loss of MHC-I is considered to be the highly common form of immune escape, observed in approximately 50% of DLBCLs and reduces recognition by cytotoxic $CD8^+$ T cells (210). Additionally, in the TME, chronic antigen stimulation impacts the functioning of $CD8^+$ T cells, ultimately driving them into an dysfunctional and "exhausted" state (229). In the context of HIV-positive DLBCL, $CD8^+$ T cells are reported to be elevated in the TME, due to the depletion of $CD4^+$ T cells (230). Within our cohort, as shown in Figure 3.3, a significantly lower proportion of $CD8^+$ T cells were observed in the HIV-positive cohort (HIV-negative vs HIV-positive; median: 2.12% vs 1.25%; $p \leq 0.05$), which may reflect reduced cytotoxic activity in the TME.

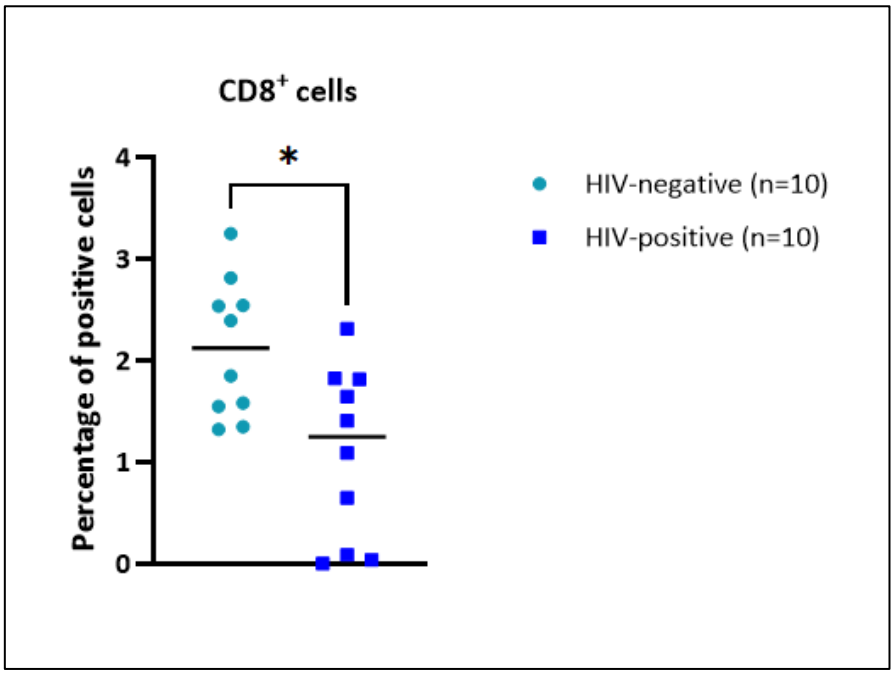

Figure 3.3: Percentage of CD8-positive cells in HIV-negative and HIV-positive DLBCL tissues. FFPE tissues were stained using a CD8 antibody to detect cytotoxic T cells. Individual data points represent the percentage of positively stained cells in each case, with the centre line indicating the median. Statistical analysis was performed using GraphPad Prism version 9 (Mann-Whitney U test; *$p \leq 0.05$).

3.3.2.2 TAM infiltration

Macrophages are an important member of the innate immune system, regulating homeostasis by engulfing microorganisms and clearing out diseased and damaged cells (231). Furthermore, macrophages are capable of infiltrating tumours to become part of the TME (TAMs) where they affect cancer progression; with M1-like TAMs exhibiting anti-tumour activity and M2-like TAMs being associated with pro-tumour properties (232) (233). While a high density of the latter group has been associated with an unfavourable outcome in DLBCL, the role of TAMs in the advancement of DLBCL remains unclear (234). Upon differentiation, macrophages are reported to be vulnerable to HIV-1 infection and serve as reservoirs due to the fact that they are long-lived and resistant to structural changes following infection (235, 236). CD68, a marker for all TAMs, was used to detect the infiltration

of TAMs within the tumours of our DLBCL samples. As shown in Figure 3.4, a significantly higher proportion of $CD68^+$ TAMs were observed in HIV-positive DLBCL tumours (HIV-negative vs HIV-positive; median: 1.56% vs 2.69%; $p \leq 0.05$).

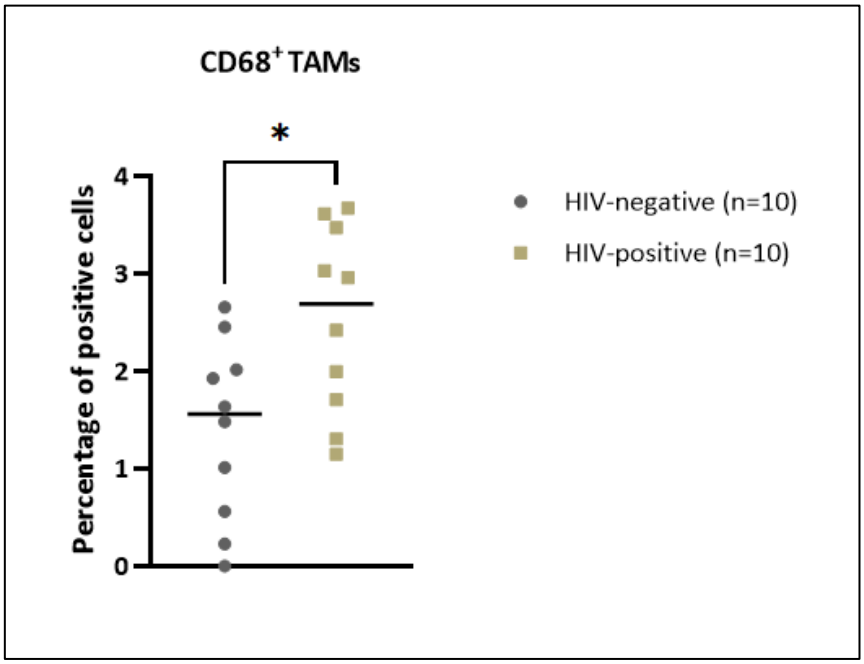

Figure 3.4: Percentage of TAMs in HIV-negative and HIV-positive DLBCL tissues. FFPE tissues were stained using a CD68 antibody to detect TAMs. Individual data points represent the percentage of positively stained cells in each case, with the centre line indicating the median. Statistical analysis was performed using GraphPad Prism version 9 (Mann-Whitney U test; *$p \leq 0.05$).

3.3.2.3 PD-L1-positivity

In the TME, PD-L1 engages with the PD-1 receptor on T cells to promote tumour immune evasion. As mentioned previously, PD-L1 can be expressed on tumour cells and several other immune cell types, including macrophages, fibroblasts and dendritic cells, within the TME (108). In DLBCL, positivity for PD-L1 expression is reported to be associated with poor clinical outcomes (210). The impact of HIV on PD-L1 status within the DLBCL TME remains largely understudied. Since PD-L1 is expressed on multiple cell types within the TME, overall PD-L1 expression was assessed which showed a significantly higher overall expression within the HIV-positive DLBCL tumours (HIV-negative vs HIV-positive; median: 0.09% vs 0.47%; $p \leq 0.05$) (Figure 3.5).

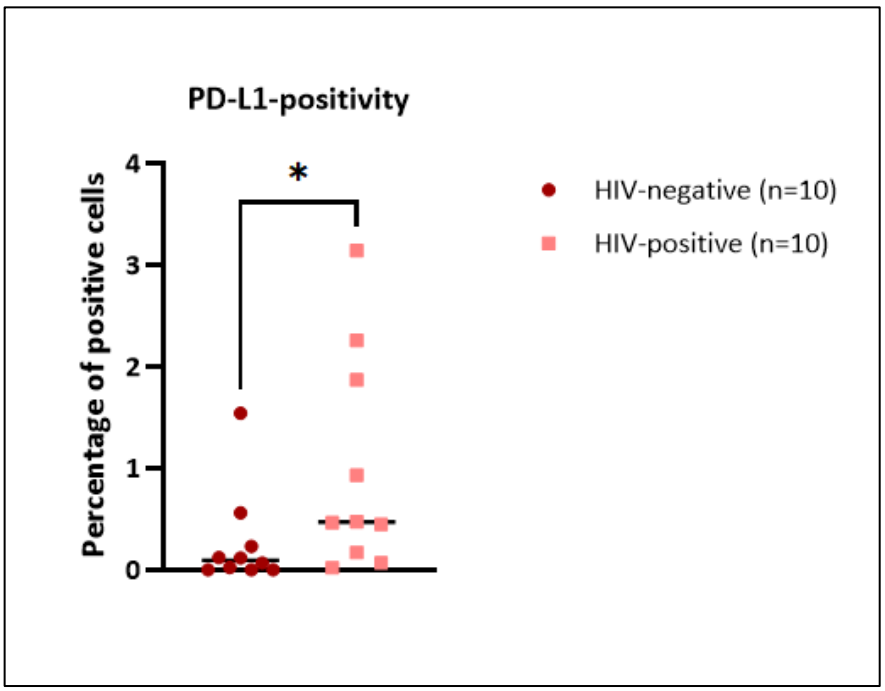

Figure 3.5: Percentage of PD-L1-positive cells in HIV-negative and HIV-positive DLBCL tissues. FFPE tissues were stained using a PD-L1 antibody to assess the status of PD-L1. Individual data points represent the percentage of positively stained cells in each case, with the centre line indicating the median. Statistical analysis was performed using GraphPad Prism version 9 (Mann-Whitney U test; *p ≤ 0.05).

3.4 Discussion

The TME is a complex niche surrounding a tumour and is typically comprised of (i) non-cellular elements such as the ECM and growth factors, and (ii) cellular elements such as tumour and non-malignant cells (237). The TME plays a pivotal role in the initiation and progression of cancer, by regulating and promoting the function and survival of tumour cells (238). In addition to creating a "favourable" environment for tumour growth, the TME has also been implicated in remodelling itself to facilitate resistance to treatment (239). Since interactions within the TME affect several aspects of tumour biology, reprogramming the TME has emerged as a promising therapeutic target to suppress tumour development, improve the efficacy of treatment and overcome drug resistance (240, 241). Furthermore, several immunotherapeutic strategies targeting components of the TME have been explored (242), but have proven to be challenging due to the highly complex nature of the TME, and thus a deeper knowledge of the TME dynamics is key to understanding how tumour growth is influenced (241, 243).

The majority of cells within the TME of DLBCL are tumour cells and several studies have reported on the infiltration of cellular components exerting either pro- and/or anti-tumorigenic properties. These cells include T cells, TAMs, tumour-associated neutrophils, NK cells and myeloid-derived suppressor cells (MDSCs) (234, 244, 245, 246, 247, 248). As mentioned, DLBCL is a highly heterogenous at the

biological and clinical levels, and the diversity of non-malignant cell types observed in TME is a contributor to the heterogeneity of this disease (249). This was demonstrated by Wright and colleagues who recently identified 3 TME categories of DLBCL, based on their microenvironmental composition: (i) immune-deficient, (ii) dendritic cell-enriched and (iii) macrophage-enriched (250). This heterogeneity further emphasizes the need for a greater understanding of the TME, specifically within an HIV positive context, which is a co-factor of DLBCL (249). Interactions between tumour cells and the TME is reported to contribute to immune evasion in DLBCL (208), and as mentioned earlier, loss of MHC molecules and PD-L1 expression is implicated in the immune escape of DLBCL cells (251). As discussed in chapter 1, in a healthy setting, the PD-1/PD-L1 axis dampens the hyperactivation of T cells and protects against autoimmunity (252), and by hijacking this axis, tumour cells evade immune recognition by impairing T cell functioning (109). While PD-1/PD-L1 blockade has achieved success in other cancers, especially cHL, the results remain suboptimal in DLBCL (253), warranting further investigation into the significance of PD-L1 in the DLBCL TME.

Our study, which we have classified as a small-scale study, assessed a total of 20 tumours, of which half were HIV-associated. The samples were chosen purely based on availability for the intended research (convenience sampling), which may constitute a limitation in terms of accuracy of the observations made. Nevertheless, some notable and interesting observations were made.

As expected, the percentage of $CD4^+$ cells were significantly reduced in HIV-positive DLBCL tumours, compared to the HIV-negative group, since these cells are the primary target of HIV. The finding correlates with the data obtained from the medical records of patients, despite 60% (n=6) being on ARTs. In an HIV-uninfected setting, $CD4^+$ T cells are crucial in modulating the activation of several immune cell types, including cytotoxic $CD8^+$ T cell responses, and maintaining a regulated and effective immune response against invading pathogens and tumour cells. In the context of HIV-infection, $CD4^+$ T cells have two roles: (i) to produce HIV virions when infected and (ii) to activate immune responses when they are uninfected (254). By infecting and reducing this population of cells, HIV is directly involved in the development of tumours and contributes to defects in immunosurveillance (165). Given the crucial function of $CD4^+$ T cells in the anti-tumour response, a depletion of $CD4^+$ T cells results in limited activity of $CD8^+$ T cells, and thus negatively impacts the anti-tumour response (255). Kusano and colleagues conducted a retrospective review of 355 DLBCL patients' medical records, after treatment was implemented, and found that a low absolute CD4 count was associated with a poor survival rate in DLBCL patients (255). While reports indicate that the survival outcomes of HIV-positive DLBCL patients on ART, and thus have had immune reconstitution, are comparable to that of HIV-negative DLBCL patients (256, 257), the same is not consistently observed in our local setting. In low socio-economic settings, such as within peri-urban and rural communities in South Africa, late

implementation of ART along with a delayed diagnosis of HIV-associated cancers remain common (82). This may therefore explain the poor survival outcomes of HIV-positive DLBCL patients at our local public hospitals. This may also explain why the CD4 counts of our HIV-positive cohort remained low, despite 60% being on ARTs. While ART suppresses viral replication which in turn replenishes $CD4^+$ T cells, it has been reported that a subset of patients who commence with ART at a very low CD4 count, may not experience normalization of their CD4 counts for up to 10 years after starting treatment (258). The risk of a suboptimal response was reported to be dependent on factors such as nadir CD4 counts prior to therapy, age as well as the extent of immunosuppression (258, 259). Additionally, within the sites where our patients are recruited, it is not uncommon that patients get diagnosed as HIV positive during the process of diagnosing their cancer.

A lower overall proportion of $CD8^+$ T cells was observed in the HIV-positive DLBCL group within our study sample. NHLs are reported to be characterized by the infiltration of activated $CD8^+$ cells and in DLBCL specifically, they account for the majority of tumour-infiltrating T cells (245). The infiltration and number of $CD8^+$ T cells in DLBCL has also been associated prognosis, whereby less $CD8^+$ T infiltration is correlated to a poorer response to treatment and outcome (260). As mentioned above, $CD4^+$ T cells are involved in stimulating and activating $CD8^+$ T cells which can be via several mechanisms: (i) by expanding $CD8^+$ T cells during primary immune response and establishing memory cells, (ii) by maintaining the survival of $CD8^+$ T cells during chronic infections, and (iii) by facilitating the localization of $CD8^+$ T cells to sites of infection (261). In the context of HIV-infection, HIV indirectly impairs the maturation of $CD8^+$ T cells by targeting and affecting $CD4^+$ T cells, leading to a reduction in their numbers and impairing their functioning (262). Previously published studies examining the TME of HIV-positive and HIV-negative DLBCLs have reported that in addition to having more angiogenic markers, HIV-positive DLBCLs also exhibit less $CD4^+$ and more $CD8^+$ T cells (221, 230). Additionally, a higher density of $CD8^+$ cytotoxic T cells in HIV-positive DLBCLs was correlated to an improved patient outcome (222). An increase and expansion of $CD8^+$ T cells takes place during the early stages on HIV-infection; however, contrasting to other viral infections where levels of $CD8^+$ T cells reduce as the infection clears, $CD8^+$ T cells remain elevated during HIV-infection (263). A majority of these cells are in a hyporesponsive state, otherwise known as T cell exhaustion, which can be promoted by PD-L1 expression (264). Interestingly, a recent study also reported on the effect of ART on T cell response in a cohort of HIV-positive DLBCL patients in Malawi (265). The authors found that the percentage of $CD8^+$ T cells were elevated in the TME of DLBCL cases that were HIV-positive. HIV-positive DLBCL cases were further stratified according to ART exposure, where patients were either classified as ART-naïve or ART-experienced depending on whether they have been on ARTs for less than or more than 6 months, respectively. They reported that $CD8^+$ T cells were even higher in patients who were

prescribed ARTs for less than 6 months (ART- naïve), compared to HIV-negative DLBCL patients. In most of the above-mentioned studies, the majority of HIV-positive DLBCL patients were on ARTs, and thus had restored $CD4^+$ T cell levels, which in turn may have impacted on the $CD8^+$ T cell population. In our cohort of HIV-positive DLBCL patients, the average CD4 count was low (<500 cells/mm^3), which ultimately maintained a low proportion of $CD8^+$ T cells across all HIV-positive patients. In addition, we observed increased PD-L1-positivity and together with the reduced $CD8^+$ T cells, relates to T cell exhaustion, a common factor associated with HIV-infection. The loss of T cell function as a result of T cell exhaustion, promoted by PD-L1, would ultimately lead to the depletion of these cells (266, 267).

It is noteworthy to mention that a separate study conducted in our laboratory which evaluated the proportion of immune cell populations, including $CD8^+$ T cells, in the peripheral blood of newly diagnosed DLBCL patients who were HIV-negative or HIV-positive found that this subpopulation of T cells was increased in the blood of the HIV-positive group (141). While the patients included for analysis in Ramorola's study and this present study do not overlap, both studies included patients recruited from the same site in Cape Town. However, since peripheral blood and TME are two exclusive biological entities, they are not expected to reflect the same trends. Taking into account the findings from this study as well as the observation by Ramorola, the results suggest that in HIV-positive DLBCL patients, there are increased $CD8^+$ T cells circulating in the peripheral blood, which could be due to the continuous antigen stimulation by HIV (141); whereas in the TME, where $CD8^+$ T cells would typically exert their cytotoxic activities, their functions and numbers are dampened, especially within an immune supressed state (i.e., low CD4 count). Thus, low infiltration of $CD8^+$ T cells in the TME likely contributes to the inferior outcome generally seen within this patient group within our setting.

In DLBCL, infiltration by TAMs within the TME has been correlated with prognosis, although the current published studies are conflicting, with some reporting poor prognostic outcomes associated with high $CD68^+$ TAM infiltration in the TME (268, 269, 270), while others report the opposite (271, 272). A recent study has also reported no association between both T cells and $CD68^+$ macrophages in the TME with overall survival in DLBCL patients (273). By retrospectively analysing DLBCL FFPE tissues using IHC, Ghorab and colleagues reported that neither high nor low expression of $CD4^+$ T cells, $CD8^+$ T cells and $CD68^+$ TAMs had an impact on the overall survival of DLBCL patients (273). Our study found increased proportion of $CD68^+$ TAMs in HIV-positive DLBCL tumours, compared to the HIV-negative group. This is in line with a previous report by Chao and colleagues where it was demonstrated that increased $CD68^+$ TAMs, along with a lower $CD4^+$ T cell count, is associated with HIV-positive DLBCL tumours, and poor prognosis (222). Because of the findings uncovered in this study, a future prospect should seek to stratify TAMs into M1- and M2-types and establish the status of PD-L1 within these two populations. This may provide insight and guide TAM-targeting strategies. As mentioned, the TME

of HIV-positive DLBCL is highly angiogenic with an increased microvessel density (165). In future studies, it would be worthwhile for us to explore and compare the expression of angiogenic markers within our cohort.

The overall percentage of cells positive for PD-L1 expression was significantly elevated within our HIV-positive DLBCL cohort, compared to the HIV-negative group. Within the TME, PD-L1 can be expressed by several different cell types, with macrophages being the primary cell type (274). In the present study, total PD-L1 positivity was assessed without considering the cell type on which it is expressed. Therefore, the increase in PD-L1-positivity observed in HIV-positive DLBCLs could be expressed by malignant or non-malignant cells in the TME. To date, only a few studies have reported on this, especially within an African cohort of patients. The available reports examining the TME of DLBCL indicate that high PD-L1 expression correlates with aggressive disease features and a poor response to therapy (275, 276). PD-L1 can be expressed on several cell types, including macrophages, APCs as well as tumour cells. Therefore, the elevated proportion of PD-L1^{+} cells in HIV-positive DLBCL tumours is a direct indication of enhanced immune evasion in this particular disease and explains the aggressive characteristics and poor outcomes associated with HIV-positive DLBCL. Recently, the microenvironment of HIV-associated DLBCL was assessed by performing single cell sequencing (277), where it was revealed that HIV-positive DLBCLs have higher expression levels of PD-L1 and that patients with this disease were at a higher risk of T-cell exhaustion. Interestingly, PD-L1 has been associated with promoting angiogenesis in several cancer types (278, 279, 280). For example, PD-L1 protein expression was shown to positively correlate with VEGF expression in glioma (278). In addition, PD-L1 was reported to promote angiogenesis via the c-JUN/VEGFR2 signalling axis in ovarian cancer (280). While such a correlation has not been described in DLBCL, it is plausible given the higher macrophage density observed within the HIV-positive DLBCL cohort in this study. This emphasizes the varied and acute role of PD-L1 in the TME, which includes dampening T cell activity and promoting angiogenesis, ultimately favouring tumour progression. As discussed in Chapter 1, DLBCLs that are positive for PD-L1 expression are often associated with EBV-infection. In the current cohort, only two cases were EBV-positive, and both were HIV-positive. However, due to this low number, an assessment of the influence of EBV within this cohort could not be made.

For interest, an analysis of correlation between cell populations within each group (HIV-positive DLBCL and HIV-uninfected DLBCL) was made, and this data is shown in supplementary Figures 1A and B. While no clear trend was seen within the HIV-negative group, in the HIV-positive DLBCL cohort, six out of ten HIV-positive DLBCLs showed an inverse association between CD8^{+} T cells and PD-L1-positivity (cases 4, 5, 7, 8, 9 10). Although this potential inverse association is suggested by Figures 3.3 and 3.5, the trend is more evident when looking at the cell populations grouped within a particular region of

the same tissue case, as shown in supplementary Figure 1B. The elevated status of PD-L1 in the HIV-positive DLBCL TME, coupled with a reduced number of $CD8^+$ T cells suggests that PD-L1 may be directly suppressing the anti-tumour effects of $CD8^+$ T cells, through engagement with PD-1, and this increase in PD-L1 expression could possibly be facilitated by HIV-infection. Since PD-L1 plays a pro-tumorigenic role by dampening the immune response, and $CD8^+$ T cells are essential for their cytotoxic activity, it is highly plausible that this inverse correlation may reflect the exhausted state of $CD8^+$ T cells. An inverse correlation between PD-L1 and $CD8^+$ T cells has been reported in several cancer types, including ovarian cancer, oesophageal squamous cell cancer and cervical adenocarcinoma (281, 282, 283, 284). As mentioned, there is a scarcity of studies exploring the status of PD-L1, in an HIV-positive DLBCL TME. In primary DLBCL of the central nervous system (PCNS DLBCL), Kim and colleagues reported that elevated expression of PD-L1 in the TME and a low number of $CD8^+$ T cells, predicted a poor prognostic outcome (285). Interestingly, high expression of PD-1 on $CD8^+$ T cells and PD-L1 on macrophages and T cells in the TME were reported to be associated with a poor survival in DLBCL patients after treatment with R-CHOP, suggesting that these mechanisms are involved in chemotherapeutic resistance and may be appealing targets for blockade of the PD-1/PD-L1 pathway in DLBCL patients with relapse or refractory disease (286).

With this being a pilot study, the primary limitation is the sample size. Nevertheless, the findings revealed some pertinent and unique TME biological workings within an HIV positive context, specifically in the absence of immune reconstitution, which aligns with the more severe phenotype of the disease seen in this patient group. A future study, including a larger sample size, is therefore warranted, which will include additional investigations, such as the role of EBV, the status of angiogenic markers, as well as a comprehensive analysis of the impact of CD4 counts.

Chapter 4

The regulation of PD-L1 in DLBCL

4.1 Introduction

In DLBCL, mutations in genes influencing the immune status are frequent, with over 70% of DLBCLs containing genetic alterations in immune evasion-related genes (251, 287). As discussed in Chapter 1 (section 1.5.3), PD-L1 is overexpressed in a subset of DLBCL cases, more commonly those assigned to the ABC subtype, which is associated with aggressive disease and inferior survival (288, 289). This alteration in expression is caused by the 9p24.1 chromosomal alterations (although at a much lower frequency than in other lymphomas such as cHL), as well as by other regulatory mechanisms at the epigenetic, transcriptional and post-transcriptional levels (110, 290, 291). Clinical trials exploring the benefit of therapeutic blockade of the PD-1/PD-L1 axis demonstrated a moderate overall response in DLBCL, which is has been attributed to the highly heterogenous nature of the disease - at the genetic level, at least five distinct molecular clusters have been described (39, 41), and the pathobiology of DLBCL within an HIV positive context remains largely undefined. While several mechanisms contributing to the dysregulation of PD-L1 in DLBCL have been explored; to date, the collective data provides only a limited insight into this regulation. The current present study sought to delineate some of the common factors involved in the pathogenesis of DLBCL, namely EBV (in particular, EBNA2), HIV and c-MYC, in the regulation of PD-L1.

c-MYC is a well-established oncogene in DLBCL, and its aberrant levels are attributed to alterations at multiple levels, including epigenetically, at the transcriptional and post-transcriptional levels, as well as by gene translocations and amplifications (242). *c-MYC* gene translocations are observed in roughly 10% of DLBCL cases, while overexpression of the MYC protein is observed in approximately 40% of cases (46). This oncogenic transcription factor is known to regulate a large range of factors in the oncogenic process, including PD-L1. Indeed, the relationship between c-MYC and PD-L1 has been described in various cancers such as acute lymphoblastic leukaemia, liver cancer, oesophageal squamous cell carcinoma, non-small cell lung cancer and human pancreatic ductal adenocarcinoma (292, 293, 294, 295). By performing chromatin immunoprecipitation (ChIP) sequencing analysis using a mouse model of MYC-induced T cell acute lymphoblastoid leukaemia (T-ALL), Casey and colleagues demonstrated direct binding of c-MYC to the *PD-L1* promoter, resulting in upregulation of the oncogene (292). To date, only one E-box element (binding site for c-MYC) has been reported in the *PD-L1* promoter, within region -164bp to -159bp, in a study involving Triple Negative Breast Cancer

(TBNC), where the site showed occupancy of c-MYC, enhanced by Mucin 1 (MUC1-C), to elevate transcription of PD-L1 (296). Furthermore, Maeda and colleagues demonstrated that c-MYC was recruited to the PD-L1 promoter by MUC1-C. In DLBCL, reports on the regulation of PD-L1 by c-MYC are few, and the relationship between c-MYC and PD-L1 in this cancer remains unclear and even contradictory. While one report indicated a positive correlation between c-MYC and PD-L1 levels in DLBCL cell lines (297), others demonstrated that there is no association in DLBCL cell lines and patients (298, 299). Contrasting to this, some studies have reported on an inverse correlation between c-MYC and PD-L1 levels in cohorts of DLBCL patients (242, 300). This evidently unclear relationship between c-MYC and PD-L1 could be explained by the complex and genetically heterogenous nature of DLBCL, as well as its association with pathogenic factors and infectious agents, including EBV and HIV, which are the most common.

In developing countries, EBV is prevalent in early-life infections, in comparison to developed countries where EBV-infection is typically delayed into post-adolescence (301). In DLBCL, infection with EBV is observed in up to 15% of tumours, with the proportion being higher in Asian and Latin American counties, compared to Western countries (151, 302, 303). While there are limited data on the prevalence of EBV in DLBCL within the sub-Saharan African region, a recent retrospective study conducted in Rwanda evaluated the incidence of EBV in several subtypes of lymphoma diagnosed over a 5-year period and reported that 11% of DLBCL cases were EBV-positive (304). Within our local setting, Cassim et al. retrospectively evaluated 131 DLBCL patient tissue specimens and reported that 7% of cases were EBV-positive (82), and as shown in Chapter 2, 9% of newly diagnosed DLBCL patients recruited in our study were positive for EBV in their tumours. Furthermore, the frequency of EBV-infection is higher in HIV-positive DLBCL relative to HIV-negative DLBCL, a trend demonstrated by this study as well as the study by Cassim and colleagues. EBV is a potent driver of B cell transformation, associated with not only the development of DLBCL (60), but also the progression of disease (303). For instance, GEP has revealed that EBV-positive DLBCL displayed enrichment in NF-kB signalling and pathways associated with cell cycle progression and proliferation, in comparison to EBV-negative DLBCL tumours (305). Additionally, in DLBCL, EBV contributes to the evasion of B cells from immune recognition, partly due to PD-L1 expression (306).

Recent studies have revealed that the EBV protein, Epstein Barr virus Nuclear Antigen 2 (EBNA2), is responsible for PD-L1 upregulation in both primary B cells and DLBCL cells (124, 125). Yanagi et al. (2021) showed marked elevated expression of PD-L1 in primary B cells infected with wild-type EBV, and alleviation of this upregulation when using an EBNA2-knockout mutant virus (124). Additionally, they also identified binding sites bound by EBNA2 within the *PD-L1* promoter region, responsible for

mediating this expression. Anastasiadou and colleagues (2019) revealed that EBV, through EBNA2, increases PD-L1 expression by downregulating the cellular microRNA miR-34a, the latter being an inhibitor of PD-L1 expression. They showed that EBNA2 recruits the transcription factor Early B cell factor 1 (EBF-1) to the promoter of miR-34a, resulting in its downregulation, which in turns leads to an increase in *PD-L1* expression. EBNA2 is crucial for the transformation of B cells by EBV and is also a potent activator of c-MYC (125).

While HIV-infection is associated with increased PD-L1 expression (183, 307), the mechanism involved remains largely undefined, and the role that important and established oncogenic factors, such as c-MYC and EBV, may be playing in mediating this deregulation, is even more obscure. For instance, while EBNA2 has been reported to activate the HIV-1 long terminal repeat (LTR) (308), the influence of EBNA2 in the regulation of PD-L1 by HIV, remains unknown.

This final aspect of the study employed a diverse approach to try and unravel the seemingly complex and largely undefined role and regulation of PD-L1 in DLBCL, within an environment where HIV infection is prevalent. The approaches involved in silico analyses, as well as molecular assays, to attempt to define firstly, the status of PD-L1 in DLBCL in association with c-MYC, and secondly, how DLBCL co-factors such as EBV, particularly EBNA2, and HIV may affect the status of PD-L1 in the disease.

4.2 Methods

4.2.1 In silico analyses

4.2.1.1 Transcriptome-based analysis of DLBCL datasets extracted from TCGA

Publicly available DLBCL datasets, comprising of clinical and transcriptome data, were retrieved from The Cancer Genome Atlas (TCGA) to perform an integrated and comprehensive analysis on *PD-L1* (*CD274*) expression in DLBCL, its effect on survival outcomes and the correlation with *c-MYC.*

4.2.1.1.1 Comparison of PD-L1 expression across DLBCL subtypes

To determine if there were significant differences in *PD-L1 (CD274)* expression levels among different subtypes of DLBCL datasets (n=48), a one-way Analysis of Variance (ANOVA) was conducted. The subtypes analysed were ABC (n=15), GCB (n=22) and Unclassified (UC) (n=11). *CD274* expression data was log-transformed to stabilise variance and meet the assumptions of ANOVA, and the data was then categorised according to the three DLBCL subtypes. ANOVA was performed to compare the mean *CD274* expression levels across these subtypes.

4.2.1.1.2 Survival analysis

To perform survival estimate analysis, the datasets were stratified into low-*CD274* and high-*CD274* expression groups based on the median *CD274* expression level. The Kaplan-Meier method was used to estimate survival distributions, and the log-rank test assessed the statistical significance of differences between the low and high *CD274* expression groups.

4.2.1.1.3 Correlation analysis

To investigate the relationship between *CD274* and *MYC* expression levels in different subtypes of DLBCL, correlation analyses were performed. In this particular analysis, one outlier dataset was removed (n=47) which did not affect the results in any way, but allowed for clear assumptions to be drawn as the data became less skewed. Pearson correlation coefficients were calculated to assess the linear relationship between *CD274* and *MYC* expression within ABC (n=14), GCB (n=22), and UC (n=11) subtypes.

4.2.1.2 Correlation between c-MYC and PD-L1 in DLBCL cell lines

Using The Human Protein Atlas (https://www.proteinatlas.org/), the expression levels of *PD-L1* and *c-MYC* was assessed in DLBCL cell lines. Each gene of interest was searched within the database and "lymphoma" cell lines were selected. Cell lines were filtered to assess only those that were specifically DLBCLs and the normalized transcript per million (nTPM) value for each gene in each DLBCL cell line was recorded for further analysis.

4.2.1.3 PD-L1 promoter analysis

The *PD-L1* promoter sequence (~2500 bp upstream of the TSS) was extracted from Ensembl (https://www.ensembl.org/index.html) and used in the PROMO online tool (https://alggen.lsi.upc.es/cgi-bin/promo_v3/promo/promoinit.cgi?dirDB=TF_8.3) to identify potential E-box motifs. A dissimilarity rate of 15% was applied.

4.2.2 DLBCL Cell lines

The OCI-LY1 and WSU-DLCL2 established DLBCL cell lines were kindly donated by Professor Bjoern Chapuy (Charité Universitätsmedizin, Berlin), while the HBL-1 and SU-DHL-4 cell lines were kindly donated by Professor Dave Sandeep (Duke University, USA). The U2932 parental and two EBNA2-expressing clones (CL1 and CLW) were kindly donated by Professor Pankaj Trivedi (Sapienza University of Rome, Italy) (309).

4.2.2.1. Culture conditions

The U2932, SU-DHL-4, HBL-1 and WSU-DLCL2 cells were maintained in Roswell Park Memorial Institute (RPMI-1640) (Sigma-Aldrich, USA) base medium, and the OCI-LY1 cell line was maintained in

Iscove's Modified Dulbecco's Medium (IMDM) (Sigma Aldrich, USA) base medium, and in all cases supplemented with 10% Fetal Bovine Serum (FBS) (ThermoFisher Scientific, USA) and 1% Penicillin/Streptomycin (P/S) (Sigma Aldrich, USA). The EBNA2-expressing U2932 clones (U2932-EBNA2-CL1 and -EBNA2-CLW) were maintained in RPMI, 10% FBS and 1% P/S, supplemented with 10ug/ml hypoxanthine (Sigma Aldrich, USA), 160ug/ml xanthine (Sigma Aldrich, USA) and 1.5ug/ml mycophenolic acid (Sigma Aldrich, USA). Culture flasks were incubated at 37°C in a humidified incubator supplemented with 5% CO_2 (Nuaire IR Direct Heat CO_2 Incubator).

For Tissue Culture Infectious Dose 50 ($TCID_{50}$) experiments, HEK293FT and TZM-bl cells were maintained in Dulbecco's Modified Eagle's Medium (DMEM) (Sigma-Aldrich, USA) supplemented with 10% FBS and 1% P/S.

All cell lines were routinely tested for Mycoplasma contamination. To do this, cells were grown in P/S free media (RPMI and 10% FBS) for 2 to 3 days, and then fixed on a microscope slide and stained with Hoechst 33342 stain (Sigma Aldrich, USA). The cells were visualized using a fluorescent microscope at 40X magnification.

4.2.3 HIV-1 Pseudovirus production

4.2.3.1 Transfection of HEK293FT cells

The plasmid constructs and protocol required to produce HIV-1 pseudoviruses (pvHIV-1) were kindly donated by Professor Zenda Woodman (Division of Medical Biochemistry & Structural Biology, UCT). These included the HIV backbone vector, pNL4-3.Luc.R-E-, and the gp160 envelope-expressing vector. A total of 1 x 10^6 HEK239FT cells were plated, and 16 hours later the cells were co-transfected with the two plasmids, using Lipofectamine LTX (ThermoFisher Scientific, USA). The medium containing viral particles was harvested at 48- and 72-hour time points post-transfection and pooled. After harvesting, the medium containing viral particles was centrifuged at 2000 rpm for 5 minutes at room temperature to remove cellular debris. The supernatant was filtered through a 0.45uM membrane into a separate tube, after which aliquots were prepared and stored at -80˚ C. For use as a negative control, a mock transfection was performed alongside the above, where only transfection reagent was used, and no plasmid constructs.

4.2.3.2 Tissue culture infectious dose 50 assay

To estimate the titre for the generated pseudoviruses, the tissue culture infectious dose 50 ($TCID_{50}$) assay was employed. In this fluorescent-based assay, 1 x 10^4 TZM-bl cells (kindly donated by Professor Zenda Woodman (Division of Medical Biochemistry & Structural Biology, UCT)) were plated 16 hours prior to infecting with various dilutions of pvHIV-1. At 48 hours post-infection, cells were lysed using

BrightGlo reagent (Brightglo Luciferase Assay System, Promega, USA) and the samples were analysed using the Glo-Max®-Multi+ multiplate reader (Promega, USA). The $TCID_{50}$ was calculated according to the method described by Reed and Muench (310).

4.2.4 Exposure of DLBCL cells to HIV-1

U2932 (parent clone) and two EBNA2-expressing U2932 clones (CL1 and CLW) were plated at a density of 4.8 x 10^5 cells/mL in 6-well cell culture dishes, in low-serum (0.5% FBS) medium. Approximately 16 hours post-plating, cells were exposed to HIV-1 or control for a period of 24 hours, following which both total protein and RNA were extracted. Two types of HIV-1 were used, independently, in this assay. This included the Aldrithiol-2-Inactivated HIV-1 (AT-2 HIV-1), paired with its microvessicle control (MV) (311). AT-2 is a mild oxidizing reagent which eliminates the infectivity of HIV (rendering it safe to manipulate under Biosafety level 2 (BSL-2) conditions), while maintaining the structural and functional integrity of the viral envelop, and ability to interact with cell surface receptors. AT-2 HIV-1 and MV particles were kindly donated by Professor Jeff Lifson (NIH, Maryland, USA) and Dr Wendy Burgers (Division of Medical Virology, Department of pathology, UCT). For all assays with AT-2 HIV-1, 500ng/ml of were used and an equivalent amount of MV control. This concentration was determined as optimal based on our previous study (312). The second type of HIV-1 particle was HIV-1 pseudovirus (pvHIV-1). Pseudotyped viruses are produced by co-transfecting an envelope-expressing vector and an envelope-deficient vector which allows for entry into a cell, but there is no replication potential and the pseudoviruses can therefore be safely handled under BSL2 conditions (313). The procedure to produce pvHIV-1 is described in section 4.3.2.1. above. An equal number of cells for each cell line was exposed to 124 $TCID_{50}$/ml of pvHIV-1 and an equal volume of media from the mock transfection to serve as controls.

4.2.5 Total soluble protein extraction and quantification

4.2.5.1 Extraction using RIPA.

Cells were transferred into centrifuge tubes and pelleted via centrifugation for 5 minutes at 1000 rpm, the pellets washed twice using cold 1X PBS (Appendix B), followed by resuspension in Radio-Immunoprecipitation Assay (RIPA) extraction solution (0.1% SDS) (Appendix B). The extracts were frozen at -80^{0}C overnight (O/N) to optimized cell lysis, followed by centrifugation at 12 000 rpm for 20 minutes at 4^{0}C to remove cell debris. The supernatant, representing soluble total protein, was stored at -80°C in aliquots. This method was used to extract protein from the U2932 panel of cells, both unexposed and AT-2 HIV-1-exposed, as well as OCI-LY1, WSU-DLCL2, SU-DHL-4 and HBL-1.

4.2.5.2 Extraction using commercial kit

Since a limited amount of pvHIV-1 was produced, a commercial kit was used to extract total protein from cells treated with pvHIV-1, which allowed for simultaneous total RNA extraction (The AllPrep DNA/RNA/Protein mini kit (Qiagen, Germany)). The procedure was followed according to the manufacturer's instructions. Briefly, cells were pelleted and homogenized using a 21-gauge needle lysed in RLT buffer containing β-mercaptoethanol. The lysate was passed through the provided AllPrep DNA spin column and the flowthrough was used for RNA isolation. 100% Ethanol was added to the lysate and the sample passed through a provided RNeasy spin column. After centrifugation at 10 000 rpm for 15 seconds, the RNeasy spin column was kept aside for RNA isolation, and the flowthrough was collected and as per manufacturer's instructions. An equal volume of Buffer APP was added to the flowthrough followed by incubation for 10 minutes at room temperature to precipitate the protein. Thereafter, the samples were centrifuged to pellet the protein, which was then washed in 70% ethanol being thoroughly air-dried. The protein pellet was dissolved in RIPA buffer (5% SDS) (Appendix B).

The Pierce™ Bicinchoninic acid (BCA) protein assay kit (ThermoFisher Scientific, USA) was used for protein quantification according to the manufacturer's instructions. Briefly, protein samples and BSA standards were diluted (1:5) and 10 µL aliquots were quantified in duplicate. 200 µL of working reagent was added to each sample in a 96-well plate. The plate was incubated at 37°C for 30 minutes, and the absorbance was thereafter measured at 560nm using the Glo-Max®-Multi+ multiplate reader (Promega, USA). The BSA standard curve was generated, and the protein concentrations were extrapolated.

4.2.6 Western blotting

4.2.6.1 Protein separation using SDS-PAGE

Protein samples were separated by molecular weight using sodium dodecyl sulphate-polyacrylamide gel electrophoresis (SDS-PAGE). The Mini-PROTEAN 3 system (Bio-Rad, USA) was used to prepare the electrophoresis gel which comprised of a 5% stacking gel and a 10-12% resolving gel.

Samples were prepared, as shown in Table 4.1.1. Thereafter, the samples were denatured at 95°C for 5-10 minutes, prior to loading. A prestained protein marker (ProteinTech, USA) was included in one of the lanes to allow for accurate identification of protein size. Samples were separated at 100V in 1X Running buffer (Appendix B) for approximately 2.5 hours.

Table 4.1.1: Preparation of samples for SDS-PAGE.

Component	Volume
Protein sample (20 – 40 µg)	X
5X SDS loading dye	4 µL
100mM DTT	1 µL
RIPA buffer	Up to 20 µL

SDS - sodium dodecyl sulphate; µg - microgram; DTT - Dithiothreitol; RIPA – Radioimmunoprecipitation assay; µL - microlitre

4.2.6.2. Protein transfer, antibody incubation and detection

Following electrophoresis, proteins were transferred onto a nitrocellulose membrane (Bio-Rad, USA) in 1X Transfer buffer (Appendix B), using Mini Trans-Blot® cell assembly (Bio-Rad, USA). The transfer was performed for 1.5 hours at 100V. After protein transfer, the membrane was incubated in blocking buffer made up of 5% fat-free milk in 1X TBS/0.1% Tween-20 (Appendix B) for 2 hours with gentle agitation. Thereafter, the membrane was washed with 1X TBS/0.1% Tween-20 (Appendix B) and incubated with primary antibody overnight at 4°C, with gentle agitation. The primary antibodies are listed in Table 4.1.2, along with the dilution used and appropriate secondary antibodies.

Table 4.1.2: Primary antibodies, dilutions and secondary antibodies used for western blotting.

Antibody	Dilution	Secondary antibody
PD-L1 (Cell Signaling, (E1L3N) 13684)	1:1000	1:3000 (Goat anti-rabbit)
EBNA2 (Novus Bio, (PE2) NBP2-50382)	1:250	1:3000 (Horse anti-mouse)
c-MYC (Abcam, (Y69) 32072)	1:1000	1:3000 (Goat anti-rabbit)
β-actin (Santa Cruz Biotechnology, sc-47778)	1:10 000	1:3000 (Horse anti-mouse)
p38 MAP Kinase (Sigma, M0800)	1:10 000	1:3000 (Goat anti-rabbit)

PD-L1 - Programmed Death-Ligand; EBNA2 - Epstein Barr Virus Nuclear Antigen 2

Following overnight incubation, the membrane was washed and incubated in the appropriate HRP-conjugated secondary antibody (as specified in Table 4.1.2) for 1 hour with gentle agitation at room temperature. The membrane was then washed and visualized by chemiluminescence using the Clarity™ Western ECL substrate (Bio-Rad, USA), in a 1:1 ratio. The membrane was exposed to X-ray film and thereafter transferred to developer and fixer solutions to visualize the protein signal. Densitometric analysis of the protein signal intensity was performed using ImageJ Version 1.54 software (NIH, USA) and protein expression levels was represented as a ratio of protein of interest/ loading control.

4.2.6.3 Membrane stripping for reprobing

The membrane was washed in 1X TBS/0.1% Tween-20 for 10 minutes and the bound antibodies were removed from the membrane by incubating in pre-heated stripping buffer (Appendix B) at 50°C for 30

minutes, with gentle agitation every 10 minutes. The membrane was then washed with 1X TBS/0.1% Tween-20 for two 10-minute cycles. The membranes were reprocessed for western blotting to detect the internal loading control, either p38 (Sigma, USA) or β-actin (Santa Cuz Biotechnology, USA).

4.2.7 RNA isolation and quantification

Prior to RNA isolation, all plasticware was treated with 0.1% diethyl pyrocarbonate (DEPC) (Sigma-Aldrich, USA) (Appendix B) overnight to inhibit nucleases, and thereafter autoclaved to remove ribonucleases (RNases).

The High Pure RNA Isolation Kit (Roche, Germany) was used to isolated total RNA from the U2932 panel of cells, both unexposed and AT-2 HIV-1-exposed, as well as OCI-LY1, WSU-DLCL2, SU-DHL-4 and HBL-1 cells. The protocol was carried out according to that of the manufacturer. Briefly, cultured cells were washed with 1X PBS (Appendix B) and centrifuged at 1500 rpm for 5 minutes. The pelleted cells were resuspended in 200 uL of 1X PBS. Cells were thereafter lysed by adding lysis buffer and the tubes were vortexed for 15 seconds. Cell lysates were then transferred to a High Pure filter column and collection tube (provided with the kit) and centrifuged for 15 seconds at 12 000rpm. The flowthrough was discarded, DNase I was added to the High Pure filters, and incubated for 15 minutes at room temperature. The filters were first washed with Wash buffer I, followed by Wash Buffer II. To ensure that all contaminants were removed, a second wash with wash buffer II was performed by centrifuging samples at maximum speed for 2 minutes. The RNA was eluted from the filters in approximately 70 uL of elution buffer and quantified using the NanoDrop™ ND-1000 (ThermoFisher Scientific™, USA). The RNA integrity was determined by 1.5% agarose gel electrophoresis (Appendix B). The RNA samples were aliquoted and stored at -80˚ C.

As mentioned in section 4.2.5.2, a limited amount of pvHIV-1 was produced, therefore a commercial kit was used to simultaneously harvest total protein and total RNA (AllPrep DNA/RNA/Protein mini kit (Qiagen, Germany)). The procedure was followed according to the manufacturer's instructions. Briefly, Buffer RW1 was passed through the RNeasy spin column (kept aside during protein isolation), followed by two washes with Buffer RPE. The RNA was eluted from the filter in RNase-Free-water and the quantified using the NanoDrop™ ND-1000 (ThermoFisher Scientific™, USA). The RNA integrity was determined as mentioned previously, aliquoted and stored at -80˚ C.

4.2.8 Reverse transcription and real-time qPCR

4.2.8.1 CDNA synthesis

The total RNA isolated from the cell lines was reverse transcribed using the iScript cDNA synthesis kit (Bio-Rad, USA). The protocol was performed according to the manufacturer's recommendations, using

1 µg of RNA (Table 4.2.1). Reagents were thawed on ice and once the components were mixed and centrifuged briefly, the reverse transcription reaction was performed according to the parameters listed in table 4.2.2. cDNA products were diluted with nuclease-free water and stored at -20˚ C.

Table 4.2.1: Reaction setup for reverse transcription using iScript cDNA synthesis kit.

Reagent	1X reaction	Final concentration
5X iScript reaction mix	4 µL	1X
iScript reverse transcriptase	1	U/µl
Nuclease-free water	Up to 20 µL	
RNA template (1µg)	X	50ng

µL - microlitre; ng - nanogram; U/µL - Units per microlitre.

Table 4.2.2: Cycling conditions for reverse transcription using iScript cDNA synthesis kit.

Step	Temperature	Duration (minutes)	Number of cycles
Initial priming	25˚C	5	1
Reverse transcription	42˚C	30	1
Inactivation	85˚C	5	1
Cool down	4˚C	Infinite	Infinite

°C - degrees Celsius

4.2.8.2 qPCR

To perform qPCR, the KAPA SYBR FAST universal kit (Roche, USA) was used. Primer sets for the genes of interest are listed Table 4.3.1 and the housekeeping gene, GAPDH, was used as an internal control. A mastermix was prepared for each gene assessed, according to the recommended protocol as shown in Table 4.3.2, accounting for 3 technical repeats of each template sample as well as a no-template control. To each corresponding PCR tube, 19 µL of mastermix was aliquoted and 1 µL of diluted cDNA (1:10) was added separately. The samples were placed in the Rotor-gene Q real-time PCR cycler (Qiagen, Germany), and the cycling parameters are listed in Table 4.3.3.

Table 4.3.1: Primer sequences used in qPCR.

Primer	Sequence	Melting temperature	Amplicon product size
PD-L1	Forward: 5'-GGAGATTAGATCCTGAGGAAAACCA-3' Reverse: 5'-AACGGAAGATGAATGTCAGTGCTA-3'	56˚C 56.3˚C	147 bp
c-MYC	Forward: 5'-CAGATCAGCAACAACC-3' Reverse: 5'-TGTGTGTTCGCCTCTTGAT-3'	55.7˚C 55.6˚C	76 bp

GAPDH	Forward: 5'-GAAGGCTGGGGCTCATTT-3' Reverse: 5'-CAGGAGGCATTGCTGATGAT-3'	55.4˚C 55.2˚C	138 bp

PD-L1 – Programmed Death-Ligand 1; GAPDH - Glyceraldehyde 3-phosphate dehydrogenase; ˚ C – degrees Celsius; bp – base pair

Table 4.3.2: qPCR reaction setup using KAPA SYB FAST universal kit.

Component	1X reaction	Final concentration
2X KAPA SYBR fast qPCR Universal MasterMix	10 µL	1X
10µM Forward Primer	0.4 µM	0.2 µM
10µM Reverse Primer	0.4 µM	0.2 µM
cDNA template	X	<20ng
Nuclease-free water	Up to 20 µL	

µL - microlitre; µM – micromolar; ng - nanogram; nM - nanomolar

Table 4.3.3: Cycling conditions set up for qPCR experiments.

Step	Temperature	Duration	Number of cycles
Pre-incubation	95˚C	3 min	1
Denaturation	95˚C	10 sec	40
Annealing	60˚C	20 sec	
Extension	72˚C	10 sec	
Cooling	40˚C	1 min	1

°C - degrees Celsius; min - minutes; sec - seconds

4.2.8.3 Data and statistical analyses

Amplification and melt curves were generated and assessed on the Rotor-gene Q series software (Qiagen, Germany). The threshold was manually set, and the data was exported. The comparative method (ΔΔCt) of relative quantification was used to measure the fold change in gene expression. GAPDH expression was used as the internal control. The $2^{-(\Delta\Delta Ct)}$ equation was used to calculate the fold induction and in U2932 EBNA2-expressing cells, data was normalized to the U2932 parental cells, while in HIV-1-exposed cells (AT-2 HIV-1 or pvHIV-1), data was normalized to the respective control (MV or mock). Statistical tests, such as an ordinary ANOVA test and two-tailed students t-test, were performed using GraphPad Prism version 9 (GraphPad Software, USA), and the cutoff for significance was considered to be $p \leq 0.05$.

4.2.8 Absolute quantification of gene expression

4.2.8.1 Generation of a standard curve

To generate standards for the standard curve, the GoTaq® Flexi DNA Polymerase kit (Promega, USA), was used to amplify regions within HBL-1 cDNA, using the primer sets listed in Table 4.3.1. PCR was

reactions were prepared according to the manufacturer's recommendations, as indicated in Table 4.4.1.

Table 4.4.1: PCR reaction set up for each primer set, using GoTaq® Flexi DNA Polymerase kit.

Component	1X reaction	Final concentration
5X Colourless GoTaq flexi buffer	5 µL	1X
25mM $MgCl_2$	3 µL	0.3 mM
10mM dNTP mix	0.5 µL	0.2 mM
10µM Forward primer	1 µL	0.4 µM
10µM Reverse primer	1 µL	0.4 µM
GoTaq G2 flexi DNA polymerase (5U/µl)	0.13 µL	1.25 U
cDNA template	1 µL	5ng
Nuclease free water	Up to 25 µL	

µL - microlitre; MgCl2 - Magnesium chloride; mM – millimolar; ng - nanogram; dNTP – deoxynucleotide triphosphate; U/µL – Units per microlitre; µM – micromolar

PCR reactions were performed according to the cycling conditions outlined in Table 4.4.2, and thereafter, 5 µL of PCR products were separated on a 1.5% agarose gel (Appendix B) by electrophoresis. The Quick-Load 100bp DNA ladder (New England Biolabs, USA) was added alongside the samples to confirm that the PCR amplicons were the correct size.

Table 4.4.2: Cycling conditions used for HBL-1 amplification using GoTaq® Flexi DNA Polymerase kit.

Step	Temperature	Duration	Number of cycles
Initial denaturation	95°C	5 min	1
Denaturation	95°C	30 sec	30 cycles
Annealing	53°C	30 sec	
Extension	72°C	30 sec	
Final extension	72°C	5 min	1
Cool down	10°C	Infinite	

°C - degrees Celsius; min - minutes; sec – seconds

4.2.8.3 Purification of PCR products

The GeneJET PCR purification kit (ThermoFisher Scientific™, USA) was used to purify the HBL-1 PCR products. All buffers were provided with the kit. Briefly, PCR products were incubated with an equal volume of Binding buffer and transferred onto the GeneJET purification columns. The columns were centrifuged at 14 000 rpm for 30 seconds and the flowthrough was discarded. The columns were washed with provided Wash buffer and centrifuged for 30 seconds. After discarding the flowthrough, the columns were centrifuged for another 1 minute to remove residual wash buffer. The DNA was

eluted in 50 µL nuclease-free water and samples were quantified using the NanoDrop™ ND-1000 (ThermoFisher Scientific™, USA). 10-fold serial dilutions of the PCR products were prepared to serve as standards.

qPCR was performed as described in section 4.2.8.2 for U2923, HBL-1, WSU-DLCL2, SU-DHL4 and OCI-LY1 cell lines, along with diluted standards. A standard curve was generated and used to determine the absolute expression in the specified cell lines.

4.2.8 Generation of CRISPR-Cas9 MYC knockout cell lines

The development of OCI-LY1 cells in which c-MYC expression is knocked out was performed in the laboratory of Professor Bjoern Chapuy, at Charité – Universitätsmedizin in Berlin, Germany, during a research visit (August 2022 to October 2022).

4.2.8.1 Single guide RNA design and cloning into LentiGuide-Puro vector backbone

To achieve CRISPR-mediated knockout of c-MYC, three single guide RNAs (sgRNAs) were designed. The first sgRNA was chosen from the Brunello Library, an optimized CRISPR-library with improved on-target effects (314). The remaining two sgRNAs were identified from the integrated DNA technologies portal (IDT) where predesigned sgRNAs can be searched for (https://eu.idtdna.com/site/order/designtool/index/CRISPR_PREDESIGN). sgRNA were selected based on two target scores: (i) the off-target score, where a higher score indicates less chance that the sgRNA binds to sequences elsewhere in the genome, and (ii) the on-target score, where a higher score represents efficiency of Cas9 at the target site. In this study, an off-target score of >70 and an on-target score of >40 was accepted. The c-MYC targeting sgRNA sequences obtained from either the Brunello library or IDT served as the forward primer, and the reverse complement was generated to act as the reverse primer. To ensure compatibility with the LentiGuide-Puro (LGP) backbone vector (Addgene, USA), which contains a puromycin selection marker, and efficient transcription of the sgRNAs, the following nucleotides were included in each primer set:

c-MYC forward primer: 5’ CACCGNNN…….N 3’

c-MYC reverse primer: 3’ CNNN……..NCAAA 5’

For cloning into the LGP vector backbone, each sgRNA pair (forward and reverse) was phosphorylated and annealed together using the 10X T4 DNA ligase buffer with ATP (New England Biolabs, USA) and 10 000U/mL T4 Polynucleotide Kinase (New England Biolabs, USA). gRNAs were stored at -20˚ C.

The LGP backbone vector was digested with BSMBi-v2-R07395 (CGTCTC) and fragments were then electrophoresed on a 1% agarose gel (Appendix B) at 100V for 40 minutes, to confirm digestion of the

vector. The Wizard SV gel and PCR cleanup kit (Promega, USA) was used to excise bands from the gel and purify the vector, which was thereafter quantified using the NanoDrop™ ND-1000 (ThermoFisher Scientific™, USA). gRNAs were ligated within the digested LGP backbone vector, and ligated constructs were transformed into STBL3 competent cells (New England Biolabs, USA) using heat shock, and colonies were grown in Lysogeny Broth (LB) (Appendix B). Plasmid extractions were performed using Mini-prep spin kit (Qiagen, Germany) and successful clones were confirmed using sequencing. To generate larger stocks of plasmids fit for transfection, the Nucleobond Xtra endotoxin free plasmid DNA purification kit (ClonTech Laboratories, USA) was used, as it contains an endotoxin-removal step. Plasmid concentrations were determined using the NanoDrop™ ND-1000 (ThermoFisher Scientific™, USA).

4.2.8.2 Lentivirus production

A total of four transfections were performed, one for each of the three MYC-gRNA and the gRNA control, PLKO.5-AAVI-GFP (kindly donated by Dr Jens Loeber, in Professor Chapuy's laboratory). For each transfection, HEK239T cells were plated at a density of 1.5 x 10^6 and incubated for 16 hours prior to transfection. On the day of transfection, transfection solutions containing the gRNA plasmid, OptiMem, polyethyleneimine (PEI) and viral packaging, psPax2 and PMD2G, were added to cells. After a 4-to-6-hour incubation period at 37˚ C, the media was replaced with fresh media, supplemented with 30% FBS, and cells were incubated at 37˚ C overnight. The media, containing viral particles, was collected 24- and 48-hours post-transfections, pooled together and filtered through a 0.45 µM filter.

4.2.8.3 Lentivirus transduction of OCI-LY1 cells

OCI-LY1 cells were plated at a density of 2 x 10^6 cells, in IMDM containing 30% FBS. Polybrene was added to cells, at a final concentration of 8 µg/mL, and spinfection was performed at 1000 RCF for 90 minutes at 30˚ C, followed by addition of IMDM, containing 30% FBS. The following day, the media was replaced with fresh IMDM containing 10% FBS and transduced cells were selected by culturing in media containing 1 µg/mL puromycin for three days. Thereafter, cells were maintained in 0.25 µg/mL puromycin, and protein was harvested. To determine whether successful knockdown of c-MYC was achieved, as well as the effect on PD-L1 expression, western blot experiments were performed as described previously. The effect of c-MYC knockdown on PD-L1 mRNA levels was assessed via qPCR experiments, as described previously.

4.3 Results

4.3.1 Status of *PD-L1* in online DLBCL patient database

A total of 48 DLBCL datasets were retrieved from The Cancer Genome Atlas (TCGA) and used to conduct an integrated and comprehensive analysis on the status of *PD-L1*. The dataset cohort comprised of 46% males and 54% females, and multiracial participants (60% White; 18% Asian; 2% Black/African American).

4.3.1.1 PD-L1 expression in DLBCL cancer database

TCGA is a publicly available repository containing genomic and clinical data, derived from a wide range of human tumour samples (315). The expression profile of *PD-L1* (*CD274*) in the available DLBCL database (primary site; n = 48) was accessed and compared per specific subtypes, namely ABC (n = 15), GCB (n = 22) and unclassified (UC) (n = 11). Using a one-way ANOVA, we observed a statistically significant difference in *PD-L1* expression levels among the DLBCL subtypes ($F(2,45) = 7.9038$, $p = 0.0011$). Post-hoc comparisons using Tukey's HSD test indicated that the mean *PD-L1* expression level for the GCB subtype (mean = 3.3277) was significantly lower than both the ABC subtype (mean = 4.8153, $p = 0.0120$) and the UC subtype (mean = 5.2584, $p = 0.0027$). There was no significant difference between the ABC and UC subtypes (mean difference = -0.4430, $p = 0.7331$). These results indicate that the GCB subtype has significantly lower *PD-L1* expression than the ABC and UC subtypes (Figure 4.1). This finding is in line with what is described in the literature where PD-L1 expression is elevated in non-GCB subtypes of DLBCL (297).

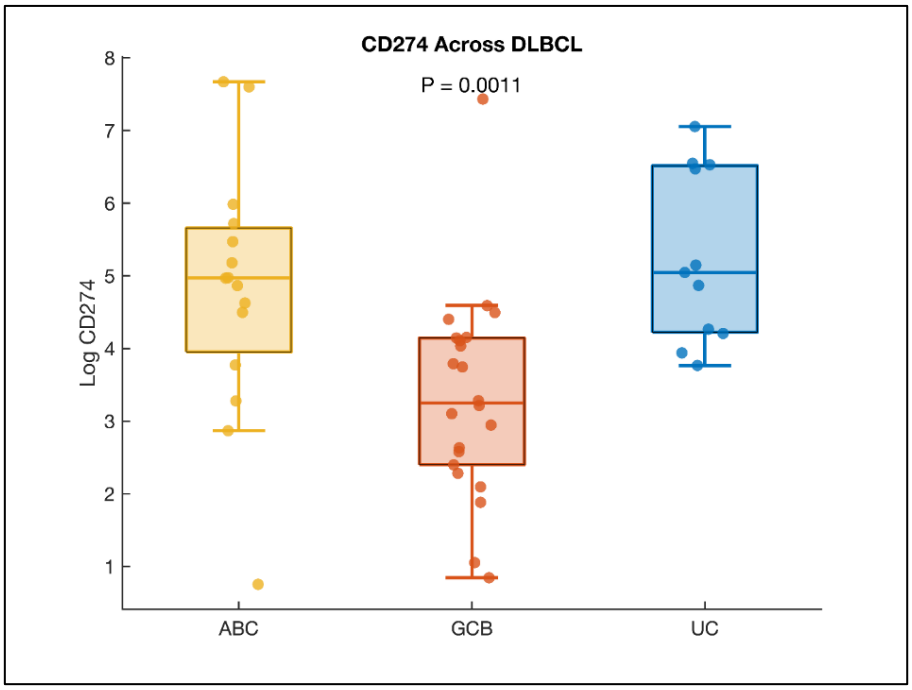

Figure 4.1: *PD-L1* expression in DLBCL TGCA database. The expression of *PD-L1* was evaluated within DLBCL (primary site DLBCL; n = 48) from TCGA available datasets, and compared within three clusters, namely ABC (n = 15), GCB (n = 22) and unclassified (n = 11) (316). One-way ANOVA, p = 0.0011; GCB vs ABC, p = 0.0120; GCB vs UC, p = 0.0027; ABC vs UC, p = 0.7331.

4.3.1.2 Association of PD-L1 status with patient survival

The TCGA *PD-L1* (*CD274*) transcriptome data was used to cluster data based on *PD-L1* mRNA expression into two groups, namely "high-*CD274*" (n = 13) and "low-*CD274*" (n = 35). Thereafter, the patient survival data was correlated with the two clusters. The resulting Kaplan-Meier plots, depicted in Figure 4.2, demonstrate that patients within the high *CD274* group had significantly lower progression free survival (PFS), where less than 30% of patients were alive after 40 months (p = 0.0139) (Figure 4.2A). Compared to a PFS of 107.013 months in patients with low-expression of *CD274*, patients in the high-expression cluster had a PFS of only 9.53414 months. The same trend is observed for overall survival (OS) (Figure 4.2B), and disease-specific survival (DSS) (Figure 4.2C), while for disease-free survival (DFS) (Figure 4.2D), the dataset included only one patient within the high-expression cluster, which, in itself, demonstrates that DFS is a rare occurrence in patients with high *CD274* expression.

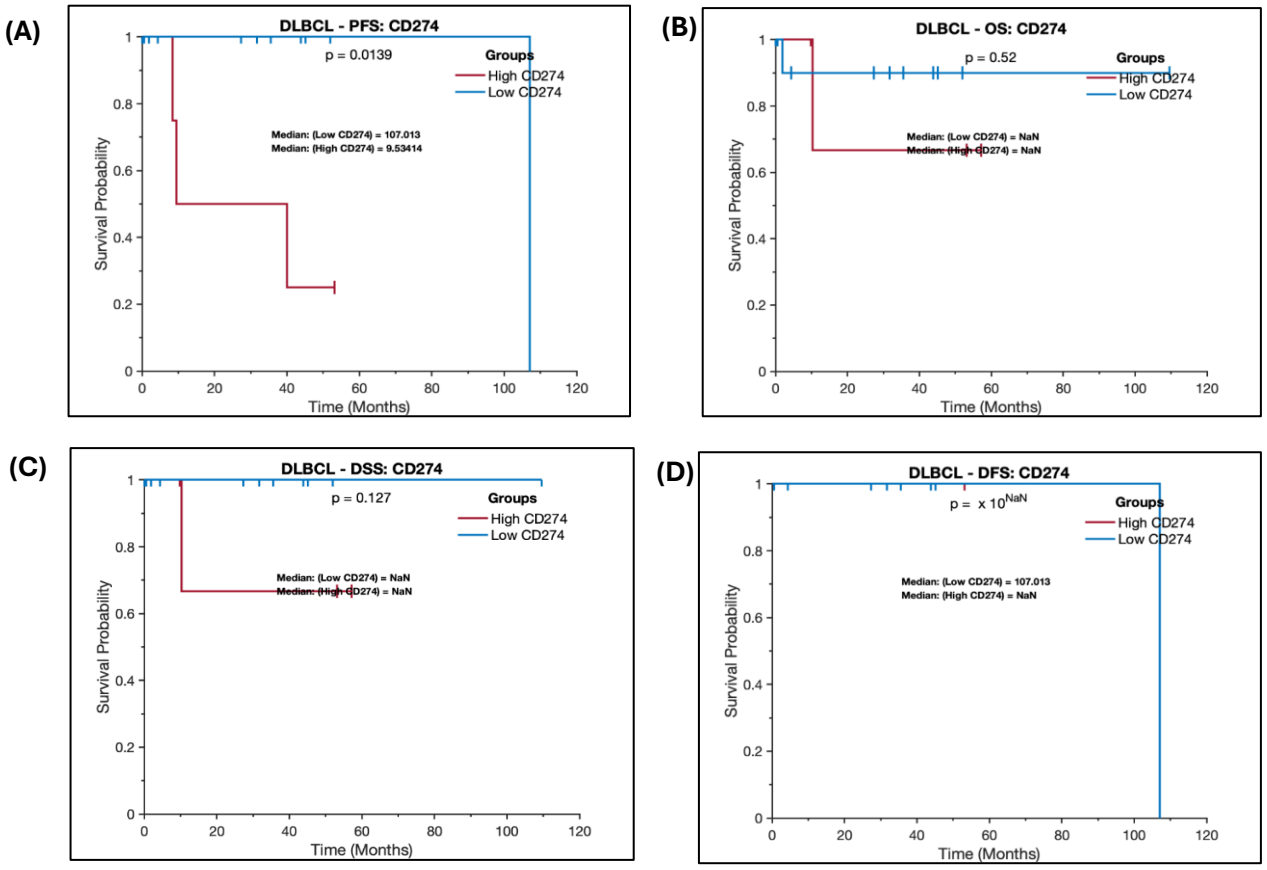

Figure 4.2: Kaplan-Meier survival estimate curves showing (A) PFS, (B) OS, (C) DSS and (D) DFS of DLBCL patients in the "low-*CD274*" (n=35) and "high-*CD274*" (=13) cluster groups. (Extracted from TCGA (316)). For the specific prognostic outcomes depicted in figures 4.2 B-C, the median survival in months is specified as not a number (NaN) and this is due to censored events which are not related to the study itself. Log-rank test.

4.3.2 Association between *PD-L1 and c-MYC* expression in online DLBCL patient database and DLBCL cell lines

As reported previously, c-MYC is a crucial oncogenic driver that is implicated in the pathogenesis of DLBCL. Because previous reports on the potential regulation of PD-L1 by c-MYC in DLBCL is contradictory, this study sought to describe this relationship using in silico techniques and DLBCL cell models.

4.3.2.1 In silico analysis of c-MYC binding elements in the human PD-L1 promoter

To date, only one E-box site, which is the DNA regulatory element via which c-MYC is known to regulate its target genes, has been reported in the human *PD-L1* promoter, located at position -164 bp to -159 bp (296). Using the PROMO software designed to predict transcription factor binding sites (TFBS) in DNA sequences, the region -2500 bp upstream of the TSS was analysed (dissimilarity rate of 15%), which revealed an additional four E-box sites located at positions -835 bp to -828 bp, -1389 bp to -1382 bp, -1876 bp to -1869 bp and -2355 bp to -2348 bp, as illustrated in Figure 4.3 below. The data suggests that *PD-L1* may indeed be regulated by the c-MYC transcription factor.

(A)

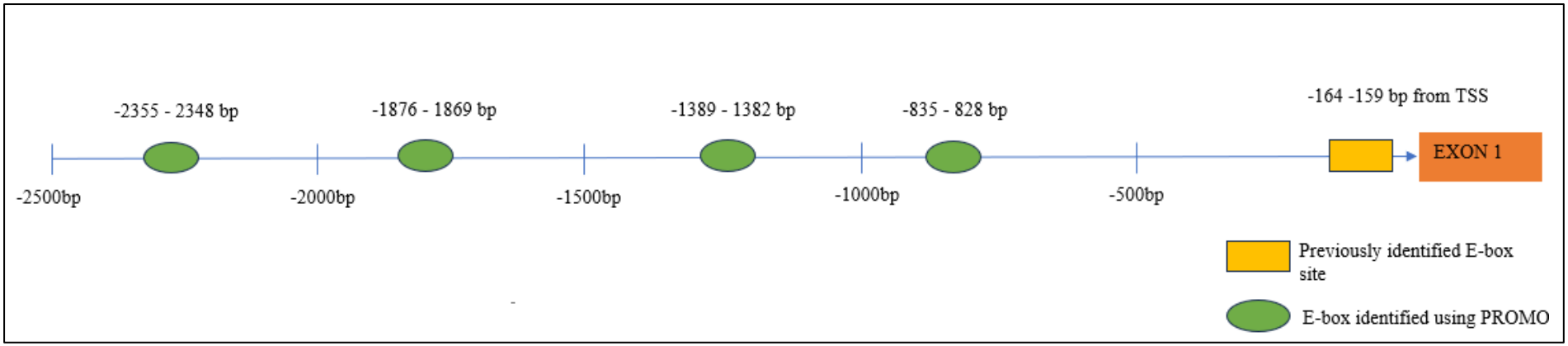

(B)

Factor	Position	Dissimilarity percentage	String
c-MYC	-2355 to - 2348	3.98%	CACCTGA
c-MYC	-1876 to -1869	3.98%	ACAGGTG
c-MYC	-1389 to -1382	7.32%	ACATGTG
c-MYC	-835 to -828	7.32%	CACTTGA

Figure 4.3: Predicted E-box sites within the human *PD-L1* promoter, analysed using the PROMO online tool. The human *PD-L1* promoter sequence (-2500bp) was extracted from Ensemble and used to identify putative c-MYC binding sites. (A) Graphical representation depicting the potential c-MYC binding sites within the *PD-L1* promoter, specified in green boxes, as labelled in the key. Yellow square represents the previously identified E-Box site described by Maeda and colleagues (296). (B) Dissimilarity score representing the extent of sequence variation from the consensus. A dissimilarity rate of 15% was specified to reflect at least 85% similarity.

4.3.2.2 Correlation analysis of PD-L1 and c-MYC expression in online DLBCL patient database

Analyses were performed to investigate correlation between *c-MYC* and *PD-L1* expressions within the TGCA DLBCL datasets. Using the non-clustered DLBCL dataset, no distinct correlation could be observed between these two genes (Figure 4.4A, p = 0.5850, n=47). When clustered, a notable inverse (negative), but not statistically significant, correlation was observed for the ABC-DLBCL subtype (Figure 4.4B, p = 0.1161, n=14), while a mild inverse (positive) correlation was seen in the GCB subtype (Figure 4.4C; p = 0.2279, n=22). As was the case for *PD-L1* status, the UC cluster followed a similar trend as the ABC cluster (Figure 4.4 D; p=0.2714, n=11).

(A)

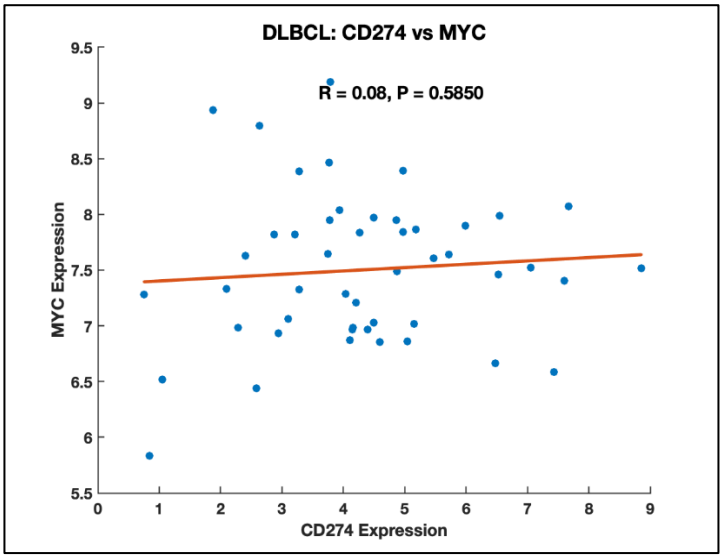

(B)

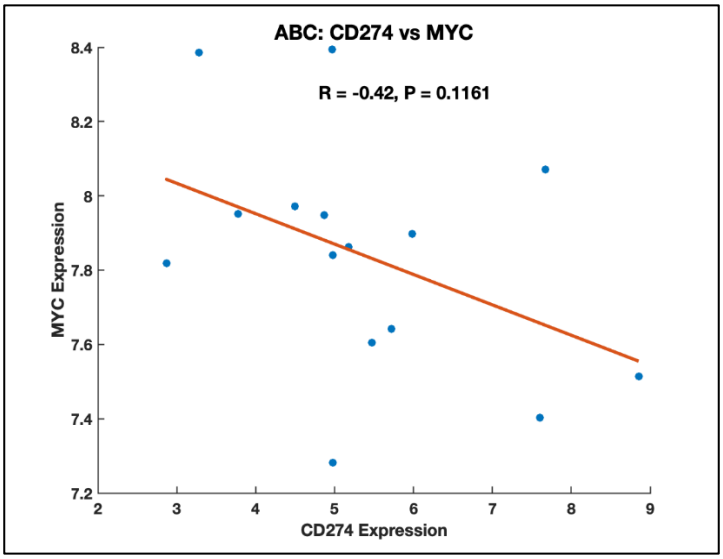

(C)

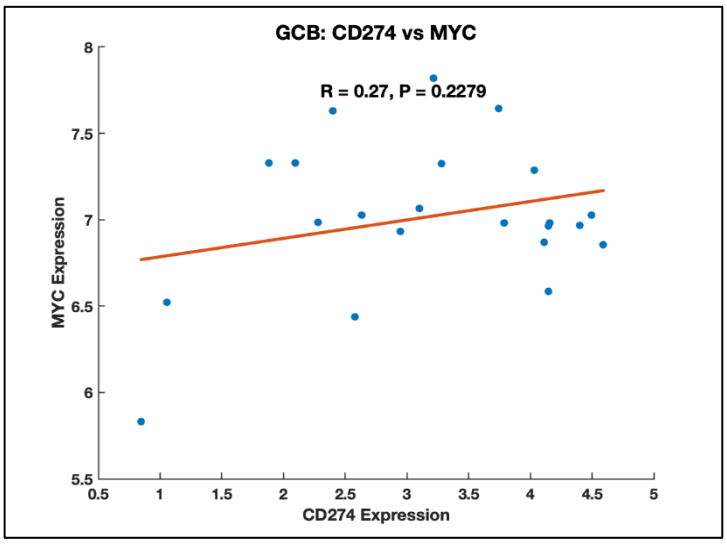

(D)

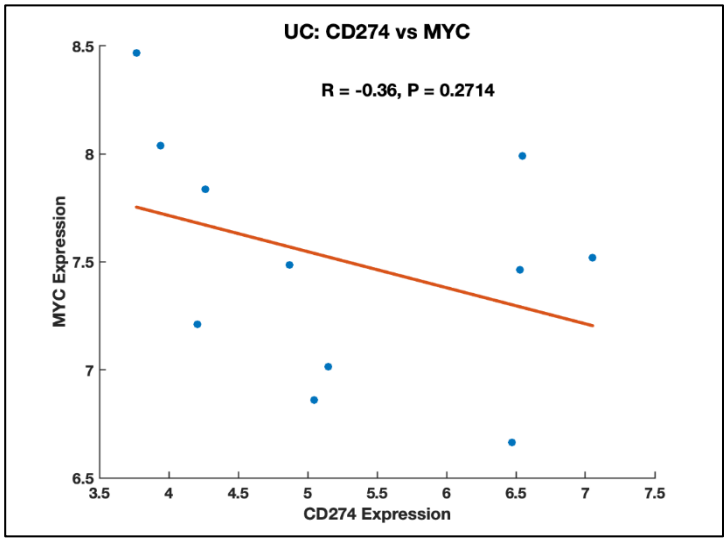

Figure 4.4: Correlation between *PD-L1 and c-MYC* expression in online TGCA DLBCL patient database. (A) Correlation analysis was performed to assess the relationship between PD-L1 and c-MYC in DLBCL dataset (n = 47). Datasets were clustered as (B) ABC (n = 14), (C) GCB (n = 22) and (D) UC (n = 11). Pearson correlation coefficients.

4.3.2.3. Assessment of c-MYC and PD-L1 expression in online DLBCL cell line database.

To further explore the correlation between *c-MYC* and *PD-L1* expression, publicly available data on The Human Protein Atlas was accessed, and gene expression values for *PD-L1* and *c-MYC* from a total of 27 DLBCL cell lines (1 unknown, 18 GCBs and 8 ABCs) were retrieved and plotted side-by-side (Figure 4.5). Of the 27 cell lines, 1 was EBV-positive (Farage), while another cell line, DoHH2, is considered to be partially EBV-positive. Both of these cell lines were assigned to the GCB subtype. *PD-L1* expression was generally higher (mean = 8.2125; pink bars) within ABC-DLBCL cell lines, relative to the GCB subtypes (mean = 0.8; pink bars), which is consistent with the findings for patient tumour data shown in Figure 4.1. The expression level of *c-MYC* (blue bars) was generally much higher than *PD-L1* in all cell lines, with a mean expression of 333.1 within GBC-DLBCL cell lines and 308.5875 within ABC-DLBCL

cell lines. From the available data, no clear association between *c-MYC* and *PD-L1* levels could be drawn in DLBCL cell lines overall, or across subtypes.

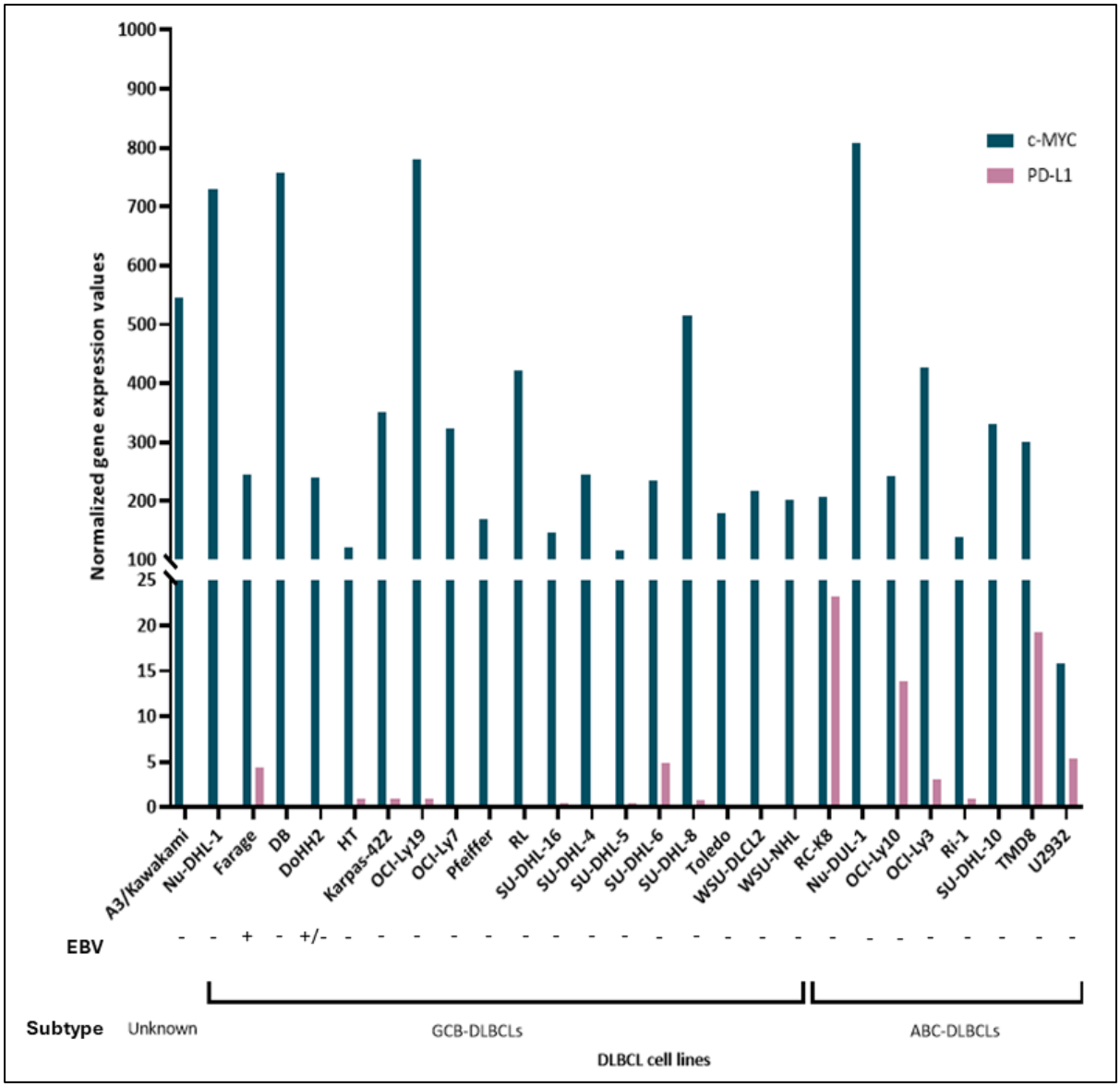

Figure 4.5: Expression levels of *PD-L1* and *c-MYC* in DLBCL cell lines, extracted from The Human Protein Atlas. A total of 27 DLBCL cell lines were identified, 18 of which were assigned to the GCB subtype and 8 cell lines to ABC subtype. The subtype of 1 cell line was unknown at the time. Of the total cell lines identified, 1 was EBV-positive and another was considered partially EBV-positive. Normalized gene expression values for *PD-L1* and *c-MYC* were recorded and plotted on the same graph, using GraphPad Prism version 9 (GraphPad Software, USA) (From The Human Protein Atlas (317)).

4.3.2.4 Assessment of PD-L1 and c-MYC mRNA and protein expressions in five DLBCL cell lines

The relationship between c-MYC and PD-L1 was evaluated in a panel of five established DLBCL cell lines which were available in the laboratory. Table 4.5 lists the cell lines and their characteristics.

Table 4.5: Characteristics of the DLBCL cell lines included for analysis.

Cell line	DLBCL subtype	EBV status	Origin	Reference
U2932	ABC-DLBCL	Negative	Established from the ascites of a 29-year-old female, previously treated for HL.	(318)
HBL-1	ABC-DLBCL	Negative	Established from the pleural effusion of a 65-year-old male.	(319)
WSU-DLCL2	GCB-DLBCL	Negative	Established from the pleural effusion of a 41-year-old male.	(320)
OCI-LY1	GCB-DLBCL	Negative	Established from the bone marrow of a 44-year-old male.	(321)
SU-DHL-4	GCB-DLBCL	Negative	Established from the peritoneal effusion of a 38-year-old male.	(322)

ABC-DLBCL - Activated B-cell (ABC)-like Diffuse Large B-cell Lymphoma; EBV – Epstein Barr Virus; HL – Hodgkin Lymphoma; GCB-DLBCL – Germinal Centre B-cell (GCB)-like Diffuse Large B-cell Lymphoma

qPCR and western blotting analyses were carried out to determine the mRNA and protein levels, respectively, of PD-L1 and c-MYC in the DLBCL cell lines. The expression of c-MYC, at both mRNA and protein expression levels, could be detected in all 5 cell lines, at varying levels, with the lowest transcriptional levels seen in the ABC-DLBCL cell lines, U2932 and HBL-1 (Figure 4.6A, upper panel); while at the protein level, this trend was slightly different, with only U2932 being a relatively low expressor of c-MYC protein (Figure 4.6A, lower panel). For PD-L1, the three GCB-DLBCL cell lines appeared to be lower expressors of PD-L1 at both the mRNA and protein levels, when compared to the two ABC-DLBCL cell lines (Figure 4.6B). In fact, under our assay conditions, PD-L1 was effectively undetectable in the three GCB-DLBCL cell lines.

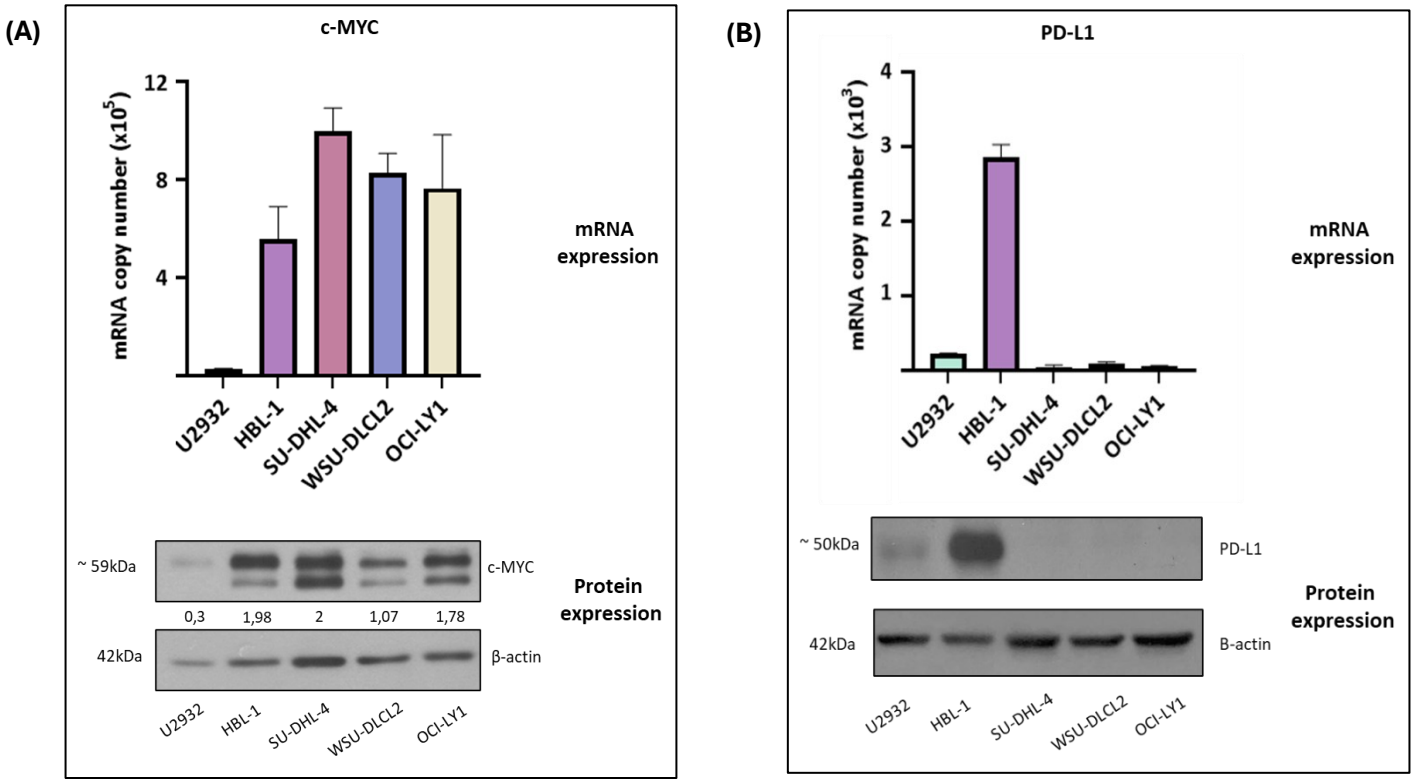

Figure 4.6: PD-L1 and c-MYC expression in a panel of DLBCL cell lines. (A) c-MYC mRNA (upper panel) and protein expression (lower panel) in DLBCL cell lines. (B) PD-L1 mRNA (upper panel) and protein expression (lower panel) in DLBCL cell lines. Western blot experiments were normalized to β-actin and quantified using ImageJ. qPCR results are a representation of two independently conducted experiments.

Overall, this finding is line with what was seen in patient datasets extracted from TCGA (Figure 4.1) and DLBCL cell lines in The Human Protein Atlas (Figure 4.3), where DLBCLs of the ABC subtype are higher expressors of PD-L1. In addition, the data indicates that GCB-DLBCLs are more frequent expressors of c-MYC, compared to ABC-DLBCLs. Another observation of the data is that it infers an inverse correlation between c-MYC and PD-L1, since the latter was detectable only in ABC-DLBCL cell lines, where c-MYC expression was lower.

4.3.2.5 Assessment of PD-L1 expression in a c-MYC knock out model.

To further explore the correlation between PD-L1 and c-MYC expressions, and the potential role that the c-MYC transcription factor might be playing in regulating the expression of PD-L1 in DLBCL, a MYC knock out model was used. Specifically, CRISPR-Cas9 technology was used with the intention to knock out c-MYC expression in the GCB-DLBCL cell line OCI-LY1. The OCI-LY1 MYC knock outs were generated during a research visit to the laboratory of collaborator and lymphoma research expert, Professor Bjoern Chapuy, at Charité – Universitätsmedizin Berlin, in Germany, where this methodology is well established. Following selection of successfully transduced cells, western blot analysis revealed that complete knock out of c-MYC expression was not achieved, despite the fact that the CRISPR-Cas9

technology aims to achieve complete knock out. Instead, partial knockdown was achieved in all three clones (Figure 4.6). The partial knockdown of c-MYC is further discussed in section 4.4. Nevertheless, we proceeded with the experiment and clone gMYC-1, which achieved the most c-MYC knockdown, was selected to assess PD-L1 expression at the mRNA and protein levels.

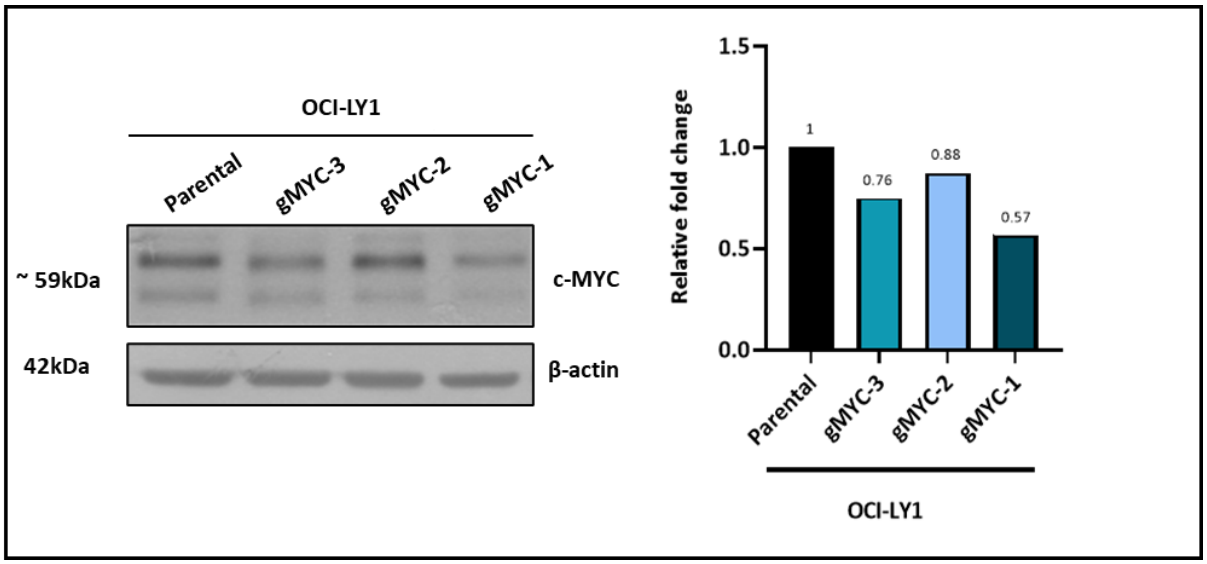

Figure 4.7: CRISPR-Cas9 leads to knockdown of c-MYC in OCI-LY1 parental and gMYC-transduced cells. Western blot experiments using anti-c-MYC antibody (Abcam, [Y69] 32072) to assess efficiency of c-MYC knockout, normalized to β-actin (Santa Cruz Biotechnology, sc-47778). Quantification was performed using ImageJ and is shown relative to parental OCI-LY1 cells.

A 2-fold increase in *PD-L1* gene transcription was observed in the OCI-LY1 gMYC-1 knock down cells, relative to the parent cell line (Figure 4.8A). However, at the protein level, under our experimental conditions, no PD-L1 protein could be detected, in either parental or MYC knockdown cells (Figure 4.8B). This data, once again, infers that an inverse correlation may exist between c-MYC and PD-L1.

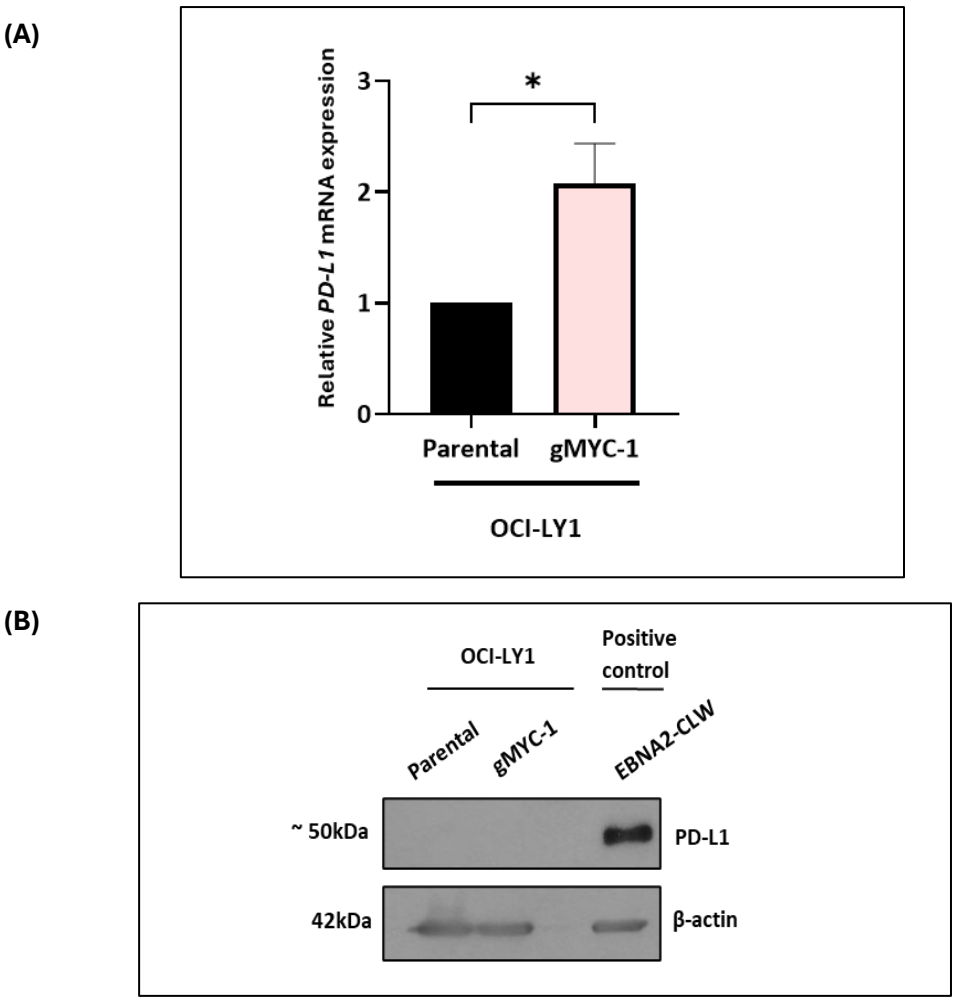

Figure 4.8: PD-L1 expression in OCI-LY1 gMYC-1 cells where c-MYC is knocked down. (A) qPCR was used to determine the effect of c-MYC knockdown on *PD-L1* mRNA expression. qPCR data is a representation of at least two independently conducted experiments, normalized to GAPDH. Statistical analysis was performed using GraphPad Prism 9 (Students t-test, two-tailed, *p ≤ 0.05). (B) Western blot experiments using anti-PD-L1 antibody (Cell Signalling, E1L3N), including a positive control in which high levels of PD-L1 is known to be expressed (EBNA2-CLW). The experiment was performed in duplicate and the above result is a representative on the result. Results were normalized to β-actin (Santa Cruz Biotechnology, sc-47778).

4.3.3 Impact of HIV and EBV on the expression of PD-L1 in DLBCL cells.

HIV-infected individuals are reported to be 17-fold more at risk of developing DLBCL compared to the general population (57), constituting a significant health care challenge in settings where the prevalence of HIV is high such as in the Southern African region. Additionally, EBV-infections are prevalent in early-life infections in developing countries, where this oncogenic virus has been shown to enhance PD-L1 expression, particularly via the activity of EBNA2. Since EBNA2 has been shown to upregulate PD-L1 expression, this study sought to investigate how that aspect is affected by HIV. For this purpose, a cell model was used, which comprises of U2932 established parent cell line (ABC subtype), and two EBNA2-expressing daughter clones. In our assays, these cells were exposed to two forms of HIV-1, namely AT-2 HIV-1 and pvHIV-1, generated independently and by different

methodologies. In brief, AT-2 HIV-1 are HIV viral particles where the infectivity has been impaired, while maintaining the structural and functional integrity of the viral envelop, and ability to interact with cell surface receptors; while pvHIV-1 are viral particles which are capable of cell entry but lack replication potential. In both cases, their respective and appropriate mock controls were used during cell treatments.

4.3.3.1 Verification of EBNA2-expressing ABC-DLBCL U2932 cell model

The EBNA2-expressing cell model consisted of the parental line (U2932; ABC-DLBCL subtype), and two EBNA2-expressing clones (CL1 and CLW) created and previously described by Prof. Pankaj Trivedi's group (309). Confirmation of stable EBNA2 expression was done using western blotting (Figure 4.9). As shown below, EBNA2-CL1 is a higher expressor of EBNA2, relative to EBNA2-CLW, while the viral protein is indetectable in the parent U2932 cells.

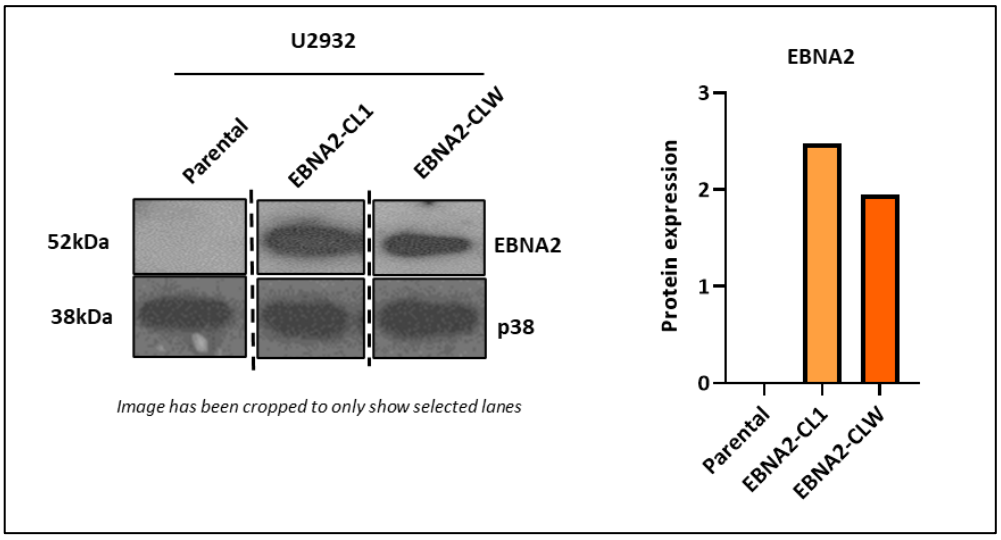

Figure 4.9: Western blot analysis confirming expression of EBNA2 in stably transfected U2932 cells. An anti-EBNA2 antibody (PE2, NBP2-50382, Novus Biologicals, USA) was used to detect EBNA2 expression and an anti-P38 antibody (M0800, Sigma-Aldrich) was used to measure p38 as an internal loading control. Quantification of protein expression, normalized to p38, was done using ImageJ. Western blot image is cropped to only show the relevant lanes on the blot.

Additionally, we confirmed, using qPCR and western blotting analyses, that PD-L1 is highly expressed in EBNA2-expressing clones, relative to the parent cell line, at both the transcriptional, and protein expression levels (Figure 4.10). While less *PD-L1* mRNA was detected in CL1, relative to CLW, the reverse was the case for PD-L1 protein expression. This observation was consistent across multiple repeats.

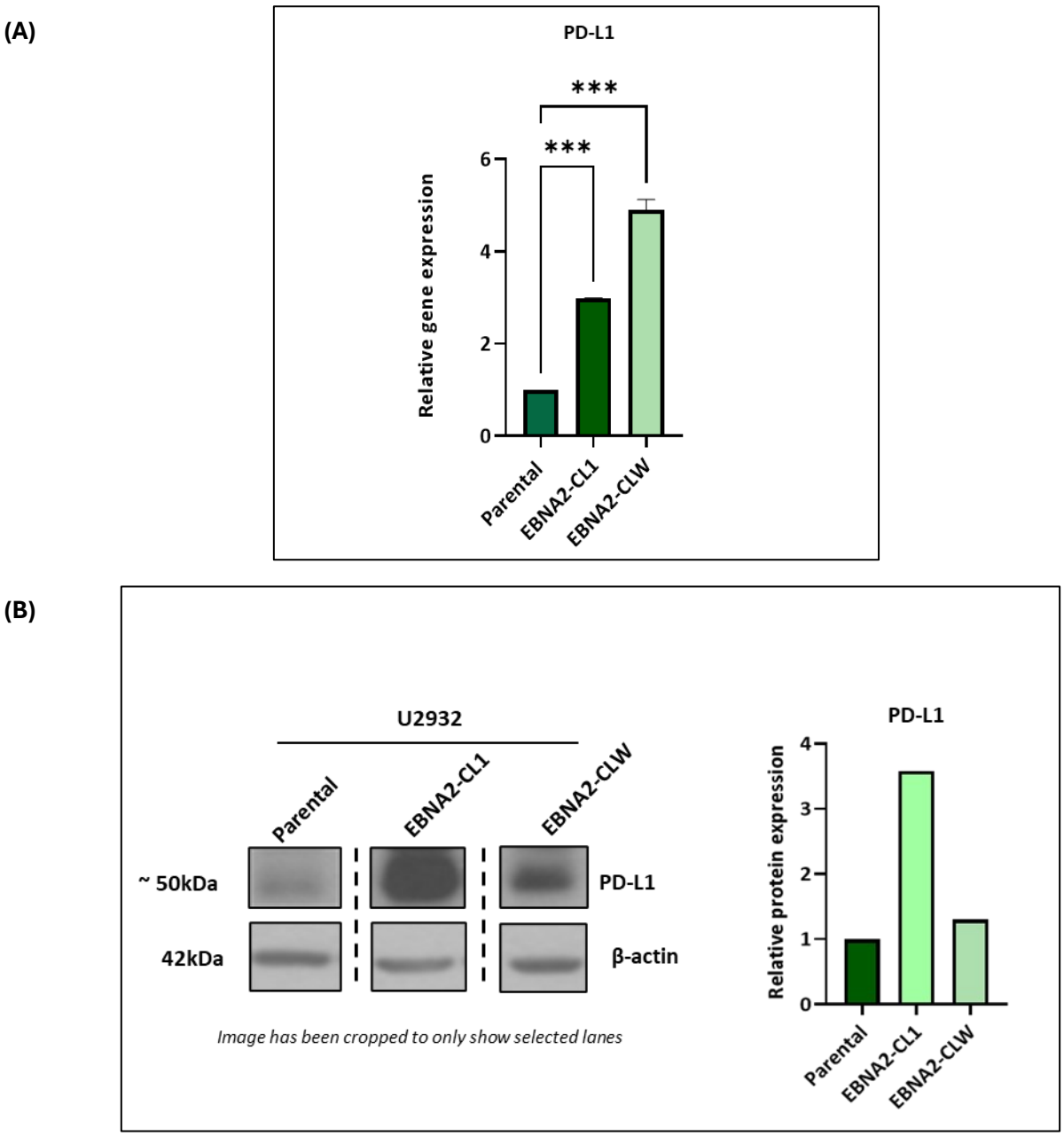

Figure 4.10: PD-L1 mRNA and protein expressions are enhanced in EBNA-expressing clones. (A) qPCR analysis confirming increased *PD-L1* mRNA expression in EBNA2-expressing cells. qPCR data is a representation of two independently conducted experiments, normalized to GAPDH. Statistical analysis was performed using GraphPad Prism 9 (ANOVA test, ***p ≤ 0.001). (B) Western blot experiments confirming upregulation of PD-L1 protein levels, using anti-PD-L1 antibody (Cell Signalling, E1L3N), in the presence of EBNA2. The experiment was performed in duplicate and the above result is a representative on the result. Results were normalized to β-actin (Santa Cruz Biotechnology, sc-47778), using ImageJ, and are shown relative to parental cells.

4.3.3.2 Assessment of c-MYC expression in EBNA2-expressing ABC-DLBCL U2932 cell model

The expression of c-MYC has been described in this cell model by Leopizzi et al. (323). As a confirmation, the expression of c-MYC, at both the mRNA and protein levels, was assessed, using qPCR and western blotting respectively. As is shown in Figure 4.11 below, c-MYC expression is higher in EBNA2-expressing clones, relative to the parent cell line, at both the transcriptional (Figure 11A), and protein expression levels (Figure 11B). Similarly to what was observed for *PD-L1* expression, less *c-*

MYC mRNA was detected in CL1, relative to CLW. At the protein level however, the expression was comparable between the two clones.

(A)

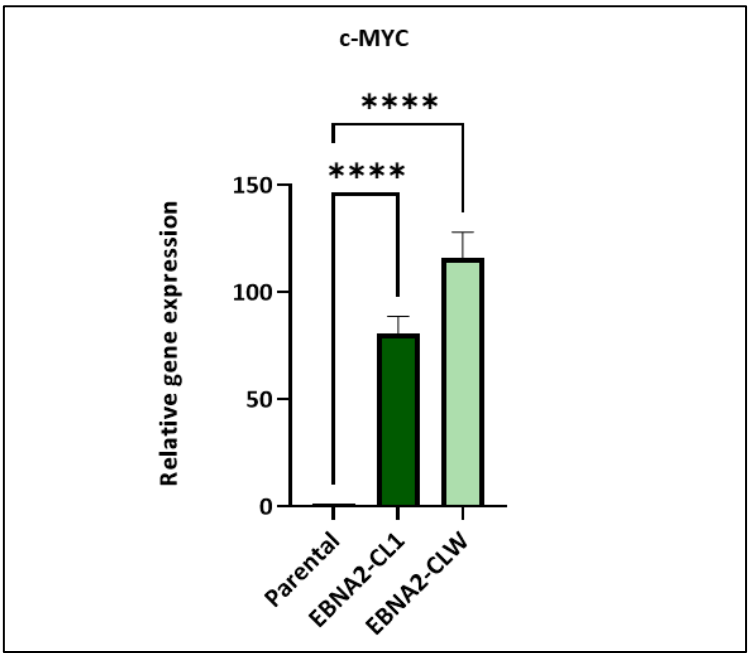

(B)

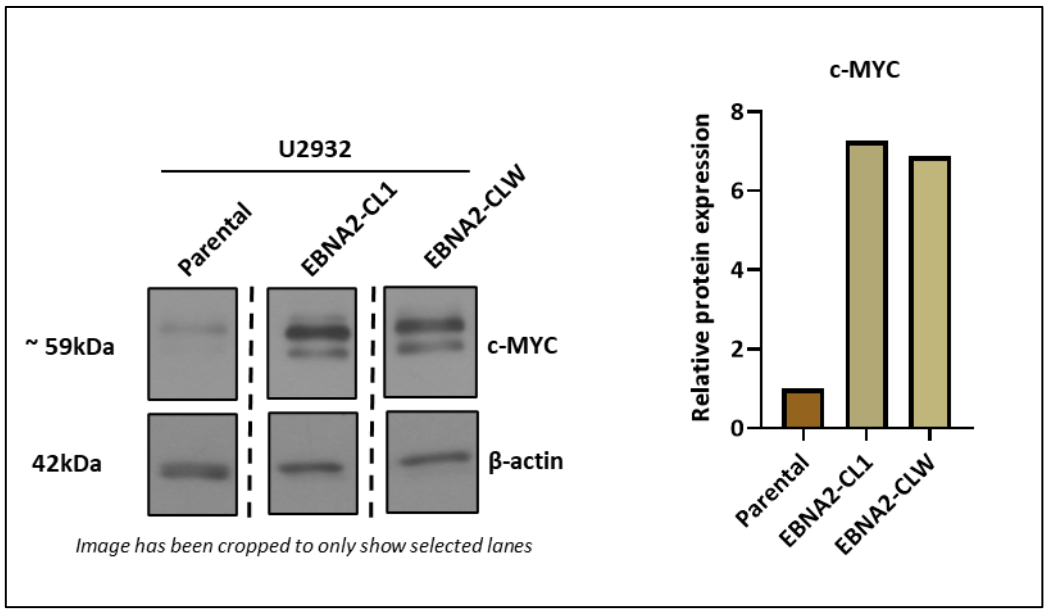

Figure 4.11: c-MYC mRNA and protein expressions are highly enhanced in EBNA-expressing clones. (A) qPCR analysis confirming increased *c-MYC* mRNA expression in EBNA2-expressing cells. qPCR data is a representation of two independently conducted experiments, normalized to GAPDH. Statistical analysis was performed using GraphPad Prism 9 (ANOVA test, ****p ≤ 0.0001). (B) Western blot experiments confirming upregulation of c-MYC protein levels, using anti-c-MYC antibody (Abcam, [Y69] 32072), in the presence of EBNA2. The experiment was performed in duplicate and the above result is a representative on the result. Results were normalized to β-actin (Santa Cruz Biotechnology, sc-47778), using ImageJ, and are shown relative to parental cells.

4.3.3.3 Effect of HIV exposure on expressions of PD-L1 and c-MYC in EBNA2-expressing ABC-DLBCL U2932 cell model

To determine the effect of HIV-1 exposure (either AT-2 HIV-1 or pvHIV-1) on the expression levels of PD-L1 and c-MYC, the cell lines were exposed to the viral particles, thereafter qPCR and western blotting analyses were carried out.

There was no significant change in *PD-L1* mRNA levels in the parental cell line following exposures to either AT-2 HIV-1 (red bars) or pvHIV-1 (green bars), while significant decreases were observed in the EBNA2-expressing clones (Figure 4.12).

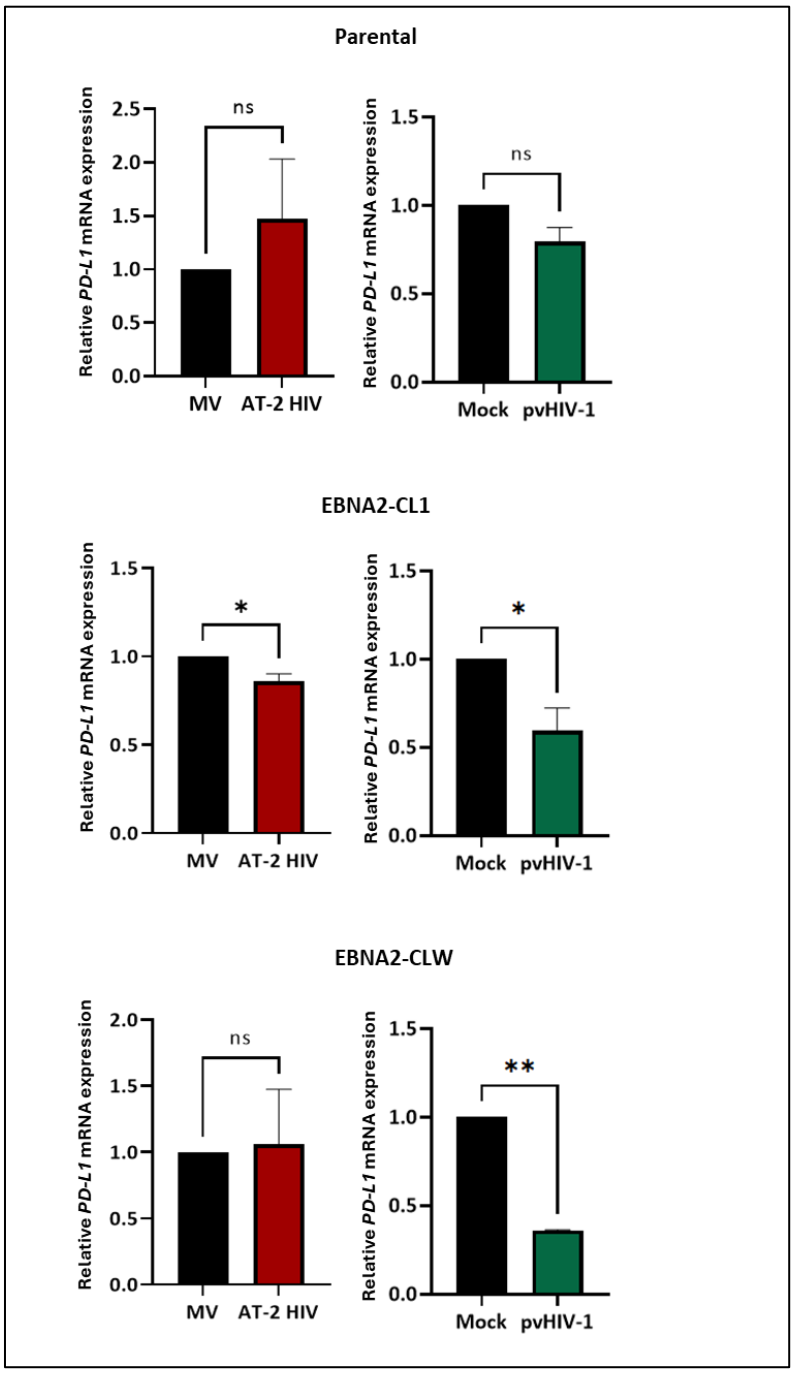

Figure 4.12: Exposure to HIV-1 affects *PD-L1* expression at the mRNA level. qPCR analysis assessing *PD-L1* mRNA levels after exposure to either AT-2 HIV-1 or pvHIV-1 in parental cells (upper panel) and EBNA2-expressing cells, CL1 (middle panel) and CLW (lower panel). Results are shown relative to the respective controls (MV or Mock). qPCR data is a representation of two independently conducted experiment normalized to GAPDH. Statistical analysis was performed using GraphPad Prism 9 (Students t test, two-tailed, *p ≤ 0.05; **p ≤ 0.01).

At the protein levels, for cells exposed to AT-2 HIV-1 (red bars), PD-L1 was downregulated within the parent cells, as well as the EBNA2-expressing clones (Figure 4.13, upper panel). The same trend was seen for cells exposed to pvHIV-1 (green bars), except for the parent cell line. Since both forms of HIV-1 exposure (AT-2 HIV-1 and pvHIV-1) affected PD-L1 in similar manner, i.e. decreased protein expression, relative to their respective controls (MV and mock), our results strongly suggest that in DLBCL cell lines, HIV-1 exposure negatively regulates PD-L1 mRNA and protein expressions, and that this effect is enhanced in the presence of EBNA2.

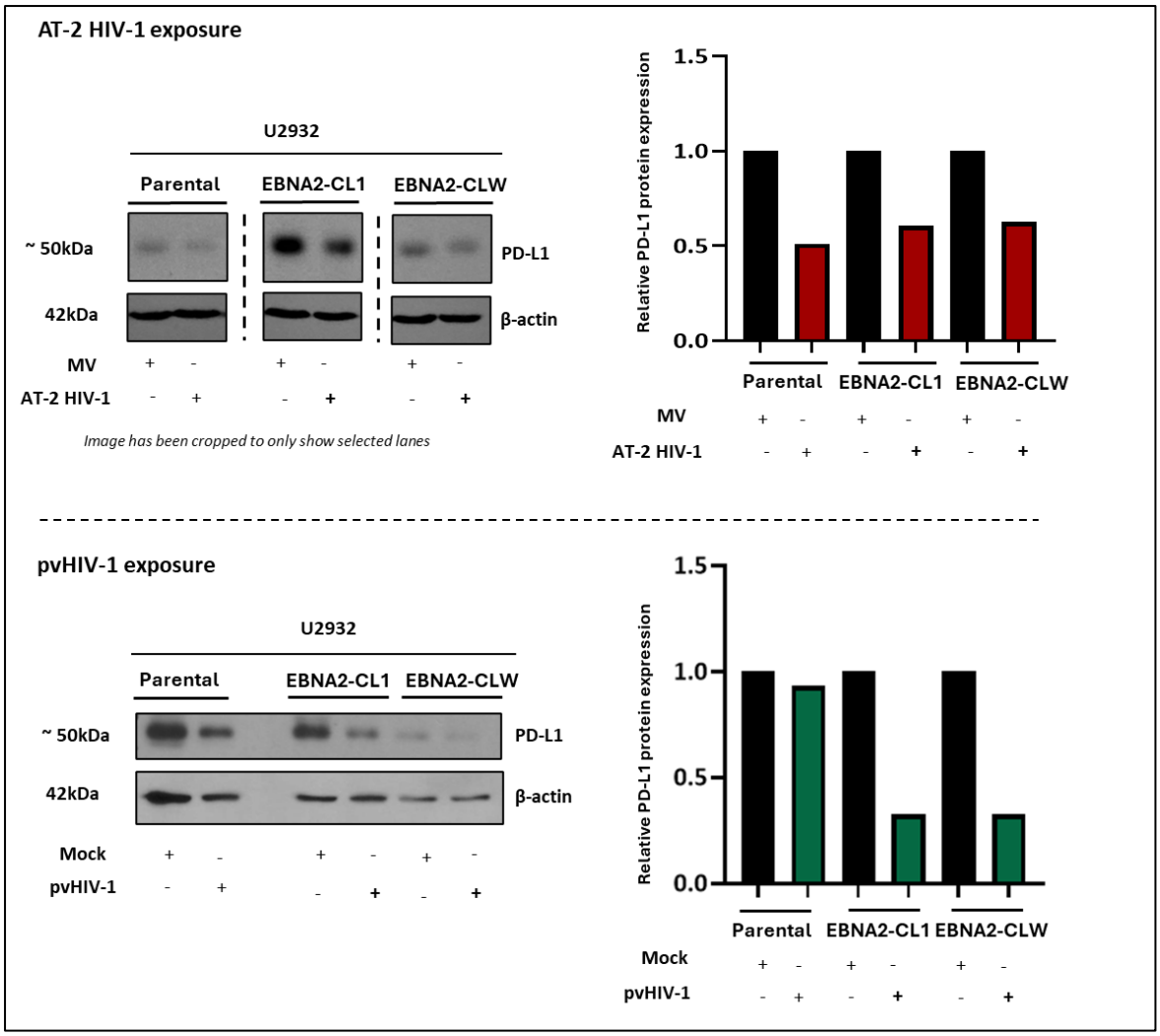

Figure 4.13: Exposure to HIV-1 affects PD-L1 expression at the protein level. Western blot experiments using anti-PD-L1 antibody (Cell Signalling, E1L3N) demonstrated reduced PD-L1 expression in cells exposed to either AT-2 HIV-1 (upper panel) or pvHIV-1 (lower panel), relative to their respective control (MV or Mock). The experiment was performed in duplicate and the above result is a representative on the result. Protein levels were normalized to β-actin (Santa Cruz Biotechnology, sc-47778), using ImageJ.

With regards to *c-MYC* expression, exposure to AT-2 HIV-1 (red bars) did not affect its mRNA expression, while a small decrease was noted in in pvHIV-1-exposed (green bars) EBNA2-expressing cells (Figure 4.14). At the protein level however, exposure to either AT-2 HIV-1 (red bars, upper panel)

or pvHIV-1 (green bars, lower panel) seemed to lead to a decrease in c-MYC expression, both in the parent and EBNA2-expressing cell lines (Figure 4.15).

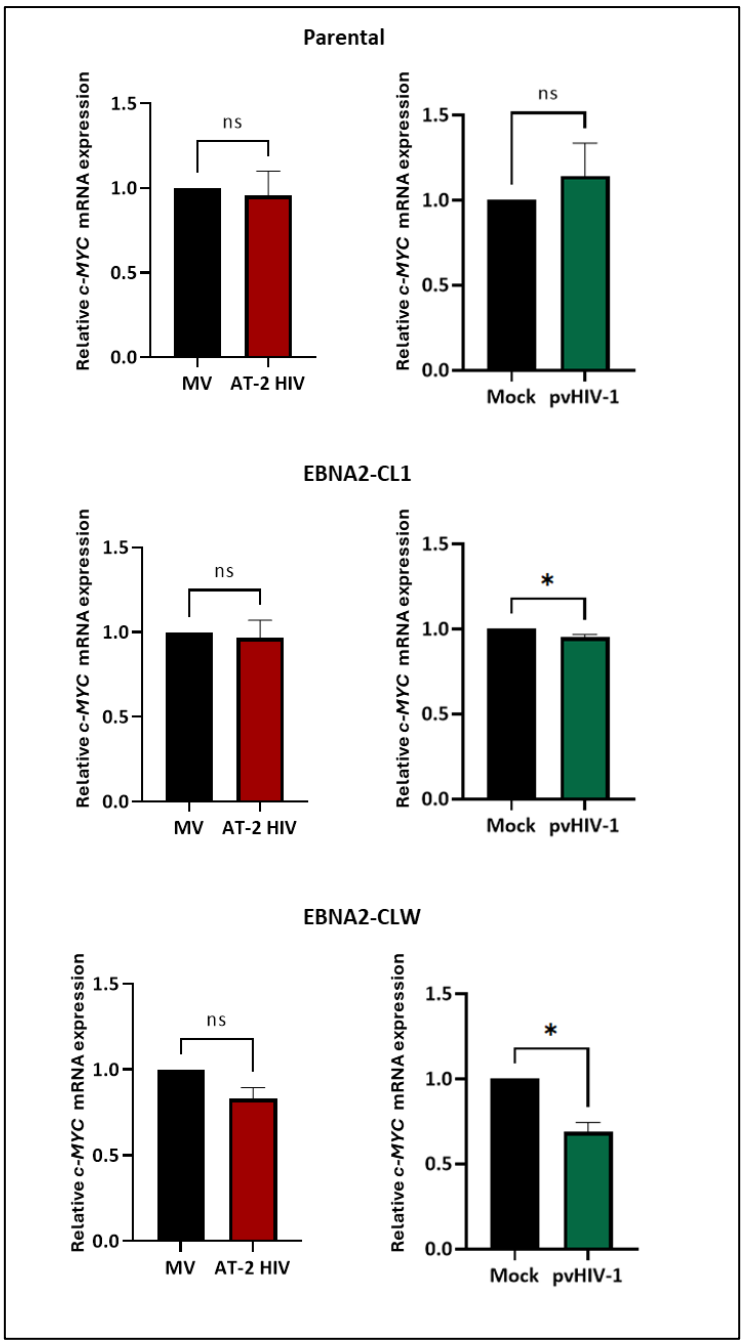

Figure 4.14: Effect of HIV-1 exposure on *c-MYC* expression. qPCR analysis assessing *c-MYC* mRNA levels after exposure to either AT-2 HIV-1 or pvHIV-1 in parental cells (upper panel) and EBNA2-expressing cells, CL1 (middle panel) and CLW (lower panel). Results are shown relative to the respective controls (MV or Mock). qPCR data is a representation of two independently conducted experiment normalized to GAPDH. Statistical analysis was performed using GraphPad Prism 9 (Students t test, two-tailed, *p ≤ 0.05).

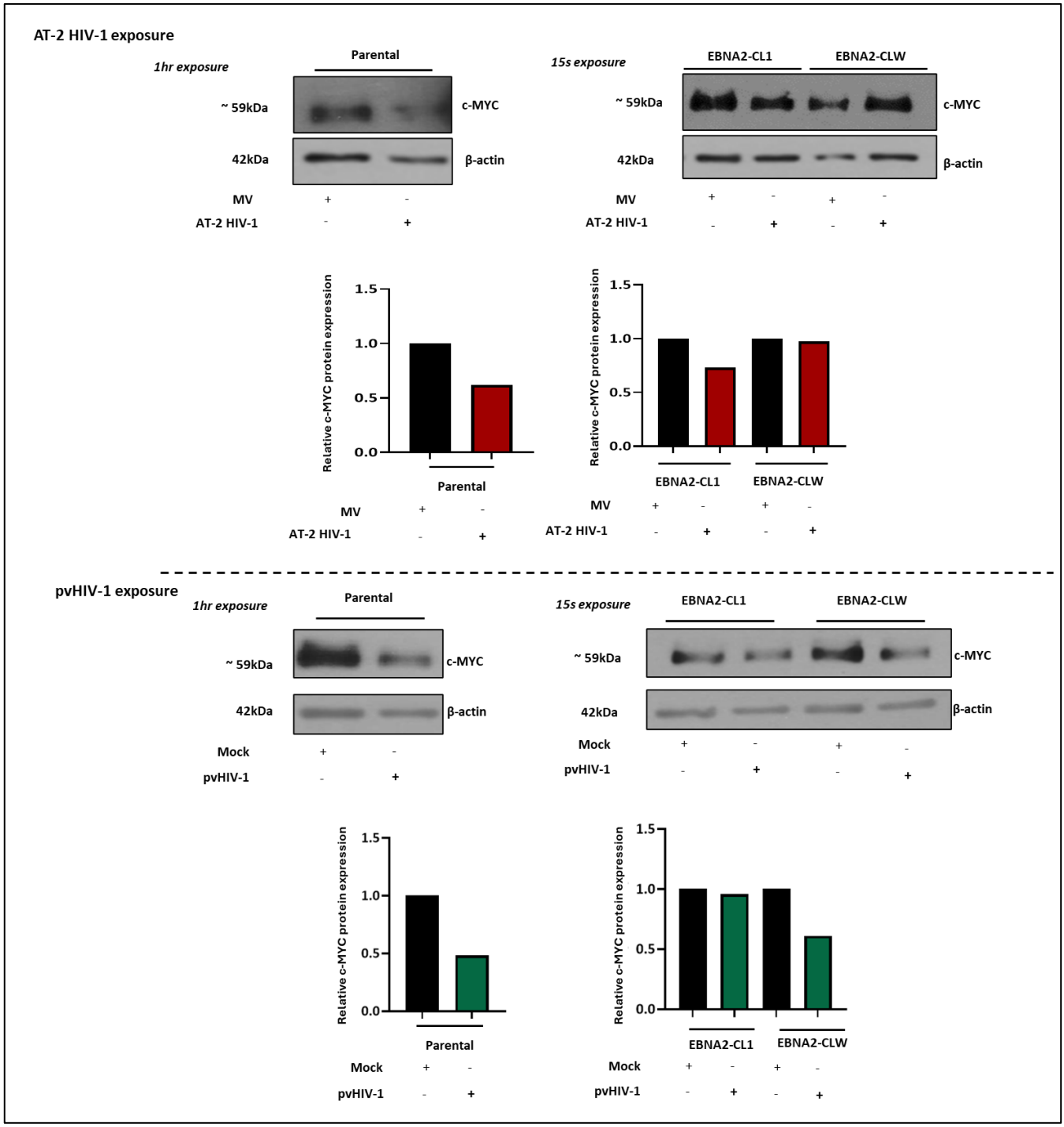

Figure 4.15: Effect of HIV-1 exposure on c-MYC expression. Western blot experiments using anti-c-MYC antibody (Abcam, [Y69] 32072), demonstrated reduced c-MYC expression in cells exposed to either AT-2 HIV-1 (upper panel) or pvHIV-1 (lower panel), relative to their respective control (MV or Mock). In cases where c-MYC expression was highly elevated in EBNA2-expressing cells, parental and EBNA2-CL1 and -CLW cells were exposed for different durations to avoid overexposure and obtain bands suitable for quantification. The experiment was performed in duplicate and the above result is a representative on the result. Protein levels were normalized to β-actin (Santa Cruz Biotechnology, sc-47778), using ImageJ.

4.4 Discussion

Due to limited and contrasting studies on the expression and relevance of PD-L1 in DLBCL, this study sought to provide insight into the significance and regulation of PD-L1, in an EBV- and HIV-positive setting, using in silico analyses, as well as a DLBCL cell model.

The ABC and GCB subtypes of DLBCL are molecularly distinct with unique alterations in specific signalling pathways and genes (324), and our in silico analyses show a probable inverse correlation between c-MYC and PD-L1 expression within the ABC subtype of DLBCL, which was consolidated through analysis of expression using a panel of established DLBCL cell lines available in our laboratory.

Several molecular alterations contributing to PD-L1 expression in the ABC subtype have been described. For example, as mentioned in chapter 1, *IGH* translocations and alterations in chromosome 9p24.1 are associated with PD-L1 expression in DLBCL and Georgiou et al. reported that cytogenetic alterations at this locus were commonly seen in the ABC subtype compared to the GCB (325). Additionally, approximately one third of ABC-DLBCLs harbour a mutation in *MYD88,* resulting in the persistent activation of the JAK/STAT pathway and ultimately inducing PD-L1 expression (326, 327). Another mechanism driving PD-L1 expression in ABC-DLBCLs implicates BCR signalling, which is constitutively activated in this subtype. In recent years, Wang and colleagues validated the link between PD-L1 expression and BCR signalling through in vitro assays. It was demonstrated that PD-L1 expression was detected in BCR-dependant cell lines and not in BCR-independent cell lines, and that loss of BCR signalling lead to reduced PD-L1 expression at the mRNA and protein levels (297). Overall, the preferential expression of PD-L1 in ABC-DLBCLs, driven by several mechanisms, most likely contributes to the aggressive nature of this subtype. Furthermore, our findings have also shown that high expression of PD-L1 is associated with a poor PFS in DLBCL patients, which is line with several other studies reporting that PD-L1 expression is related to a poor prognosis (242, 328, 329, 330, 331). Therefore, since we have shown that PD-L1 is elevated in the ABC subtype, which is known to be highly aggressive, one can infer that the more aggressive nature of ABC-DLBCLs may in part be attributed to elevated PD-L1 expression which ultimately promotes immune evasion and tumour progression; whereas GCB-DLBCL is associated with a better clinical outcome, as there is little to no PD-L1 expression (332, 333).

Expression of c-MYC was detected at relatively high levels in all DLBCL cell lines included in this study, at both the mRNA and protein levels, which is expected, since c-MYC is a known driver of DLBCL (59). Our findings suggested a higher expression level of c-MYC in cell lines assigned to the GCB subtype, compared to the ABC subtypes. As discussed in chapter 1, approximately 30% of DLBCLs carry overexpression of c-MYC which, along with BCL2, is defined as double-expressor DLBCL (DEL), while

up to 10% of cases harbour a *c-MYC* translocation, with *BCL2/BCL6*, termed as double-hit DLBCL (DHL) (46). According to reports, most of DHLs are of a GCB subtype while DELs occur more frequently within the ABC subtype (334, 335), indicating that c-MYC dysregulation is associated with both subtypes of DLBCL, and the mechanism of dysregulation varies based on the subtype.

Interestingly, in-silico analysis using TCGA data suggests a potential inverse correlation between PD-L1 and c-MYC in the ABC subtype. While the TCGA analysis comprised of less ABC datasets (n=15) than GCB datasets (n=22), the association between *c-MYC* and *PD-L1* expression was stronger in the ABC subtype, which may potentially reflect a true scenario. Furthermore, similarly to what was observed for the ABC subtype, the unclassified subtype of DLBCL (UC) was associated with elevated expression of *PD-L1*, and an inverse correlation between *c-MYC* and *PD-L1*. Although the UC category of DLBCL is a distinct subtype, it is classified as having complex genetic and molecular features which is closer in form to the ABC subtype, rather than the GBC subtype (335). The inverse correlation between c-MYC and PD-L1 was further demonstrated in a c-MYC knock down model, using CRISPR-Cas9 technology, at the transcriptional level.

This inverse trend has also been reported by other investigators (242, 300). Two retrospective studies, conducted by independent researchers examined the expression of PD-L1 in tissues from DLBCL patients. By performing IHC assays on 204 DLBCL patient FFPE tissues, Hu and colleagues demonstrated a negative correlation between PD-L1 and c-MYC in the TME (242). Interestingly, Elbæk and colleagues employed an IHC-based approach coupled with RNA sequencing, and concluded that PD-L1 mRNA and protein levels were significantly lower in patients with a MYC translocation (300). This is especially interesting since, as mentioned, most DHL cases, which contain c-MYC translocations, are assigned to the GCB subtype. This may suggest that c-MYC acts as negative regulator of PD-L1 in GCB-DLBCL, keeping in mind that we have demonstrated higher c-MYC expression in our GCB-like cell lines, coupled with very low *PD-L1* mRNA copy numbers. As discussed earlier, several other molecular mechanisms are implicated in the upregulation of PD-L1 in ABC-DLBCL, so it is highly probable that in the ABC subtype, c-MYC is not a fundamental regulator of PD-L1, whereas in the GCB subtype, it may function as a repressor.

The inability to detect PD-L1 expression at the protein level within the OCY-LY1 cell line could be due to the fact that this protein is already expressed at low levels, since this is cell line is derived from a GCB tumour. This, combined with technical aspects, including inadequate sensitivity of the western blot assay and antibody. Another possibility to consider is that, while c-MYC altered PD-L1 expression at the transcriptional level, there may be post-transcriptional mechanisms in place which negatively regulate PD-L1 protein expression. Indeed, glycosylation, ubiquitination and phosphorylation are but

a few of several post-transcriptional modifications of the protein which influence its stability and availability within cells (336). Additionally, miRNA-mediated regulation may also be a possible post-transcriptional mechanism negatively regulating PD-L1 expression.

While total knock out of c-MYC was expected, this was not achieved. Recently, evidence has emerged demonstrating that the CRISPR-Cas9 gene editing system does not always guarantee a complete gene knockout (337). Mechanisms responsible for incomplete knockout using the CRISPR-Cas9 system include (i) altered splicing, which skips the exon containing the premature termination codon and ultimately allows for functional proteins to be produced, and (ii) initiation of translation from an alternative site, preventing gene disruption (337, 338). It is important to mention that c-MYC has three isoforms as a result of alternative promoters which produces c-MYC proteins with slight variations in size (339). The two primary isoforms of c-MYC (p65 and p67) are generated by alternative initiation of translation (340), which may explain the partial knockdown observed with CRISPR-Cas9 editing.

Furthermore, the multiple isoforms associated with c-MYC also explains why in some western blotting experiments, two bands were observed for c-MYC. Interestingly, the western blot experiments that produced one single band of c-MYC (Figure 4.15) included protein samples isolated using the commercial AllPrep DNA/RNA/Protein mini kit (Qiagen, Germany), which was used to obtain matched protein and RNA products simultaneously from the same sample. These protein pellets were resuspended in a buffer containing a higher concentration of SDS (5%), which is a strong protein denaturant. Since high SDS concentration as well as its ratio to protein is reported to affect protein structure (341), it is possible that the double band observed is as a result of incomplete denaturation of the protein samples during gel separation.

While our findings strongly suggest that c-MYC is a negative regulator of PD-L1 expression, whether or not this occurs through a direct or indirect mechanism remains unclear and was not assessed within the scope of this study. To the best of our knowledge, only one E-box element within the *PD-L1* promoter has been previously described, by Maeda and colleagues, who demonstrated mechanistically, using a TNBC cell model, that c-MYC was recruited to the promoter of *PD-L1* by MUC1-C to promote activation. Furthermore, Maeda et al. demonstrated that targeting of MUC1-C resulted in downregulated c-MYC, which in turn reduced c-MYC occupancy on the *PD-L1* promoter, and ultimately reduced PD-L1 activation (296). Our study identified four other putative MYC-binding sites within the *PD-L1* promoter and warrants further studies into the relevance of these sites in the potential transcriptional regulation of PD-L1, not only in DLBCL, but in other cancers as well.

As stated in previous sections, EBNA2 is a known up-regulator of both PD-L1 and c-MYC expression. This was confirmed in our study where we observed significant increased expression of these factors

in EBNA2-expressing DLBCL cells, at both the mRNA and protein levels. In 1999, Kaiser et al. demonstrated that *c-MYC* is induced by EBNA2, using a cell model system (342). Furthermore, EBNA2 was reported to activate *MYC* through recruitment of EBF1, thereby promoting cellular proliferation of infected B cells (343). Earlier this year, a study was published offering more insight into the upregulation of c-MYC by EBNA2. Interestingly, EBNA2 was shown to not only positively impact c-MYC expression, but also that of miR-24, a negative regulator of c-MYC (323). It was demonstrated that transfection with anti-miR-24 compounds led to an even further increase in c-MYC expression, which ultimately resulted in apoptosis (323). c-MYC is capable of exerting both pro-apoptotic and pro-proliferative functions (344) and the investigation by Leopizzi and colleagues demonstrated that EBNA2 supports pro-proliferative levels of c-MYC by inducing miR-24, avoiding c-MYC-induced apoptosis (323). As mentioned earlier, Anastasiadou and colleagues showed that EBNA2 upregulates PD-L1 by downregulating its negative regulator, miR-34a; and a study by Yanagi and colleagues confirmed EBNA2 binding sites in the PD-L1 promoter (124, 125). Interestingly, between the two EBNA2-expressing clones, we consistently observed more PD-L1 protein levels in CL1, and our earlier results also showed that CL1 had a higher expression level of EBNA2, compared to CLW. This demonstrates the correlation between EBNA2 and PD-L1. The two EBNA2-expressing clones were generated by Boccellato and colleagues, and variability between clones is a common phenomenon (309).

To study the effect of HIV-1 on PD-L1 expression in DLBCL cells, the latter were exposed to two different laboratory strains of HIV-1, both non-infectious, and designed to facilitate and reduce the risk of performing in vitro studies using an infectious pathogen. Since the AT-2 HIV-1 viral particles are non-infectious, it is impossible to assess its viability after it is produced, and thus we decided to use two independent systems, with the second HIV-1 viral particle being the pseudovirus HIV-1. A major difference between AT-2 HIV-1 and pvHIV-1 particles is that AT-2 HIV-1 virions can bind cells, and are unable to enter the cells, while pvHIV-1 can enter host cells, but no replication or further growth can take place. However, since B cells lack the CD4 surface receptors, they cannot be host cells for HIV. Nevertheless, early reports demonstrated that HIV could interact with B cells via CD21 expressed on the surface of B cells (190). The data generated using both systems were consistent, thus conferring validity and reliability to our experimental approach. Additionally, in both instances, the appropriate and corresponding controls were used, to further validate and strengthen the data.

Following either form of HIV-1 exposure, DLBCL cells displayed reduced PD-L1 protein levels relative to the control, and this appeared to be regardless of EBNA2 expression. While this finding does not align with our observations presented in the investigations performed in aims 1 and 2 (presented in chapters 2 and 3), where PD-L1 levels were elevated in the blood and tumour tissues of HIV-positive

DLBCL patients, it is important to note that, in the current case, the investigation involved the use of a DLBCL cell line, cultured in vitro, and without cytokine stimulations or a co-culture set-up. While cell lines are important tools in molecular biology, they do not accurately represent primary cells and/or the disease physiology and/or the tumour microenvironment. This likely explains the non-concordant result obtained, but also indicates that the upregulation of PD-L1, in the context of HIV infection, happens within other immune cell populations, and not necessarily on within the DLBCL tumour cells. It is also plausible that PD-L1 may be elevated on DLBCL tumour cells in the presence of HIV but in an indirect manner. A way to explore this would be to perform the study using a co-/ multi-culture system and use primary cells rather than cell lines. An example of a co-culture system was demonstrated in the context of EBV-positive DLBCL, performed by Quan and colleagues, whereby they co-cultured T cells and DLBCL cell lines and demonstrated that DLBCL cells augmented PD-1 expression on T cells and altered the proliferation and cytokine secretion of T cells (345).

Similarly to the findings for PD-L1 expression in response to HIV-1 exposure, we have also demonstrated that exposing DLBCL cells to HIV-1 decreased expression of c-MYC at the protein level. This contradicts findings in the literature where c-MYC is reported to be further elevated in DLBCL in the presence of HIV, again, highlighting the difference in results observed between cell lines and patient-derived specimens, and the importance of supporting microenvironmental cells. Studies have reported high expression of c-MYC in HIV-positive DLBCL tumours (346, 347), and in addition, a recent report revealed that HIV-positive DLBCL patients were more prone to MYC mutations, and this was associated with a worse prognosis when compared to HIV-negative DLBCL patients (57). Two independent studies within our laboratory have shown that c-MYC expression is enhanced in Burkitt Lymphoma (BL) cells exposed to HIV proteins, Nef and Tat (20, 21). Rios et al. demonstrated that c-MYC expression was elevated in BL cells electroporated to express Tat; while Mdletshe and colleagues demonstrated that exposing BL cells to recombinant Nef increased transcription of c-MYC (20, 21). These studies suggested that HIV proteins can directly contribute to the HIV-associated BL by, in part, upregulating c-MYC. In DLBCL specifically, there are hardly any mechanistic reports on the effect of HIV on c-MYC levels in cell models, and our result in DLBCL, relative to our previous findings in BL, indicate that the pathophysiology of BL and DLBCL, in the presence of HIV, are quite distinct.

In an attempt to further consolidate the findings of our in vitro study using DLBCL cell lines, we explored the mRNA expression of *PD-L1* in a HIV-1 Tat-expressing HBL-1 DLBCL cell line model which had been developed in the laboratory to study the oncogenic potential of this viral protein. Although HIV does not directly infect B cells, Tat is secreted from infected cells and we and others have shown that this viral protein can be internalized by B cells where it enhances oncogenic events (20, 348). The Tat-transduced HBL-1 cell line was generated through lentivirus transduction by Dr Leonardo Alves de

Souza Rios, who kindly donated cDNA for a qPCR experiment. As shown in Supplemental Figure 2 (Appendix C), *PD-L1* expression was significantly decreased in HBL-1 cells expressing Tat relative to the cells transduced with the empty control. This finding is in concordance with our findings presented here, and thus confirms that the data is true and valid, albeit, not a reflection of what may be seen within the in vivo context.

Interestingly, several investigations have explored co-culture systems in DLBCL. For example, in 2015, Appollonio and colleagues established through a co-culture set-up that DLBCL tumour cells were able to reprogram primary human lymphatic fibroblasts into cancer-associated fibroblasts, which were shown to express markedly high levels of PD-L1 (349).

Overall, our study has revealed novel and important findings on the status of PD-L1 in DLBCL and its regulation by c-MYC and HIV-1, using in silico analyses and cell culture models, emphasizing the necessity of the use of co-culture systems in cancer-immunology studies.

Chapter 5

Summary and concluding remarks

Although the majority of DLBCL patients achieve remission after treatment with R-CHOP, there remains an urgent need for improved therapeutic strategies since up to 40% of patients experience relapsed or refractory disease and will eventually succumb to their disease (350, 351). The outcome of HIV-associated DLBCL is even worse and remains inferior despite the introduction of cART, within low-income settings, where the prevalence of these cancers are higher than elsewhere in the world (65, 67, 68). DLBCL is an extremely heterogenous disease, and a deeper insight into the biological mechanisms influencing its clinical behaviour remains a persisting need if we are to improve treatment and management of this disease (352, 353). DLBCL has conventionally been classified into two main subtypes based on the COO and upon further in-depth molecular profiling, additional genetic groups of DLBCL have been uncovered, according to distinct mutational profiles (39, 41, 354). These kinds of studies expand the molecular understanding of DLBCL and ultimately aid in improving therapeutic strategies and disease outcomes.

In South Africa, which has the highest HIV incidence worldwide, DLBCL represents up to 43% of diagnosed NHLs (153). HIV-associated DLBCL is a distinct entity, and the molecular events promoting the aggressive nature of HIV-associated DLBCL remains poorly understood (160). In the last few decades, the PD-1/PD-L1 axis has been shown to be a significant driver of immune evasion of tumour cells, and blockade of this signalling axis via monoclonal antibody therapy has achieved significant success in several cancer types, but the same success has not been achieved in DLBCL (355). Collectively, current published data show that the role and regulation of the PD-1/PD-L1 axis is ill-defined. For example, the oncogene c-MYC is a well-established driver of lymphomagenesis, and a number of investigators have reported contradictory findings of the association between c-MYC and PD-L1 in DLBCL (306). Additionally, although recent studies have shown that PD-L1 is elevated in HIV-positive patients (96, 104, 356), there is a scarcity of studies exploring the molecular mechanisms associated with overexpression and even more so, the status of PD-L1 in HIV-associated DLBCL remains largely unstudied. This study therefore sought to provide insight into the significance and regulation of PD-L1 in DLBCL, and specifically within the context of HIV-infection, using patient samples, in silico modelling, and established cell line models.

The findings from chapter 2 and 3 uncovered an elevation of PD-L1-expressing cells in both the peripheral blood and tumour specimens of HIV-positive DLBCL patients, despite the two sites being

two different biological entities. This aligns with the clinical characteristic of HIV-associated DLBCLs as being more aggressive than HIV-negative DLBCLs, having poorer response to treatment, and poorer patient outcomes (17). In HIV-infection, PD-L1 was reported to be highly expressed on regulatory T cells (Tregs), which are involved in promoting an immunosuppressive state (357). Furthermore, PD-L1 was also demonstrated to be elevated on another immunosuppressive cell type, Bregs, in HIV-positive patients prior to the onset of DLBCL (126). In our study, we observed high variability in the proportions of Bregs and PD-L1$^+$ Bregs in HIV-positive and -negative newly diagnosed DLBCL patients, and no noticeable difference between the two patient groups; suggesting that while HIV promotes upregulation of PD-L1, this phenomenon may be required to drive lymphoma development but may not necessarily be maintained once the cancer is established. Within the TME, we observed a lower infiltration rate of CD8$^+$ cytotoxic T cells and while this finding is not commonly reported in the literature, this subpopulation of T cells represents a crucial component of the immune system, and a lower infiltration of CD8$^+$ T cells indicate less cytotoxic activity occurring in the presence of HIV, and thus higher tolerance for this virus. The reduced infiltration of CD8$^+$ T cells may be directly caused by HIV through its action on CD4$^+$ T cells, or indirectly, via the dysregulation of other entities, or both. Although upregulation of PD-L1 by HIV was not demonstrated using cell models (Chapter 4), this highlights the importance of the surrounding microenvironment, which directly interacts with tumour cells, influencing all aspects of tumour biology (197). Additionally, PD-L1 expression can be found on multiple other cell types, in addition to tumour cells, and therefore HIV may be upregulating PD-L1 expression on other cell types, resulting in the elevated status we observed in patient-derived specimens (chapters 2 and 3). Additionally, increased expression of c-MYC in HIV-associated DLBCL is well-established in the literature (153, 347) but exposure to inactivated forms of HIV-1 on a DLBCL cell model did not mimic this phenomenon. This further signifies that tumour cells are dependent on signals from their surroundings and do not act independently (210, 358).

An aspect of this study focussed on exploring the potential regulation of PD-L1 by c-MYC in DLBCL, since current literature indicates contrasting findings (Chapter 4). In-silico analyses suggested an inverse association between PD-L1 and c-MYC, specifically within the ABC-DLBCL subtype, and this was consolidated using in vitro approaches, which strongly implies that c-MYC acts a negative regulator of PD-L1 in DLBCL, but that this axis is restricted to certain DLBCL subtypes.

5.1 Conclusion

Collectively, this study uncovered a unique status of elevated PD-L1 in patient-derived peripheral blood and tumour tissue samples of HIV-positive DLBCL patients in South Africa, suggesting that infection with HIV promotes an immunosuppressive state in DLBCL through overexpression of PD-L1 on multiple immune cell populations. While DLBCL tumour cells were not high expressors of PD-L1 in the presence of HIV, when using a cell model approach, this does not rule out the expression of PD-L1 by DLBCL tumour cells. Instead, it highlights the importance of surrounding immune cells which interacts with and influences tumour cells. In the present context, it is possible that surrounding immune cells may either (a) act as the primary expressors of PD-L1, or (b) serve as a mediator between HIV-1 and DLBCL tumour cells, facilitating the necessary signals for tumour cells to express PD-L1. This study uncovered the significance of PD-L1 in HIV-associated DLBCL and indicates that the PD-L1 blockade within this patient group may prove beneficial. The study also highlights the need for further comprehensive analyses to disentangle the deep complexity of this disease.

References

1. Storck K, Brandstetter M, Keller U, Knopf A. Clinical presentation and characteristics of lymphoma in the head and neck region. Head & face medicine. 2019;15(1):1.
2. Ninkovic S, Lambert J. Non-Hodgkin lymphoma. Medicine. 2017;45(5):297-304.
3. Jitani AK, Khonglah Y, Kumar R, Gogoi BB, Jajodia E. Natural Killer Cell Lymphoma: A Case with Classification Dilemma. Journal of clinical and diagnostic research : JCDR. 2016;10(2):Ed07-8.
4. Ekstrom-Smedby K. Epidemiology and etiology of non-Hodgkin lymphoma--a review. Acta Oncol. 2006;45(3):258-71.
5. Pasqualucci L, Bereshchenko O, Niu H, Klein U, Basso K, Guglielmino R, et al. Molecular pathogenesis of non-Hodgkin's lymphoma: the role of Bcl-6. Leuk Lymphoma. 2003;44 Suppl 3:S5-12.
6. Crisci S, Di Francia R, Mele S, Vitale P, Ronga G, De Filippi R, et al. Overview of Targeted Drugs for Mature B-Cell Non-hodgkin Lymphomas. Front Oncol. 2019;9:443.
7. Ansell SM. Non-Hodgkin Lymphoma: Diagnosis and Treatment. Mayo Clin Proc. 2015;90(8):1152-63.
8. Singh R, Shaik S, Negi BS, Rajguru JP, Patil PB, Parihar AS, et al. Non-Hodgkin's lymphoma: A review. J Family Med Prim Care. 2020;9(4):1834-40.
9. Bowzyk Al-Naeeb A, Ajithkumar T, Behan S, Hodson DJ. Non-Hodgkin lymphoma. BMJ. 2018;362:k3204.
10. Xie M, Leroy H, Mascarau R, Woottum M, Dupont M, Ciccone C, et al. Cell-to-Cell Spreading of HIV-1 in Myeloid Target Cells Escapes SAMHD1 Restriction. mBio. 2019;10(6):10.1128/mbio.02457-19.
11. Welsh RA, Song N, Sadegh-Nasseri S. How Does B Cell Antigen Presentation Affect Memory CD4 T Cell Differentiation and Longevity? Frontiers in immunology. 2021;12.
12. Saharia KK, Koup RA. T Cell Susceptibility to HIV Influences Outcome of Opportunistic Infections. Cell. 2013;155(3):505-14.
13. Kirkoyun Uysal H, Koksal MO, Sarsar K, Soguksu P, Erkose Genc G, Yapar G, et al. Distribution of Opportunistic Pathogens in People Living with HIV at a University Hospital in Istanbul over a One-Year Treatment Period and Its Association with CD4 T Cell Counts. Pathogens. 2023;12(10):1226.
14. Hübel K. The Changing Landscape of Lymphoma Associated with HIV Infection. Current Oncology Reports. 2020;22(11):111.
15. Chen Y, Zhao J, Sun P, Cheng M, Xiong Y, Sun Z, et al. Estimates of the global burden of non-Hodgkin lymphoma attributable to HIV: a population attributable modeling study. EClinicalMedicine. 2024;67:102370.
16. Somay K, Çöpür S, Osmanbaşoğlu E, Masyan H, Arslan H, Akay OM, et al. HIV-ASSOCIATED NON HODGKIN LYMPHOMA: A CASE SERIES STUDY FROM TURKEY. Afr J Infect Dis. 2020;14(2):42-7.
17. Huguet M, Navarro JT, Moltó J, Ribera JM, Tapia G. Diffuse Large B-Cell Lymphoma in the HIV Setting. Cancers (Basel). 2023;15(12).
18. Breen EC, Hussain SK, Magpantay L, Jacobson LP, Detels R, Rabkin CS, et al. B-cell stimulatory cytokines and markers of immune activation are elevated several years prior to the diagnosis of systemic AIDS-associated non-Hodgkin B-cell lymphoma. Cancer Epidemiol Biomarkers Prev. 2011;20(7):1303-14.
19. Mowla S. Addressing the Challenges of HIV/AIDS-Defining NonHodgkin's Lymphomas in Sub-Saharan Africa. Clinics in Oncology. 2017;2(1366).
20. Alves de Souza Rios L, Mapekula L, Mdletshe N, Chetty D, Mowla S. HIV-1 Transactivator of Transcription (Tat) Co-operates With AP-1 Factors to Enhance c-MYC Transcription. Front Cell Dev Biol. 2021;9:693706.
21. Mdletshe N, Nel A, Shires K, Mowla S. HIV Nef enhances the expression of oncogenic c-MYC and activation-induced cytidine deaminase in Burkitt lymphoma cells, promoting genomic instability. Infectious Agents and Cancer. 2020;15(1):54.
22. Zhang Y, Dai Y, Zheng T, Ma S. Risk Factors of Non-Hodgkin Lymphoma. Expert opinion on medical diagnostics. 2011;5(6):539-50.

23. Susanibar-Adaniya S, Barta SK. 2021 Update on Diffuse large B cell lymphoma: A review of current data and potential applications on risk stratification and management. Am J Hematol. 2021;96(5):617-29.
24. Chen B-J, Fend F, Campo E, Quintanilla-Martinez LJAoL. Aggressive B-cell lymphomas—from morphology to molecular pathogenesis. 2019. 2019;3.
25. Dubey AP, Singh R, Rathore A, Kapoor R, Sharma D, Singh N, et al. Diffuse large b-cell lymphoma-review. Journal of Medical Sciences. 2018;0(0).
26. Pratap S, Scordino TS. Molecular and cellular genetics of non-Hodgkin lymphoma: Diagnostic and prognostic implications. Exp Mol Pathol. 2019;106:44-51.
27. Clipson A, Barrans S, Zeng N, Crouch S, Grigoropoulos NF, Liu H, et al. The prognosis of MYC translocation positive diffuse large B-cell lymphoma depends on the second hit. J Pathol Clin Res. 2015;1(3):125-33.
28. Stebegg M, Kumar SD, Silva-Cayetano A, Fonseca VR, Linterman MA, Graca L. Regulation of the Germinal Center Response. 2018;9(2469).
29. Wen R, Wang D. MCD-DLBCL arises from germinal center B cells. Blood. 2022;140(10):1058-9.
30. Nowakowski GS, Czuczman MSJASoCOEB. ABC, GCB, and double-hit diffuse large B-cell lymphoma: does subtype make a difference in therapy selection? 2015;35(1):e449-e57.
31. Armitage JO, Gascoyne RD, Lunning MA, Cavalli F. Non-Hodgkin lymphoma. The Lancet. 2017;390(10091):298-310.
32. Quintanilla-Martinez L. IX. Is it only about MYC? How to approach the diagnosis of diffuse large B-cell lymphomas. Hematological Oncology. 2015;33(S1):50-5.
33. Frick M, Dorken B, Lenz G. The molecular biology of diffuse large B-cell lymphoma. Ther Adv Hematol. 2011;2(6):369-79.
34. Pfeifer M, Lenz G. PI3K/AKT addiction in subsets of diffuse large B-cell lymphoma. Cell Cycle. 2013;12(21):3347-8.
35. Frontzek F, Lenz G. Novel insights into the pathogenesis of molecular subtypes of diffuse large B-cell lymphoma and their clinical implications. Expert Rev Clin Pharmacol. 2019;12(11):1059-67.
36. Crombie JL, LaCasce AS. Epstein Barr Virus Associated B-Cell Lymphomas and Iatrogenic Lymphoproliferative Disorders. 2019;9(109).
37. Bojarczuk K, Chapuy B. Molecular classification of aggressive B-cell lymphoma. HemaSphere. 2019;3:116-8.
38. Dubois S, Jardin F. The role of next-generation sequencing in understanding the genomic basis of diffuse large B cell lymphoma and advancing targeted therapies. Expert Rev Hematol. 2016;9(3):255-69.
39. Schmitz R, Wright GW, Huang DW, Johnson CA, Phelan JD, Wang JQ, et al. Genetics and Pathogenesis of Diffuse Large B-Cell Lymphoma. N Engl J Med. 2018;378(15):1396-407.
40. Wright GW, Huang DW, Phelan JD, Coulibaly ZA, Roulland S, Young RM, et al. A Probabilistic Classification Tool for Genetic Subtypes of Diffuse Large B Cell Lymphoma with Therapeutic Implications. Cancer cell. 2020;37(4):551-68.e14.
41. Chapuy B, Stewart C, Dunford AJ, Kim J, Kamburov A, Redd RA, et al. Molecular subtypes of diffuse large B cell lymphoma are associated with distinct pathogenic mechanisms and outcomes. Nat Med. 2018;24(5):679-90.
42. Weber T, Schmitz R. Molecular Subgroups of Diffuse Large B Cell Lymphoma: Biology and Implications for Clinical Practice. Curr Oncol Rep. 2022;24(1):13-21.
43. Pophali PA, Marinelli LM, Ketterling RP, Meyer RG, McPhail ED, Kurtin PJ, et al. High level MYC amplification in B-cell lymphomas: is it a marker of aggressive disease? Blood Cancer Journal. 2020;10(1):5.
44. Jha RK, Kouzine F, Levens D. MYC function and regulation in physiological perspective. Frontiers in Cell and Developmental Biology. 2023;11.

45. Xia Y, Zhang X. The Spectrum of MYC Alterations in Diffuse Large B-Cell Lymphoma. Acta Haematol. 2020;143(6):520-8.
46. Laude M-C, Lebras L, Sesques P, Ghesquieres H, Favre S, Bouabdallah K, et al. First-line treatment of double-hit and triple-hit lymphomas: Survival and tolerance data from a retrospective multicenter French study. American Journal of Hematology. 2021;96(3):302-11.
47. Huang W, Medeiros LJ, Lin P, Wang W, Tang G, Khoury J, et al. MYC/BCL2/BCL6 triple hit lymphoma: a study of 40 patients with a comparison to MYC/BCL2 and MYC/BCL6 double hit lymphomas. Modern Pathology. 2018;31(9):1470-8.
48. Wang Y, Liu D, Zhang X, Zhang M, Li S, Feng X, et al. MYC overexpression but not MYC/BCL2 double expression predicts survival in bulky mass diffuse large B-cell lymphoma patients. Cancer Medicine. 2023;12(18):18568-77.
49. Spinner MA, Advani RH. Current Frontline Treatment of Diffuse Large B-Cell Lymphoma. Oncology (Williston Park). 2022;36(1):51-8.
50. Jakobsen LH, Øvlisen AK, Severinsen MT, Bæch J, Kragholm KH, Glimelius I, et al. Patients in complete remission after R-CHOP(-like) therapy for diffuse large B-cell lymphoma have limited excess use of health care services in Denmark. Blood Cancer Journal. 2022;12(1):16.
51. Nowakowski GS, Feldman T, Rimsza LM, Westin JR, Witzig TE, Zinzani PL. Integrating precision medicine through evaluation of cell of origin in treatment planning for diffuse large B-cell lymphoma. Blood Cancer J. 2019;9(6):48.
52. Salles G, Barrett M, Foa R, Maurer J, O'Brien S, Valente N, et al. Rituximab in B-Cell Hematologic Malignancies: A Review of 20 Years of Clinical Experience. Adv Ther. 2017;34(10):2232-73.
53. Held G, Pöschel V, Pfreundschuh M. Rituximab for the treatment of diffuse large B-cell lymphomas. Expert review of anticancer therapy. 2006;6(8):1175-86.
54. Thieblemont C, Brière J. MYC, BCL2, BCL6 in DLBCL: impact for clinics in the future? Blood. 2013;121(12):2165-6.
55. Xie Y, Pittaluga S, Jaffe ES. The histological classification of diffuse large B-cell lymphomas. Semin Hematol. 2015;52(2):57-66.
56. Cesarman E. Pathology of lymphoma in HIV. Curr Opin Oncol. 2013;25(5):487-94.
57. Peng Y, Ran L, Zhao M, Yang Z, Liu Y. High Frequency Mutant Genes and Prognosis Value of HIV-Related Diffuse Large B-Cell Lymphoma. Blood. 2023;142(Supplement 1):5723-.
58. Rubinstein PG, Aboulafia DM, Zloza A. Malignancies in HIV/AIDS: from epidemiology to therapeutic challenges. Aids. 2014;28(4):453-65.
59. McNally GA. HIV and Cancer: An Overview of AIDS-Defining and Non-AIDS-Defining Cancers in Patients With HIV. Clin J Oncol Nurs. 2019;23(3):327-31.
60. Ross AM, Leahy CI, Neylon F, Steigerova J, Flodr P, Navratilova M, et al. Epstein-Barr Virus and the Pathogenesis of Diffuse Large B-Cell Lymphoma. Life (Basel). 2023;13(2).
61. Morales D, Beltran B, De Mendoza FH, Riva L, Yabar A, Quiñones P, et al. Epstein–Barr virus as a prognostic factor in de novo nodal diffuse large B-cell lymphoma. Leukemia & Lymphoma. 2010;51(1):66-72.
62. Verdu-Bou M, Tapia G, Hernandez-Rodriguez A, Navarro JT. Clinical and Therapeutic Implications of Epstein-Barr Virus in HIV-Related Lymphomas. Cancers (Basel). 2021;13(21).
63. Chapman JR, Bouska AC, Zhang W, Alderuccio JP, Lossos IS, Rimsza LM, et al. EBV-positive HIV-associated diffuse large B cell lymphomas are characterized by JAK/STAT (STAT3) pathway mutations and unique clinicopathologic features. British Journal of Haematology. 2021;194(5):870-8.
64. de Carvalho PS, Leal FE, Soares MA. Clinical and Molecular Properties of Human Immunodeficiency Virus-Related Diffuse Large B-Cell Lymphoma. Front Oncol. 2021;11:675353.
65. Baptista MJ, Garcia O, Morgades M, Gonzalez-Barca E, Miralles P, Lopez-Guillermo A, et al. HIV-infection impact on clinical-biological features and outcome of diffuse large B-cell lymphoma treated with R-CHOP in the combination antiretroviral therapy era. AIDS. 2015;29(7):811-8.

66. Dwyer-Lindgren L, Cork MA, Sligar A, Steuben KM, Wilson KF, Provost NR, et al. Mapping HIV prevalence in sub-Saharan Africa between 2000 and 2017. Nature. 2019;570(7760):189-93.
67. Chen J, Wu Y, Kang Z, Qin S, Ruan G, Zhao H, et al. A promising prognostic model for predicting survival of patients with HIV-related diffuse large B-cell lymphoma in the cART era. Cancer Med. 2023;12(11):12470-81.
68. Vaccher E, Gloghini A, Volpi CC, Carbone A. Lymphomas in People Living with HIV. Hemato. 2022;3(3):527-42.
69. Coelho J, Roush SM, Xu AM, Puranam K, Mponda M, Kasonkanji E, et al. HIV and prior exposure to antiretroviral therapy alter tumour composition and tumour: T-cell associations in diffuse large B-cell lymphoma. British Journal of Haematology. 2024;n/a(n/a).
70. Kimani S, Painschab MS, Kaimila B, Kasonkanji E, Zuze T, Tomoka T, et al. Safety and efficacy of rituximab in patients with diffuse large B-cell lymphoma in Malawi: a prospective, single-arm, non-randomised phase 1/2 clinical trial. The Lancet Global Health. 2021;9(7):e1008-e16.
71. Pather S, Mohamed Z, McLeod H, Pillay K. Large cell lymphoma: correlation of HIV status and prognosis with differentiation profiles assessed by immunophenotyping. Pathol Oncol Res. 2013;19(4):695-705.
72. Magangane PS, Mohamed Z, Naidoo R. Diffuse large B-cell lymphoma in a high human immunodeficiency virus (HIV) prevalence, low-resource setting. 2020. 2020;4.
73. Noy A. Optimizing treatment of HIV-associated lymphoma. Blood. 2019;134(17):1385-94.
74. Little RF, Pittaluga S, Grant N, Steinberg SM, Kavlick MF, Mitsuya H, et al. Highly effective treatment of acquired immunodeficiency syndrome–related lymphoma with dose-adjusted EPOCH: impact of antiretroviral therapy suspension and tumor biology. Blood. 2003;101(12):4653-9.
75. Sparano JA, Lee JY, Kaplan LD, Levine AM, Ramos JC, Ambinder RF, et al. Rituximab plus concurrent infusional EPOCH chemotherapy is highly effective in HIV-associated B-cell non-Hodgkin lymphoma. Blood. 2010;115(15):3008-16.
76. Carbone A, Vaccher E, Gloghini A. Hematologic cancers in individuals infected by HIV. Blood. 2022;139(7):995-1012.
77. Cai Q, Medeiros LJ, Xu X, Young KH. MYC-driven aggressive B-cell lymphomas: biology, entity, differential diagnosis and clinical management. Oncotarget. 2015;6(36):38591-616.
78. Ghoreschi K, Laurence A, O'Shea JJ. Janus kinases in immune cell signaling. Immunol Rev. 2009;228(1):273-87.
79. Knoops L, Hornakova T, Royer Y, Constantinescu SN, Renauld JC. JAK kinases overexpression promotes in vitro cell transformation. Oncogene. 2008;27(11):1511-9.
80. Ding BB, Yu JJ, Yu RY-L, Mendez LM, Shaknovich R, Zhang Y, et al. Constitutively activated STAT3 promotes cell proliferation and survival in the activated B-cell subtype of diffuse large B-cell lymphomas. Blood. 2008;111(3):1515-23.
81. Chao C, Silverberg MJ, Xu L, Chen LH, Castor B, Martinez-Maza O, et al. A comparative study of molecular characteristics of diffuse large B-cell lymphoma from patients with and without human immunodeficiency virus infection. Clin Cancer Res. 2015;21(6):1429-37.
82. Cassim S, Antel K, Chetty DR, Oosthuizen J, Opie J, Mohamed Z, et al. Diffuse large B-cell lymphoma in a South African cohort with a high HIV prevalence: an analysis by cell-of-origin, Epstein-Barr virus infection and survival. Pathology. 2020;52(4):453-9.
83. Huber F, Zwickl-Traxler E, Pecherstorfer M, Singer J. Evaluation of Ki-67 as a Prognostic Marker in Diffuse Large B-Cell Lymphoma-A Single-Center Retrospective Cohort Study. Curr Oncol. 2021;28(6):4521-9.
84. Liu R, Li H-F, Li S. PD-1-mediated inhibition of T cell activation: Mechanisms and strategies for cancer combination immunotherapy. Cell Insight. 2024;3(2):100146.
85. Han Y, Liu D, Li L. PD-1/PD-L1 pathway: current researches in cancer. American journal of cancer research. 2020;10(3):727-42.
86. Velu V, Shetty RD, Larsson M, Shankar EM. Role of PD-1 co-inhibitory pathway in HIV infection and potential therapeutic options. Retrovirology. 2015;12:14.

87. Dong Y, Sun Q, Zhang X. PD-1 and its ligands are important immune checkpoints in cancer. Oncotarget. 2017;8(2):2171-86.
88. Riella LV, Paterson AM, Sharpe AH, Chandraker A. Role of the PD-1 pathway in the immune response. Am J Transplant. 2012;12(10):2575-87.
89. Sharpe AH, Pauken KE. The diverse functions of the PD1 inhibitory pathway. Nat Rev Immunol. 2018;18(3):153-67.
90. Qin W, Hu L, Zhang X, Jiang S, Li J, Zhang Z, et al. The Diverse Function of PD-1/PD-L Pathway Beyond Cancer. 2019;10(2298).
91. Chen R-Y, Zhu Y, Shen Y-Y, Xu Q-Y, Tang H-Y, Cui N-X, et al. The role of PD-1 signaling in health and immune-related diseases. Frontiers in immunology. 2023;14.
92. Sharpe AH, Pauken KE. The diverse functions of the PD1 inhibitory pathway. Nature Reviews Immunology. 2018;18(3):153-67.
93. Wang B, Chen C, Liu X, Zhou S, Xu T, Wu M. The effect of combining PD-1 agonist and low-dose Interleukin-2 on treating systemic lupus erythematosus. Frontiers in immunology. 2023;14.
94. Carosio R, Fontana V, Mastracci L, Ferro P, Grillo F, Banelli B, et al. Characterization of soluble PD-L1 in pleural effusions of mesothelioma patients: potential implications in the immune response and prognosis. J Cancer Res Clin Oncol. 2021;147(2):459-68.
95. vom Berg J, Kobold S. The need for speed: how PD1-blockade only works if T cells are properly activated. Translational Cancer Research. 2017;6(S6):S1018-S21.
96. Porichis F, Kaufmann DE. Role of PD-1 in HIV pathogenesis and as target for therapy. Curr HIV/AIDS Rep. 2012;9(1):81-90.
97. Trabattoni D, Saresella M, Biasin M, Boasso A, Piacentini L, Ferrante P, et al. B7-H1 is up-regulated in HIV infection and is a novel surrogate marker of disease progression. Blood. 2003;101(7):2514-20.
98. Velu V, Shetty RD, Larsson M, Shankar EM. Role of PD-1 co-inhibitory pathway in HIV infection and potential therapeutic options. Retrovirology. 2015;12(1):14.
99. Ensoli B, Moretti S, Borsetti A, Maggiorella MT, Buttò S, Picconi O, et al. New insights into pathogenesis point to HIV-1 Tat as a key vaccine target. Archives of Virology. 2021;166(11):2955-74.
100. Planès R, BenMohamed L, Leghmari K, Delobel P, Izopet J, Bahraoui E. HIV-1 Tat Protein Induces PD-L1 (B7-H1) Expression on Dendritic Cells through Tumor Necrosis Factor Alpha- and Toll-Like Receptor 4-Mediated Mechanisms. Journal of Virology. 2014;88(12):6672-89.
101. Wang X, Duan Z, Yu G, Fan M, Scharff MD. Human Immunodeficiency Virus Tat Protein Aids V Region Somatic Hypermutation in Human B Cells. mBio. 2018;9(2):10.1128/mbio.02315-17.
102. Nicoli F, Finessi V, Sicurella M, Rizzotto L, Gallerani E, Destro F, et al. The HIV-1 Tat Protein Induces the Activation of CD8+ T Cells and Affects In Vivo the Magnitude and Kinetics of Antiviral Responses. PLOS ONE. 2013;8(11):e77746.
103. Opi S, Péloponèse J-M, Esquieu D, Campbell G, de Mareuil J, Walburger A, et al. Tat HIV-1 Primary and Tertiary Structures Critical to Immune Response Against Non-homologous Variants*. Journal of Biological Chemistry. 2002;277(39):35915-9.
104. Munoz O, Banga R, Schelling R, Procopio FA, Mastrangelo A, Nortier P, et al. Active PD-L1 incorporation within HIV virions functionally impairs T follicular helper cells. PLOS Pathogens. 2022;18(7):e1010673.
105. Fiorentini S, Marini E, Caracciolo S, Caruso A. Functions of the HIV-1 matrix protein p17. New Microbiol. 2006;29(1):1-10.
106. Caccuri F, Marsico S, Fiorentini S, Caruso A, Giagulli C. HIV-1 Matrix Protein p17 and its Receptors. Curr Drug Targets. 2016;17(1):23-32.
107. Wu Y, Chen W, Xu ZP, Gu W. PD-L1 Distribution and Perspective for Cancer Immunotherapy-Blockade, Knockdown, or Inhibition. Frontiers in immunology. 2019;10:2022.
108. Cha JH, Chan LC, Li CW, Hsu JL, Hung MC. Mechanisms Controlling PD-L1 Expression in Cancer. Molecular cell. 2019;76(3):359-70.

109. Yi M, Niu M, Xu L, Luo S, Wu K. Regulation of PD-L1 expression in the tumor microenvironment. Journal of Hematology & Oncology. 2021;14(1):10.
110. Takahara T, Sakakibara A, Tsuyuki Y, Satou A, Kato S, Nakamura S. Diagnostic approach for classic Hodgkin lymphoma in small samples with an emphasis on PD-L1 expression and EBV harboring in tumor cells: a brief review from morphology to biology. J Clin Exp Hematop. 2023;63(2):58-64.
111. Glorieux C, Xia X, Huang P. The Role of Oncogenes and Redox Signaling in the Regulation of PD-L1 in Cancer. Cancers (Basel). 2021;13(17).
112. Prestipino A, Emhardt AJ, Aumann K, O'Sullivan D, Gorantla SP, Duquesne S, et al. Oncogenic JAK2(V617F) causes PD-L1 expression, mediating immune escape in myeloproliferative neoplasms. Sci Transl Med. 2018;10(429).
113. Wu M, Huang Q, Xie Y, Wu X, Ma H, Zhang Y, et al. Improvement of the anticancer efficacy of PD-1/PD-L1 blockade via combination therapy and PD-L1 regulation. Journal of Hematology & Oncology. 2022;15(1):24.
114. Guan J, Zhang J, Zhang X, Yuan Z, Cheng J, Chen B. Efficacy and safety of PD-1/PD-L1 immune checkpoint inhibitors in treating non-Hodgkin lymphoma: A systematic review and meta-analysis of clinical trials. Medicine (Baltimore). 2022;101(50):e32333.
115. Ansell SM. PD-1 Blockade in Classic Hodgkin Lymphoma. JCO Oncology Practice. 2021;17(2):72-3.
116. Green MR, Rodig S, Juszczynski P, Ouyang J, Sinha P, O'Donnell E, et al. Constitutive AP-1 Activity and EBV Infection Induce PD-L1 in Hodgkin Lymphomas and Posttransplant Lymphoproliferative Disorders: Implications for Targeted Therapy. Clinical Cancer Research. 2012;18(6):1611-8.
117. Dong C, Flavell RA. Cell fate decision: T-helper 1 and 2 subsets in immune responses. Arthritis Research & Therapy. 2000;2(3):179.
118. Alberts B, Johnson A, Lewis J, Raff M, Roberts K, Walter P. Molecular biology of the cell (4th ed.). New York: Garland Science,; 2002.
119. Wu X, Gu Z, Chen Y, Chen B, Chen W, Weng L, et al. Application of PD-1 Blockade in Cancer Immunotherapy. Computational and structural biotechnology journal. 2019;17:661-74.
120. Godfrey J, Tumuluru S, Bao R, Leukam M, Venkataraman G, Phillip J, et al. PD-L1 gene alterations identify a subset of diffuse large B-cell lymphoma harboring a T-cell–inflamed phenotype. Blood. 2019;133(21):2279-90.
121. Nakamura S, Ye H, Bacon CM, Goatly A, Liu H, Kerr L, et al. Translocations Involving the Immunoglobulin Heavy Chain Gene Locus Predict Better Survival in Gastric Diffuse Large B-Cell Lymphoma. Clinical Cancer Research. 2008;14(10):3002-10.
122. Wang Y, Wenzl K, Manske MK, Asmann YW, Sarangi V, Greipp PT, et al. Amplification of 9p24.1 in diffuse large B-cell lymphoma identifies a unique subset of cases that resemble primary mediastinal large B-cell lymphoma. Blood Cancer J. 2019;9(9):73.
123. Bi XW, Wang H, Zhang WW, Wang JH, Liu WJ, Xia ZJ, et al. PD-L1 is upregulated by EBV-driven LMP1 through NF-κB pathway and correlates with poor prognosis in natural killer/T-cell lymphoma. J Hematol Oncol. 2016;9(1):109.
124. Yanagi Y, Okuno Y, Narita Y, Masud H, Watanabe T, Sato Y, et al. RNAseq analysis identifies involvement of EBNA2 in PD-L1 induction during Epstein-Barr virus infection of primary B cells. Virology. 2021;557:44-54.
125. Anastasiadou E, Stroopinsky D, Alimperti S, Jiao AL, Pyzer AR, Cippitelli C, et al. Epstein-Barr virus-encoded EBNA2 alters immune checkpoint PD-L1 expression by downregulating miR-34a in B-cell lymphomas. Leukemia. 2019;33(1):132-47.
126. Epeldegui M, Conti DV, Guo Y, Cozen W, Penichet ML, Martinez-Maza O. Elevated numbers of PD-L1 expressing B cells are associated with the development of AIDS-NHL. Sci Rep. 2019;9(1):9371.

127. Lu T, Zhang J, Xu-Monette ZY, Young KH. The progress of novel strategies on immune-based therapy in relapsed or refractory diffuse large B-cell lymphoma. Experimental Hematology & Oncology. 2023;12(1):72.
128. Ansell SM, Minnema MC, Johnson P, Timmerman JM, Armand P, Shipp MA, et al. Nivolumab for Relapsed/Refractory Diffuse Large B-Cell Lymphoma in Patients Ineligible for or Having Failed Autologous Transplantation: A Single-Arm, Phase II Study. Journal of clinical oncology : official journal of the American Society of Clinical Oncology. 2019;37(6):481-9.
129. Frigault MJ, Armand P, Redd RA, Jeter E, Merryman RW, Coleman KC, et al. PD-1 blockade for diffuse large B-cell lymphoma after autologous stem cell transplantation. Blood Adv. 2020;4(1):122-6.
130. Younes A, Burke JM, Cheson BD, Diefenbach CS, Ferrari S, Hahn UH, et al. Safety and efficacy of atezolizumab with rituximab and CHOP in previously untreated diffuse large B-cell lymphoma. Blood Advances. 2023;7(8):1488-95.
131. Chekol Abebe E, Asmamaw Dejenie T, Mengie Ayele T, Dagnew Baye N, Agegnehu Teshome A, Tilahun Muche Z. The Role of Regulatory B Cells in Health and Diseases: A Systemic Review. J Inflamm Res. 2021;14:75-84.
132. Rosser EC, Mauri C. Regulatory B cells: origin, phenotype, and function. Immunity. 2015;42(4):607-12.
133. Mauri C, Bosma A. Immune Regulatory Function of B Cells. Annual Review of Immunology. 2012;30(Volume 30, 2012):221-41.
134. Catalán D, Mansilla MA, Ferrier A, Soto L, Oleinika K, Aguillón JC, et al. Immunosuppressive Mechanisms of Regulatory B Cells. Frontiers in immunology. 2021;12.
135. Shang J, Zha H, Sun Y. Phenotypes, Functions, and Clinical Relevance of Regulatory B Cells in Cancer. Frontiers in immunology. 2020;11:582657.
136. Jiao Y, Wang X, Zhang T, Sun L, Wang R, Li W, et al. Regulatory B cells correlate with HIV disease progression. Microbiol Immunol. 2014;58(8):449-55.
137. Miedema F, Tesselaar K, Baarle D, Borghans J, Hazenberg M, De Boer R. Immune Activation and Collateral Damage in AIDS Pathogenesis. Frontiers in immunology. 2013;4.
138. Association WM. World Medical Association Declaration of Helsinki: Ethical Principles for Medical Research Involving Human Subjects. JAMA. 2013;310(20):2191-4.
139. Schnizlein-Bick CT, Mandy FF, O'Gorman MRG, Paxton H, Nicholson JKA, Hultin LE, et al. Use of CD45 gating in three and four-color flow cytometric immunophenotyping: Guideline from the national institute of allergy and infectious diseases, division of AIDS. Cytometry. 2002;50(2):46-52.
140. Abbasi-Kenarsari H, Shafaghat F, Baradaran B, Movassaghpour AA, Shanehbandi D, Kazemi T. Cloning and Expression of CD19, a Human B-Cell Marker in NIH-3T3 Cell Line. Avicenna J Med Biotechnol. 2015;7(1):39-44.
141. Ramorola B. Molecular Characterisation of Diffuse Large B-cell Lymphoma in South Africa [PhD]. Cape Town, South Africa: University of Cape Town; 2022.
142. Dunleavy K, Wilson WH. Chapter 82 - Diagnosis and Treatment of Diffuse Large B-Cell Lymphoma and Burkitt Lymphoma. In: Hoffman R, Benz EJ, Silberstein LE, Heslop HE, Weitz JI, Anastasi J, et al., editors. Hematology (Seventh Edition): Elsevier; 2018. p. 1309-17.
143. Huang D, Berglund M, Damdimopoulos A, Antonson P, Lindskog C, Enblad G, et al. Sex- and Female Age-Dependent Differences in Gene Expression in Diffuse Large B-Cell Lymphoma-Possible Estrogen Effects. Cancers (Basel). 2023;15(4).
144. Chen B, Mao T, Qin X, Zhang W, Watanabe N, Li J. Role of estrogen receptor signaling pathway-related genes in diffuse large B-cell lymphoma and identification of key targets via integrated bioinformatics analysis and experimental validation. Front Oncol. 2022;12:1029998.
145. Bakhshi TJ, Georgel PT. Genetic and epigenetic determinants of diffuse large B-cell lymphoma. Blood Cancer Journal. 2020;10(12):123.

146. Yakimchuk K, Iravani M, Hasni MS, Rhönnstad P, Nilsson S, Jondal M, et al. Effect of ligand-activated estrogen receptor β on lymphoma growth in vitro and in vivo. Leukemia. 2011;25(7):1103-10.
147. Luo J, Wang SS, Lu Y, Sullivan-Halley J, Cozen W, Ma H, et al. Pregnancy-related factors and risk of B-cell non-Hodgkin lymphoma among women in Los Angeles. British Journal of Haematology. 2019;186(1):133-7.
148. Machailo J. Diffuse Large B-cell Lymphoma in adults at Chris Hani Baragwanath Academic Hospital [MMED]. Johannesburg, South Africa: University of the Witwatersrand; 2016.
149. Govender K, Beckett S, Reddy T, Cowden RG, Cawood C, Khanyile D, et al. Association of HIV Intervention Uptake With HIV Prevalence in Adolescent Girls and Young Women in South Africa. JAMA Network Open. 2022;5(4):e228640-e.
150. Chao C, Silverberg MJ, Martínez-Maza O, Chi M, Abrams DI, Haque R, et al. Epstein-Barr virus infection and expression of B-cell oncogenic markers in HIV-related diffuse large B-cell Lymphoma. Clin Cancer Res. 2012;18(17):4702-12.
151. Li J-W, Deng C, Zhou X-Y, Deng R. The biology and treatment of Epstein-Barr virus-positive diffuse large B cell lymphoma, NOS. Heliyon. 2024;10(1):e23921.
152. Olivier C, Luies L. WHO Goals and Beyond: Managing HIV/TB Co-infection in South Africa. SN Comprehensive Clinical Medicine. 2023;5(1):251.
153. Pather S, Patel M. HIV-associated DLBCL: Clinicopathological factors including dual-colour chromogenic in situ hybridisation to assess MYC gene copies. Annals of Diagnostic Pathology. 2022;58:151913.
154. Magangane PS, Mohamed Z, Naidoo R. Diffuse large B-cell lymphoma in a high human immunodeficiency virus (HIV) prevalence, low-resource setting. South African Journal of Oncology. 2020;4.
155. Hleyhel M, Belot A, Bouvier AM, Tattevin P, Pacanowski J, Genet P, et al. Risk of AIDS-Defining Cancers Among HIV-1–Infected Patients in France Between 1992 and 2009: Results From the FHDH-ANRS CO4 Cohort. Clinical Infectious Diseases. 2013;57(11):1638-47.
156. Risher KA, Cori A, Reniers G, Marston M, Calvert C, Crampin A, et al. Age patterns of HIV incidence in eastern and southern Africa: a modelling analysis of observational population-based cohort studies. The Lancet HIV. 2021;8(7):e429-e39.
157. Mamgain G, Singh PK, Patra P, Naithani M, Nath UK. Diffuse large B-cell lymphoma and new insights into its pathobiology and implication in treatment. Journal of Family Medicine and Primary Care. 2022;11(8):4151-8.
158. Morton LM, Kim CJ, Weiss LM, Bhatia K, Cockburn M, Hawes D, et al. Molecular characteristics of diffuse large B-cell lymphoma in human immunodeficiency virus-infected and -uninfected patients in the pre-highly active antiretroviral therapy and pre-rituximab era. Leuk Lymphoma. 2014;55(3):551-7.
159. Fedoriw Y, Selitsky S, Montgomery ND, Kendall SM, Richards KL, Du W, et al. Identifying transcriptional profiles and evaluating prognostic biomarkers of HIV-associated diffuse large B-cell lymphoma from Malawi. Mod Pathol. 2020;33(8):1482-91.
160. Maguire A, Chen X, Wisner L, Malasi S, Ramsower C, Kendrick S, et al. Enhanced DNA repair and genomic stability identify a novel HIV-related diffuse large B-cell lymphoma signature. Int J Cancer. 2019;145(11):3078-88.
161. Wu J, Miao Y, Qian C, Tao P, Wang X, Dong X, et al. Clinical characteristics and outcomes in HIV-associated diffuse large B-cell lymphoma in China: A retrospective single-center study. J Cancer. 2021;12(10):2903-11.
162. Grogg KL, Miller RF, Dogan A. HIV infection and lymphoma. J Clin Pathol. 2007;60(12):1365-72.
163. Bobillo S, Joffe E, Lavery JA, Sermer D, Ghione P, Noy A, et al. Clinical characteristics and outcomes of extranodal stage I diffuse large B-cell lymphoma in the rituximab era. Blood. 2021;137(1):39-48.

164. Ollila TA, Olszewski AJ. Extranodal Diffuse Large B Cell Lymphoma: Molecular Features, Prognosis, and Risk of Central Nervous System Recurrence. Curr Treat Options Oncol. 2018;19(8):38.
165. Huguet M, Navarro J-T, Moltó J, Ribera J-M, Tapia G. Diffuse Large B-Cell Lymphoma in the HIV Setting. Cancers. 2023;15(12):3191.
166. Tilahun M, Gedefie A, Ebrahim E, Seid A, Ali A, Shibabaw A, et al. Immuno-Haematological Abnormalities of HIV-Infected Patients Before and After Initiation of Highly Active Antiretroviral Therapy in the Antiretroviral Therapy Clinics of Six Health Facilities at Dessie Town, Northeast Ethiopia. J Blood Med. 2022;13:243-53.
167. Wallis ZK, Williams KC. Monocytes in HIV and SIV Infection and Aging: Implications for Inflamm-Aging and Accelerated Aging. Viruses. 2022;14(2).
168. Knudsen AD, Bouazzi R, Afzal S, Gelpi M, Benfield T, Høgh J, et al. Monocyte count and soluble markers of monocyte activation in people living with HIV and uninfected controls. BMC Infectious Diseases. 2022;22(1):451.
169. Vaughan J, Wiggill T, Lawrie D, Machaba M, Patel M. The prognostic impact of monocyte fluorescence, immunosuppressive monocytes and peripheral blood immune cell numbers in HIV-associated Diffuse Large B-cell Lymphoma. PLoS One. 2023;18(1):e0280044.
170. Chirumbolo S, Bjørklund G, Sboarina A, Vella A. The role of basophils as innate immune regulatory cells in allergy and immunotherapy. Human vaccines & immunotherapeutics. 2018;14(4):815-31.
171. Marone G, Varricchi G, Loffredo S, Galdiero MR, Rivellese F, de Paulis A. Are Basophils and Mast Cells Masters in HIV Infection? International Archives of Allergy and Immunology. 2016;171(3-4):158-65.
172. Jiang AP, Jiang JF, Guo MG, Jin YM, Li YY, Wang JH. Human Blood-Circulating Basophils Capture HIV-1 and Mediate Viral trans-Infection of CD4+ T Cells. J Virol. 2015;89(15):8050-62.
173. de Paulis A, De Palma R, Di Gioia L, Carfora M, Prevete N, Tosi G, et al. Tat Protein Is an HIV-1-Encoded β-Chemokine Homolog That Promotes Migration and Up-Regulates CCR3 Expression on Human FcεRI+ Cells1. The Journal of Immunology. 2000;165(12):7171-9.
174. Rossi FW, Prevete N, Rivellese F, Lobasso A, Napolitano F, Granata F, et al. HIV-1 Nef promotes migration and chemokine synthesis of human basophils and mast cells through the interaction with CXCR4. Clinical and Molecular Allergy. 2016;14(1):15.
175. Moir S, Malaspina A, Ho J, Wang W, DiPoto AC, O'Shea MA, et al. Normalization of B Cell Counts and Subpopulations after Antiretroviral Therapy in Chronic HIV Disease. The Journal of Infectious Diseases. 2008;197(4):572-9.
176. Madzime M, Rossouw TM, Theron AJ, Anderson R, Steel HC. Interactions of HIV and Antiretroviral Therapy With Neutrophils and Platelets. Frontiers in immunology. 2021;12.
177. Zhou M, Cheng J, Zhao H, Yang M, Yu W, Qin J, et al. Clinical Features, Phenotypic Markers and Outcomes of Diffuse Large B-Cell Lymphoma between HIV-Infected and HIV-Uninfected Chinese Patients. Cancers. 2022;14(21):5380.
178. Shi X, Sims MD, Hanna MM, Xie M, Gulick PG, Zheng YH, et al. Neutropenia during HIV infection: adverse consequences and remedies. Int Rev Immunol. 2014;33(6):511-36.
179. Petrina M, Martin J, Basta S. Granulocyte macrophage colony-stimulating factor has come of age: From a vaccine adjuvant to antiviral immunotherapy. Cytokine Growth Factor Rev. 2021;59:101-10.
180. Wang L, Cao C, Qiu J, Zhang J, He Q, Song L, et al. Correlation between PD-1 and sPD-L1 expression levels in peripheral blood of DLBCL patients and their clinicopathological characteristics. Cell Mol Biol (Noisy-le-grand). 2024;70(2):44-50.
181. Rossille D, Gressier M, Damotte D, Maucort-Boulch D, Pangault C, Semana G, et al. High level of soluble programmed cell death ligand 1 in blood impacts overall survival in aggressive diffuse large B-Cell lymphoma: results from a French multicenter clinical trial. Leukemia. 2014;28(12):2367-75.

182. Meier A, Bagchi A, Sidhu HK, Alter G, Suscovich TJ, Kavanagh DG, et al. Upregulation of PD-L1 on monocytes and dendritic cells by HIV-1 derived TLR ligands. Aids. 2008;22(5):655-8.
183. Bowers NL, Helton ES, Huijbregts RPH, Goepfert PA, Heath SL, Hel Z. Immune Suppression by Neutrophils in HIV-1 Infection: Role of PD-L1/PD-1 Pathway. PLOS Pathogens. 2014;10(3):e1003993.
184. Said EA, Dupuy FP, Trautmann L, Zhang Y, Shi Y, El-Far M, et al. Programmed death-1-induced interleukin-10 production by monocytes impairs CD4+ T cell activation during HIV infection. Nat Med. 2010;16(4):452-9.
185. Moir S, Fauci AS. B cells in HIV infection and disease. Nat Rev Immunol. 2009;9(4):235-45.
186. Bussmann BM, Reiche S, Bieniek B, Krznaric I, Ackermann F, Jassoy C. Loss of HIV-specific memory B-cells as a potential mechanism for the dysfunction of the humoral immune response against HIV. Virology. 2010;397(1):7-13.
187. Luckheeram RV, Zhou R, Verma AD, Xia B. CD4+T Cells: Differentiation and Functions. Journal of Immunology Research. 2012;2012(1):925135.
188. Nicholas KJ, Zern EK, Barnett L, Smith RM, Lorey SL, Copeland CA, et al. B Cell Responses to HIV Antigen Are a Potent Correlate of Viremia in HIV-1 Infection and Improve with PD-1 Blockade. PLOS ONE. 2013;8(12):e84185.
189. Cherukuri A, Cheng PC, Sohn HW, Pierce SK. The CD19/CD21 complex functions to prolong B cell antigen receptor signaling from lipid rafts. Immunity. 2001;14(2):169-79.
190. Moir S, Malaspina A, Ogwaro KM, Donoghue ET, Hallahan CW, Ehler LA, et al. HIV-1 induces phenotypic and functional perturbations of B cells in chronically infected individuals. Proceedings of the National Academy of Sciences. 2001;98(18):10362-7.
191. García F, Vidal C, Gatell JM, Miró JM, Soriano A, Pumarola T. Viral load in asymptomatic patients with CD4+ lymphocyte counts above 500 x 10(6)/l. Aids. 1997;11(1):53-7.
192. Correa-Rocha R, Lopez-Abente J, Gutierrez C, Pérez-Fernández VA, Prieto-Sánchez A, Moreno-Guillen S, et al. CD72/CD100 and PD-1/PD-L1 markers are increased on T and B cells in HIV-1+ viremic individuals, and CD72/CD100 axis is correlated with T-cell exhaustion. PLOS ONE. 2018;13(8):e0203419.
193. Siewe B, Stapleton JT, Martinson J, Keshavarzian A, Kazmi N, Demarais PM, et al. Regulatory B cell frequency correlates with markers of HIV disease progression and attenuates anti-HIV CD8$^+$ T cell function in vitro. J Leukoc Biol. 2013;93(5):811-8.
194. Gutiérrez C, Lopez-Abente J, Pérez-Fernández V, Prieto-Sánchez A, Correa-Rocha R, Moreno-Guillen S, et al. Analysis of the dysregulation between regulatory B and T cells (Breg and Treg) in human immunodeficiency virus (HIV)-infected patients. PLoS One. 2019;14(3):e0213744.
195. Mishina T, Miyoshi H, Takeuchi M, Miyawaki K, Nakashima K, Yamada K, et al. Co-expression of regulatory B-cell markers, transforming growth factor β and interleukin-10 as a prognostic factor in diffuse large B-cell lymphoma. Pathology - Research and Practice. 2024;254:155117.
196. Jiang X, Wang J, Deng X, Xiong F, Ge J, Xiang B, et al. Role of the tumor microenvironment in PD-L1/PD-1-mediated tumor immune escape. Mol Cancer. 2019;18(1):10.
197. Mayer S, Milo T, Isaacson A, Halperin C, Miyara S, Stein Y, et al. The tumor microenvironment shows a hierarchy of cell-cell interactions dominated by fibroblasts. Nature Communications. 2023;14(1):5810.
198. Khalaf K, Hana D, Chou JT, Singh C, Mackiewicz A, Kaczmarek M. Aspects of the Tumor Microenvironment Involved in Immune Resistance and Drug Resistance. Frontiers in immunology. 2021;12:656364.
199. Dzobo K, Senthebane DA, Dandara C. The Tumor Microenvironment in Tumorigenesis and Therapy Resistance Revisited. Cancers. 2023;15(2):376.
200. Salemme V, Centonze G, Cavallo F, Defilippi P, Conti L. The Crosstalk Between Tumor Cells and the Immune Microenvironment in Breast Cancer: Implications for Immunotherapy. Frontiers in Oncology. 2021;11.

201. Lu C, Liu Y, Ali NM, Zhang B, Cui X. The role of innate immune cells in the tumor microenvironment and research progress in anti-tumor therapy. Frontiers in immunology. 2022;13:1039260.
202. Martínez-Lostao L, Anel A, Pardo J. How Do Cytotoxic Lymphocytes Kill Cancer Cells? Clin Cancer Res. 2015;21(22):5047-56.
203. Maimela NR, Liu S, Zhang Y. Fates of CD8+ T cells in Tumor Microenvironment. Computational and structural biotechnology journal. 2019;17:1-13.
204. Venkatesh H, Tracy SI, Farrar MA. Cytotoxic CD4 T cells in the mucosa and in cancer. Frontiers in immunology. 2023;14.
205. Bied M, Ho WW, Ginhoux F, Blériot C. Roles of macrophages in tumor development: a spatiotemporal perspective. Cellular & Molecular Immunology. 2023;20(9):983-92.
206. Boutilier AJ, Elsawa SF. Macrophage Polarization States in the Tumor Microenvironment. Int J Mol Sci. 2021;22(13).
207. Anderson NM, Simon MC. The tumor microenvironment. Curr Biol. 2020;30(16):R921-R5.
208. Ennishi D. The biology of the tumor microenvironment in DLBCL: Targeting the "don't eat me" signal. J Clin Exp Hematop. 2021;61(4):210-5.
209. Janeway CA J, Travers P, Walport M, Shlomchik M. The major histocompatibility complex and its functions. Immunobiology: The Immune System in Health and Disease. 5th ed. New York: Garland Science; 2001.
210. Takahara T, Nakamura S, Tsuzuki T, Satou A. The Immunology of DLBCL. Cancers (Basel). 2023;15(3).
211. Chen BJ, Chapuy B, Ouyang J, Sun HH, Roemer MG, Xu ML, et al. PD-L1 expression is characteristic of a subset of aggressive B-cell lymphomas and virus-associated malignancies. Clin Cancer Res. 2013;19(13):3462-73.
212. Kiyasu J, Miyoshi H, Hirata A, Arakawa F, Ichikawa A, Niino D, et al. Expression of programmed cell death ligand 1 is associated with poor overall survival in patients with diffuse large B-cell lymphoma. Blood. 2015;126(19):2193-201.
213. Laurent C, Charmpi K, Gravelle P, Tosolini M, Franchet C, Ysebaert L, et al. Several immune escape patterns in non-Hodgkin's lymphomas. Oncoimmunology. 2015;4(8):e1026530.
214. Menter T, Bodmer-Haecki A, Dirnhofer S, Tzankov A. Evaluation of the diagnostic and prognostic value of PDL1 expression in Hodgkin and B-cell lymphomas. Human pathology. 2016;54:17-24.
215. Kwon D, Kim S, Kim P-J, Go H, Nam SJ, Paik JH, et al. Clinicopathological analysis of programmed cell death 1 and programmed cell death ligand 1 expression in the tumour microenvironments of diffuse large B cell lymphomas. Histopathology. 2016;68(7):1079-89.
216. Roussel M, Le KS, Granier C, Llamas Gutierrez F, Foucher E, Le Gallou S, et al. Functional characterization of PD1+TIM3+ tumor-infiltrating T cells in DLBCL and effects of PD1 or TIM3 blockade. Blood Adv. 2021;5(7):1816-29.
217. Banerjee H, Kane LP. Immune regulation by Tim-3. F1000Res. 2018;7:316.
218. Das M, Zhu C, Kuchroo VK. Tim-3 and its role in regulating anti-tumor immunity. Immunol Rev. 2017;276(1):97-111.
219. Chadburn A, Chiu A, Lee JY, Chen X, Hyjek E, Banham AH, et al. Immunophenotypic analysis of AIDS-related diffuse large B-cell lymphoma and clinical implications in patients from AIDS Malignancies Consortium clinical trials 010 and 034. Journal of clinical oncology : official journal of the American Society of Clinical Oncology. 2009;27(30):5039-48.
220. Dandachi D, Morón F. Effects of HIV on the Tumor Microenvironment. Tumor Microenvironment. 2020:45-54.
221. Liapis K, Clear A, Owen A, Coutinho R, Greaves P, Lee AM, et al. The microenvironment of AIDS-related diffuse large B-cell lymphoma provides insight into the pathophysiology and indicates possible therapeutic strategies. Blood. 2013;122(3):424-33.

222. Chao C, Xu L, Silverberg MJ, Martínez-Maza O, Chen LH, Castor B, et al. Stromal immune infiltration in HIV-related diffuse large B-cell lymphoma is associated with HIV disease history and patient survival. Aids. 2015;29(15):1943-51.
223. Battistini Garcia SA, Guzman N. Acquired Immune Deficiency Syndrome CD4+ Count. StatPearls. Treasure Island (FL): StatPearls Publishing

224. Wilkinson ST, Vanpatten KA, Fernandez DR, Brunhoeber P, Garsha KE, Glinsmann-Gibson BJ, et al. Partial plasma cell differentiation as a mechanism of lost major histocompatibility complex class II expression in diffuse large B-cell lymphoma. Blood. 2012;119(6):1459-67.
225. Rimsza LM, Roberts RA, Miller TP, Unger JM, LeBlanc M, Braziel RM, et al. Loss of MHC class II gene and protein expression in diffuse large B-cell lymphoma is related to decreased tumor immunosurveillance and poor patient survival regardless of other prognostic factors: a follow-up study from the Leukemia and Lymphoma Molecular Profiling Project. Blood. 2004;103(11):4251-8.
226. Jesionek-Kupnicka D, Bojo M, Prochorec-Sobieszek M, Szumera-Ciećkiewicz A, Jabłońska J, Kalinka-Warzocha E, et al. HLA-G and MHC Class II Protein Expression in Diffuse Large B-Cell Lymphoma. Archivum Immunologiae et Therapiae Experimentalis. 2016;64(3):225-40.
227. Raskov H, Orhan A, Christensen JP, Gögenur I. Cytotoxic CD8+ T cells in cancer and cancer immunotherapy. British Journal of Cancer. 2021;124(2):359-67.
228. Durgeau A, Virk Y, Corgnac S, Mami-Chouaib F. Recent Advances in Targeting CD8 T-Cell Immunity for More Effective Cancer Immunotherapy. Frontiers in immunology. 2018;9.
229. Guan Q, Han M, Guo Q, Yan F, Wang M, Ning Q, et al. Strategies to reinvigorate exhausted CD8+ T cells in tumor microenvironment. Frontiers in immunology. 2023;14.
230. Taylor JG, Liapis K, Gribben JG. The role of the tumor microenvironment in HIV-associated lymphomas. Biomarkers in medicine. 2015;9(5):473-82.
231. Hirayama D, Iida T, Nakase H. The Phagocytic Function of Macrophage-Enforcing Innate Immunity and Tissue Homeostasis. Int J Mol Sci. 2017;19(1).
232. Wang S, Wang J, Chen Z, Luo J, Guo W, Sun L, et al. Targeting M2-like tumor-associated macrophages is a potential therapeutic approach to overcome antitumor drug resistance. npj Precision Oncology. 2024;8(1):31.
233. Lin Y, Xu J, Lan H. Tumor-associated macrophages in tumor metastasis: biological roles and clinical therapeutic applications. Journal of Hematology & Oncology. 2019;12(1):76.
234. Lin M, Ma S, Sun L, Qin Z. The prognostic value of tumor-associated macrophages detected by immunostaining in diffuse large B cell lymphoma: A meta-analysis. Front Oncol. 2022;12:1094400.
235. Waki K, Freed EO. Macrophages and Cell-Cell Spread of HIV-1. Viruses. 2010;2(8):1603-20.
236. Kruize Z, Kootstra NA. The Role of Macrophages in HIV-1 Persistence and Pathogenesis. Front Microbiol. 2019;10:2828.
237. Zhao Y, Shen M, Wu L, Yang H, Yao Y, Yang Q, et al. Stromal cells in the tumor microenvironment: accomplices of tumor progression? Cell Death & Disease. 2023;14(9):587.
238. Wang Q, Shao X, Zhang Y, Zhu M, Wang FXC, Mu J, et al. Role of tumor microenvironment in cancer progression and therapeutic strategy. Cancer Medicine. 2023;12(10):11149-65.
239. Meng L, Zheng Y, Liu H, Fan D. The tumor microenvironment: a key player in multidrug resistance in cancer. Oncologie. 2024;26(1):41-58.
240. Sun Y. Tumor microenvironment and cancer therapy resistance. Cancer Letters. 2016;380(1):205-15.
241. Zhang L, Wang Z, Liu K, Liu Y, Wang S, Jiang W, et al. Targets of tumor microenvironment for potential drug development. MedComm – Oncology. 2024;3(1):e68.
242. Hu LY, Xu XL, Rao HL, Chen J, Lai RC, Huang HQ, et al. Expression and clinical value of programmed cell death-ligand 1 (PD-L1) in diffuse large B cell lymphoma: a retrospective study. Chin J Cancer. 2017;36(1):94.
243. Tiwari A, Trivedi R, Lin S-Y. Tumor microenvironment: barrier or opportunity towards effective cancer therapy. Journal of Biomedical Science. 2022;29(1):83.

244. Zhou H, Zheng C, Huang DS. A prognostic gene model of immune cell infiltration in diffuse large B-cell lymphoma. PeerJ. 2020;8:e9658.
245. Greenbaum AM, Fromm JR, Gopal AK, Houghton AM. Diffuse large B-cell lymphoma (DLBCL) is infiltrated with activated CD8(+) T-cells despite immune checkpoint signaling. Blood Res. 2022;57(2):117-28.
246. Tamma R, Ranieri G, Ingravallo G, Annese T, Oranger A, Gaudio F, et al. Inflammatory Cells in Diffuse Large B Cell Lymphoma. Journal of Clinical Medicine. 2020;9(8):2418.
247. Azzaoui I, Uhel F, Rossille D, Pangault C, Dulong J, Le Priol J, et al. T-cell defect in diffuse large B-cell lymphomas involves expansion of myeloid-derived suppressor cells. Blood. 2016;128(8):1081-92.
248. Song JY, Nwangwu M, He T-F, Zhang W, Meawad H, Bedell V, et al. Low T-cell proportion in the tumor microenvironment is associated with immune escape and poor survival in diffuse large B-cell lymphoma. Haematologica. 2023;108(8):2167-77.
249. Steen CB, Luca BA, Esfahani MS, Azizi A, Sworder BJ, Nabet BY, et al. The landscape of tumor cell states and ecosystems in diffuse large B cell lymphoma. Cancer cell. 2021;39(10):1422-37.e10.
250. Wright KT, Weirather JL, Jiang S, Kao KZ, Sigal Y, Giobbie-Hurder A, et al. Diffuse large B-cell lymphomas have spatially defined, tumor immune microenvironments revealed by high-parameter imaging. Blood Advances. 2023;7(16):4633-46.
251. Kossow KW, Bennett JG, Hoffmann MS. Mechanisms of Immune Evasion and Novel Treatments for Relapsed and Refractory Diffuse Large B-cell Lymphoma. Oncology Advances. 2024;2(2):59-71.
252. Sun C, Mezzadra R, Schumacher TN. Regulation and Function of the PD-L1 Checkpoint. Immunity. 2018;48(3):434-52.
253. Hatic H, Sampat D, Goyal G. Immune checkpoint inhibitors in lymphoma: challenges and opportunities. Annals of Translational Medicine. 2021;9(12):1037.
254. Aavani P, Allen LJS. The role of CD4 T cells in immune system activation and viral reproduction in a simple model for HIV infection. Applied Mathematical Modelling. 2019;75:210-22.
255. Kusano Y, Yokoyama M, Terui Y, Nishimura N, Mishima Y, Ueda K, et al. Low absolute peripheral blood CD4+ T-cell count predicts poor prognosis in R-CHOP-treated patients with diffuse large B-cell lymphoma. Blood Cancer J. 2017;7(4):e558.
256. Besson C, Lancar R, Prevot S, Algarte-Genin M, Delobel P, Bonnet F, et al. Outcomes for HIV-associated diffuse large B-cell lymphoma in the modern combined antiretroviral therapy era. Aids. 2017;31(18):2493-501.
257. Kanemasa Y, Shimoyama T, Sasaki Y, Tamura M, Sawada T, Omuro Y, et al. Outcome Analysis of DLBCL in HIV-infected and non-HIV-infected patients. Annals of Oncology. 2016;27:vii86.
258. Kelley CF, Kitchen CM, Hunt PW, Rodriguez B, Hecht FM, Kitahata M, et al. Incomplete peripheral CD4+ cell count restoration in HIV-infected patients receiving long-term antiretroviral treatment. Clin Infect Dis. 2009;48(6):787-94.
259. Battegay M, Nüesch R, Hirschel B, Kaufmann GR. Immunological recovery and antiretroviral therapy in HIV-1 infection. The Lancet Infectious Diseases. 2006;6(5):280-7.
260. Ye Z, Huang N, Fu Y, Tian R, Huang W. Tumor Purity-Related Genes for Predicting the Prognosis and Drug Sensitivity of DLBCL Patients. Cold Spring Harbor Laboratory; 2023.
261. Phares TW, Stohlman SA, Hwang M, Min B, Hinton DR, Bergmann CC. CD4 T cells promote CD8 T cell immunity at the priming and effector site during viral encephalitis. J Virol. 2012;86(5):2416-27.
262. Gulzar N, Copeland KF. CD8+ T-cells: function and response to HIV infection. Curr HIV Res. 2004;2(1):23-37.
263. Cao W, Mehraj V, Kaufmann DE, Li T, Routy JP. Elevation and persistence of CD8 T-cells in HIV infection: the Achilles heel in the ART era. J Int AIDS Soc. 2016;19(1):20697.
264. Jiang Y, Li Y, Zhu B. T-cell exhaustion in the tumor microenvironment. Cell Death & Disease. 2015;6(6):e1792-e.

265. Coelho J, Roush SM, Xu AM, Puranam K, Mponda M, Kasonkanji E, et al. HIV and prior exposure to antiretroviral therapy alter tumour composition and tumour: T-cell associations in diffuse large B-cell lymphoma. British Journal of Haematology.n/a(n/a).
266. Yi JS, Cox MA, Zajac AJ. T-cell exhaustion: characteristics, causes and conversion. Immunology. 2010;129(4):474-81.
267. Shi L, Chen S, Yang L, Li Y. The role of PD-1 and PD-L1 in T-cell immune suppression in patients with hematological malignancies. J Hematol Oncol. 2013;6(1):74.
268. Cai QC, Liao H, Lin SX, Xia Y, Wang XX, Gao Y, et al. High expression of tumor-infiltrating macrophages correlates with poor prognosis in patients with diffuse large B-cell lymphoma. Med Oncol. 2012;29(4):2317-22.
269. Li Y-L, Shi Z-H, Wang X, Gu K-S, Zhai Z-M. Tumor-associated macrophages predict prognosis in diffuse large B-cell lymphoma and correlation with peripheral absolute monocyte count. BMC Cancer. 2019;19(1):1049.
270. Carreras J, Kikuti YY, Hiraiwa S, Miyaoka M, Tomita S, Ikoma H, et al. High PTX3 expression is associated with a poor prognosis in diffuse large B-cell lymphoma. Cancer Sci. 2022;113(1):334-48.
271. Nam SJ, Go H, Paik JH, Kim TM, Heo DS, Kim CW, et al. An increase of M2 macrophages predicts poor prognosis in patients with diffuse large B-cell lymphoma treated with rituximab, cyclophosphamide, doxorubicin, vincristine and prednisone. Leuk Lymphoma. 2014;55(11):2466-76.
272. Nam SJ, Kim S, Kwon D, Kim H, Kim S, Lee E, et al. Prognostic implications of tumor-infiltrating macrophages, M2 macrophages, regulatory T-cells, and indoleamine 2,3-dioxygenase-positive cells in primary diffuse large B-cell lymphoma of the central nervous system. Oncoimmunology. 2018;7(7):e1442164.
273. Ghorab DS, Helaly AM, El Mahdi HS, Khatatbeh M, Ibrahiem AT. Prognostic Role of Tumor Microenvironment in DLBCL and Relation to Patients' Clinical Outcome: A Clinical and Immunohistochemical Study. Anal Cell Pathol (Amst). 2022;2022:9993496.
274. Xu T, Chai J, Wang K, Jia Q, Liu Y, Wang Y, et al. Tumor Immune Microenvironment Components and Checkpoint Molecules in Anaplastic Variant of Diffuse Large B-Cell Lymphoma. Front Oncol. 2021;11:638154.
275. Ibrahim EM, Refat S, El-Ashwah S, Fahmi MW, Ibrahiem AT. Programmed death ligand 1 expression in diffuse large B cell lymphoma: correlation with clinicopathological prognostic factors. Journal of the Egyptian National Cancer Institute. 2023;35(1):12.
276. Kiyasu J, Miyoshi H, Hirata A, Arakawa F, Ichikawa A, Niino D, et al. Expression of programmed cell death ligand 1 is associated with poor overall survival in patients with diffuse large B-cell lymphoma. Blood. 2015;126(19):2193-201.
277. Jiang T, Peng Y, Tang X, Chen S, Yang Z, Liu Y. HIV-Related Diffuse Large B Cell Lymphoma Influences on T Cell Exhaustion. Blood. 2023;142:3013.
278. Xue S, Hu M, Li P, Ma J, Xie L, Teng F, et al. Relationship between expression of PD-L1 and tumor angiogenesis, proliferation, and invasion in glioma. Oncotarget. 2017;8(30):49702-12.
279. Cavazzoni A, Digiacomo G, Volta F, Alfieri R, Giovannetti E, Gnetti L, et al. PD-L1 overexpression induces STAT signaling and promotes the secretion of pro-angiogenic cytokines in non-small cell lung cancer (NSCLC). Lung Cancer. 2024;187.
280. Yang Y, Xia L, Wu Y, Zhou H, Chen X, Li H, et al. Programmed death ligand-1 regulates angiogenesis and metastasis by participating in the c-JUN/VEGFR2 signaling axis in ovarian cancer. Cancer Communications. 2021;41(6):511-27.
281. Farrag MS, Abdelwahab K, Farrag NS, Elrefaie WE, Emarah Z. Programmed death ligand-1 and CD8 tumor-infiltrating lymphocytes (TILs) as prognostic predictors in ovarian high-grade serous carcinoma (HGSC). Journal of the Egyptian National Cancer Institute. 2021;33(1):16.
282. Ishikawa M, Nakayama K, Nakamura K, Yamashita H, Ishibashi T, Minamoto T, et al. High PD-1 expression level is associated with an unfavorable prognosis in patients with cervical adenocarcinoma. Archives of Gynecology and Obstetrics. 2020;302(1):209-18.

283. Hamanishi J, Mandai M, Iwasaki M, Okazaki T, Tanaka Y, Yamaguchi K, et al. Programmed cell death 1 ligand 1 and tumor-infiltrating CD8+ T lymphocytes are prognostic factors of human ovarian cancer. Proc Natl Acad Sci U S A. 2007;104(9):3360-5.
284. Zhu Y, Li M, Mu D, Kong L, Zhang J, Zhao F, et al. CD8+/FOXP3+ ratio and PD-L1 expression associated with survival in pT3N0M0 stage esophageal squamous cell cancer. Oncotarget. 2016;7(44).
285. Kim S, Nam SJ, Park C, Kwon D, Yim J, Song SG, et al. High tumoral PD-L1 expression and low PD-1+ or CD8+ tumor-infiltrating lymphocytes are predictive of a poor prognosis in primary diffuse large B-cell lymphoma of the central nervous system. OncoImmunology. 2019;8(9):e1626653.
286. Xu-Monette ZY, Xiao M, Au Q, Padmanabhan R, Xu B, Hoe N, et al. Immune Profiling and Quantitative Analysis Decipher the Clinical Role of Immune-Checkpoint Expression in the Tumor Immune Microenvironment of DLBCL. Cancer Immunology Research. 2019;7(4):644-57.
287. Tomas-Roca L, Rodriguez M, Alonso-Alonso R, Rodriguez-Pinilla SM, Piris MA. Diffuse Large B-Cell Lymphoma: Recognition of Markers for Targeted Therapy. Hemato. 2021;2(2):281-304.
288. Song S, Li Y, Zhang K, Zhang X, Huang Y, Xu M, et al. Cancer Stem Cells of Diffuse Large B Cell Lymphoma Are Not Enriched in the CD45(+)CD19(-) cells but in the ALDH(high) Cells. J Cancer. 2020;11(1):142-52.
289. Zanelli M, Fragliasso V, Parente P, Bisagni A, Sanguedolce F, Zizzo M, et al. Programmed Death Ligand 1 (PD-L1) Expression in Lymphomas: State of the Art. Int J Mol Sci. 2024;25(12).
290. Deng S, Hu Q, Zhang H, Yang F, Peng C, Huang C. HDAC3 Inhibition Upregulates PD-L1 Expression in B-Cell Lymphomas and Augments the Efficacy of Anti–PD-L1 Therapy. Molecular Cancer Therapeutics. 2019;18(5):900-8.
291. Alsaadi M, Khan MY, Dalhat MH, Bahashwan S, Khan MU, Albar A, et al. Dysregulation of miRNAs in DLBCL: Causative Factor for Pathogenesis, Diagnosis and Prognosis. Diagnostics (Basel). 2021;11(10).
292. Casey SC, Tong L, Li Y, Do R, Walz S, Fitzgerald KN, et al. MYC regulates the antitumor immune response through CD47 and PD-L1. Science (New York, NY). 2016;352(6282):227-31.
293. Zhou C, Che G, Zheng X, Qiu J, Xie Z, Cong Y, et al. Expression and clinical significance of PD-L1 and c-Myc in non-small cell lung cancer. J Cancer Res Clin Oncol. 2019;145(11):2663-74.
294. Pan Y, Fei Q, Xiong P, Yang J, Zhang Z, Lin X, et al. Synergistic inhibition of pancreatic cancer with anti-PD-L1 and c-Myc inhibitor JQ1. Oncoimmunology. 2019;8(5):e1581529.
295. Liang MQ, Yu FQ, Chen C. C-Myc regulates PD-L1 expression in esophageal squamous cell carcinoma. American journal of translational research. 2020;12(2):379-88.
296. Maeda T, Hiraki M, Jin C, Rajabi H, Tagde A, Alam M, et al. MUC1-C Induces PD-L1 and Immune Evasion in Triple-Negative Breast Cancer. Cancer research. 2018;78(1):205-15.
297. Wang WG, Jiang XN, Sheng D, Sun CB, Lee J, Zhou XY, et al. PD-L1 over-expression is driven by B-cell receptor signaling in diffuse large B-cell lymphoma. Lab Invest. 2019;99(10):1418-27.
298. Li W, Gupta SK, Han W, Kundson RA, Nelson S, Knutson D, et al. Targeting MYC activity in double-hit lymphoma with MYC and BCL2 and/or BCL6 rearrangements with epigenetic bromodomain inhibitors. Journal of Hematology & Oncology. 2019;12(1):73.
299. Xu P-p, Sun C, Cao X, Zhao X, Dai H-j, Lu S, et al. Immune Characteristics of Chinese Diffuse Large B-Cell Lymphoma Patients: Implications for Cancer Immunotherapies. eBioMedicine. 2018;33:94-104.
300. Elbæk MV, Pedersen MØ, Breinholt MF, Reddy A, Love C, Clasen-Linde E, et al. PD-L1 expression is low in large B-cell lymphoma with MYC or double-hit translocation. Hematological Oncology. 2019;37(4):375-82.
301. Langer-Gould A, Wu J, Lucas R, Smith J, Gonzales E, Amezcua L, et al. Epstein-Barr virus, cytomegalovirus, and multiple sclerosis susceptibility. Neurology. 2017;89(13):1330-7.
302. Murthy SL, Hitchcock MA, Endicott-Yazdani TR, Watson JT, Krause JR. Epstein-Barr virus-positive diffuse large B-cell lymphoma. Proceedings (Baylor University Medical Center). 2017;30(4):443-4.

303. Ross AM, Leahy CI, Neylon F, Steigerova J, Flodr P, Navratilova M, et al. Epstein–Barr Virus and the Pathogenesis of Diffuse Large B-Cell Lymphoma. Life. 2023;13(2):521.
304. Mpunga T, Clifford GM, Morgan EA, Milner Jr. DA, de Martel C, Munyanshongore C, et al. Epstein-Barr virus prevalence among subtypes of malignant lymphoma in Rwanda, 2012 to 2018. International Journal of Cancer. 2022;150(5):753-60.
305. Ok CY, Li L, Xu-Monette ZY, Visco C, Tzankov A, Manyam GC, et al. Prevalence and clinical implications of epstein-barr virus infection in de novo diffuse large B-cell lymphoma in Western countries. Clin Cancer Res. 2014;20(9):2338-49.
306. de Jonge AV, Mutis T, Roemer MGM, Scheijen B, Chamuleau MED. Impact of MYC on Anti-Tumor Immune Responses in Aggressive B Cell Non-Hodgkin Lymphomas: Consequences for Cancer Immunotherapy. Cancers (Basel). 2020;12(10).
307. Trabattoni D, Saresella M, Biasin M, Boasso A, Piacentini L, Ferrante P, et al. B7-H1 is up-regulated in HIV infection and is a novel surrogate marker of disease progression. Blood. 2003;101(7):2514-20.
308. da Silva SR, de Oliveira DE. HIV, EBV and KSHV: viral cooperation in the pathogenesis of human malignancies. Cancer Lett. 2011;305(2):175-85.
309. Boccellato F, Anastasiadou E, Rosato P, Kempkes B, Frati L, Faggioni A, et al. EBNA2 Interferes with the Germinal Center Phenotype by Downregulating BCL6 and TCL1 in Non-Hodgkin's Lymphoma Cells. Journal of Virology. 2007;81(5):2274-82.
310. Reed LJ, Muench H. A SIMPLE METHOD OF ESTIMATING FIFTY PER CENT ENDPOINTS12. American Journal of Epidemiology. 1938;27(3):493-7.
311. Rutebemberwa A, Bess JW, Jr., Brown B, Arroyo M, Eller M, Slike B, et al. Evaluation of aldrithiol-2-inactivated preparations of HIV type 1 subtypes A, B, and D as reagents to monitor T cell responses. AIDS Res Hum Retroviruses. 2007;23(4):532-42.
312. Ramorola BR, Goolam-Hoosen T, Alves de Souza Rios L, Mowla S. Modulation of Cellular MicroRNA by HIV-1 in Burkitt Lymphoma Cells-A Pathway to Promoting Oncogenesis. Genes (Basel). 2021;12(9).
313. Adachi A, Gendelman HE, Koenig S, Folks T, Willey R, Rabson A, et al. Production of acquired immunodeficiency syndrome-associated retrovirus in human and nonhuman cells transfected with an infectious molecular clone. Journal of Virology. 1986;59(2):284-91.
314. Sanson KR, Hanna RE, Hegde M, Donovan KF, Strand C, Sullender ME, et al. Optimized libraries for CRISPR-Cas9 genetic screens with multiple modalities. Nature Communications. 2018;9(1):5416.
315. Kadali SSK, Gowlikar R, Fatima SN. The Cancer Genomic Atlas – "TO CONQUER CANCER". International Journal of Molecular and Immuno Oncology. 2021;6.
316. Weinstein JN, Collisson EA, Mills GB, Shaw KR, Ozenberger BA, Ellrott K, et al. The Cancer Genome Atlas Pan-Cancer analysis project. Nat Genet. 2013;45(10):1113-20.
317. Pontén F, Jirström K, Uhlen M. The Human Protein Atlas--a tool for pathology. The Journal of pathology. 2008;216(4):387-93.
318. Amini R-M, Berglund M, Rosenquist R, von Heideman A, Lagercrantz S, Thunberg U, et al. A Novel B-cell Line (U-2932) Established from a Patient with Diffuse Large B-cell Lymphoma Following Hodgkin Lymphoma. Leukemia & Lymphoma. 2002;43(11):2179-89.
319. Nozawa Y, Abe M, Wakasa H, Ohno H, Fukuhara S, Kinoshita T, et al. Establishment and Characterization of an Epstein-Barr Virus Negative B-Cell Lymphoma Cell Line and Successful Heterotransplantation. The Tohoku Journal of Experimental Medicine. 1988;156(4):319-30.
320. Al-Katib AM, Smith MR, Kamanda WS, Pettit GR, Hamdan M, Mohamed AN, et al. Bryostatin 1 down-regulates mdr1 and potentiates vincristine cytotoxicity in diffuse large cell lymphoma xenografts. Clin Cancer Res. 1998;4(5):1305-14.
321. Tweeddale ME, Lim B, Jamal N, Robinson J, Zalcberg J, Lockwood G, et al. The presence of clonogenic cells in high-grade malignant lymphoma: a prognostic factor. Blood. 1987;69(5):1307-14.

322. Epstein AL, Herman MM, Kim H, Dorfman RF, Kaplan HS. Biology of the human malignant lymphomas. III. Intracranial heterotransplantation in the nude, athymic mouse. Cancer. 1976;37(5):2158-76.
323. Leopizzi M, Mundo L, Messina E, Campolo F, Lazzi S, Angeloni A, et al. Epstein-Barr virus–encoded EBNA2 downregulates ICOSL by inducing miR-24 in B-cell lymphoma. Blood. 2024;143(5):429-43.
324. Roschewski M, Phelan JD, Wilson WH. Molecular Classification and Treatment of Diffuse Large B-Cell Lymphoma and Primary Mediastinal B-Cell Lymphoma. Cancer J. 2020;26(3):195-205.
325. Georgiou K, Chen L, Berglund M, Ren W, de Miranda NFCC, Lisboa S, et al. Genetic basis of PD-L1 overexpression in diffuse large B-cell lymphomas. Blood. 2016;127(24):3026-34.
326. Gravelle P, Burroni B, Péricart S, Rossi C, Bezombes C, Tosolini M, et al. Mechanisms of PD-1/PD-L1 expression and prognostic relevance in non-Hodgkin lymphoma: a summary of immunohistochemical studies. Oncotarget. 2017;8(27):44960-75.
327. Chen R, Zhou D, Wang L, Zhu L, Ye X. MYD88(L265P) and CD79B double mutations type (MCD type) of diffuse large B-cell lymphoma: mechanism, clinical characteristics, and targeted therapy. Ther Adv Hematol. 2022;13:20406207211072839.
328. Kwon HJ, Yang JM, Lee J-O, Lee JS, Paik JH. Clinicopathologic implication of PD-L1 and phosphorylated STAT3 expression in diffuse large B cell lymphoma. Journal of Translational Medicine. 2018;16(1):320.
329. Fang X, Xiu B, Yang Z, Qiu W, Zhang L, Zhang S, et al. The expression and clinical relevance of PD-1, PD-L1, and TP63 in patients with diffuse large B-cell lymphoma. Medicine (Baltimore). 2017;96(15):e6398.
330. Xing W, Dresser K, Zhang R, Evens AM, Yu H, Woda BA, et al. PD-L1 expression in EBV-negative diffuse large B-cell lymphoma: clinicopathologic features and prognostic implications. Oncotarget. 2016;7(37).
331. Sun C, Jia Y, Wang W, Bi R, Wu L, Bai Q, et al. Integrative analysis of PD-L1 DNA status, mRNA status and protein status, and their clinicopathological correlation, in diffuse large B-cell lymphoma. Histopathology. 2019;74(4):618-28.
332. Garcia-Lacarte M, Grijalba SC, Melchor J, Arnaiz-Leché A, Roa S. The PD-1/PD-L1 Checkpoint in Normal Germinal Centers and Diffuse Large B-Cell Lymphomas. Cancers (Basel). 2021;13(18).
333. Winter AM, Landsburg DJ, Mato AR, Isaac K, Hernandez-Ilizaliturri FJ, Reddy N, et al. A multi-institutional outcomes analysis of patients with relapsed or refractory DLBCL treated with ibrutinib. Blood. 2017;130(14):1676-9.
334. Nowakowski GS, Czuczman MS. ABC, GCB, and Double-Hit Diffuse Large B-Cell Lymphoma: Does Subtype Make a Difference in Therapy Selection? American Society of Clinical Oncology Educational Book. 2015(35):e449-e57.
335. Liu Y, Barta SK. Diffuse large B-cell lymphoma: 2019 update on diagnosis, risk stratification, and treatment. American Journal of Hematology. 2019;94(5):604-16.
336. Feng C, Zhang L, Chang X, Qin D, Zhang T. Regulation of post-translational modification of PD-L1 and advances in tumor immunotherapy. Frontiers in immunology. 2023;14.
337. Komori T, Hata S, Mabuchi A, Genova M, Harada T, Fukuyama M, et al. A CRISPR-del-based pipeline for complete gene knockout in human diploid cells. J Cell Sci. 2023;136(6).
338. Tuladhar R, Yeu Y, Tyler Piazza J, Tan Z, Rene Clemenceau J, Wu X, et al. CRISPR-Cas9-based mutagenesis frequently provokes on-target mRNA misregulation. Nat Commun. 2019;10(1):4056.
339. Ibrahim D, Prévaud L, Faumont N, Troutaud D, Feuillard J, Diab-Assaf M, et al. Alternative c-MYC mRNA Transcripts as an Additional Tool for c-Myc2 and c-MycS Production in BL60 Tumors. Biomolecules. 2022;12(6).
340. Kubickova A, De Sanctis JB, Hajduch M. Isoform-Directed Control of c-Myc Functions: Understanding the Balance from Proliferation to Growth Arrest. Int J Mol Sci. 2023;24(24).
341. Xu Q, Keiderling TA. Effect of sodium dodecyl sulfate on folding and thermal stability of acid-denatured cytochrome c: a spectroscopic approach. Protein Sci. 2004;13(11):2949-59.

342. Kaiser C, Laux G, Eick D, Jochner N, Bornkamm GW, Kempkes B. The proto-oncogene c-myc is a direct target gene of Epstein-Barr virus nuclear antigen 2. J Virol. 1999;73(5):4481-4.
343. Beer S, Wange LE, Zhang X, Kuklik-Roos C, Enard W, Hammerschmidt W, et al. The EBNA2-EBF1 complex promotes oncogenic MYC expression levels and metabolic processes required for cell cycle progression of Epstein-Barr virus-infected B cells. bioRxiv. 2022:2021.12.29.474426.
344. Edwards-Hicks J, Su H, Mangolini M, Yoneten KK, Wills J, Rodriguez-Blanco G, et al. MYC sensitises cells to apoptosis by driving energetic demand. Nature Communications. 2022;13(1):4674.
345. Quan L, Chen X, Liu A, Zhang Y, Guo X, Yan S, et al. PD-1 Blockade Can Restore Functions of T-Cells in Epstein-Barr Virus-Positive Diffuse Large B-Cell Lymphoma In Vitro. PLoS One. 2015;10(9):e0136476.
346. Shponka V, Reveles CY, Alam S, Jaramillo M, Maguire A, Rimsza LM, et al. Frequent expression of activation-induced cytidine deaminase in diffuse large B-cell lymphoma tissues from persons living with HIV. Aids. 2020;34(14):2025-35.
347. Chao C, Silverberg MJ, Xu L, Chen L-H, Castor B, Martínez-Maza O, et al. A Comparative Study of Molecular Characteristics of Diffuse Large B-cell Lymphoma from Patients with and without Human Immunodeficiency Virus Infection. Clinical Cancer Research. 2015;21(6):1429-37.
348. Musinova YR, Sheval EV, Dib C, Germini D, Vassetzky YS. Functional roles of HIV-1 Tat protein in the nucleus. Cell Mol Life Sci. 2016;73(3):589-601.
349. Apollonio B, Nicholas NS, Sutton L-A, Salisbury J, Patten PE, Kassam S, et al. Diffuse Large B-Cell Lymphoma (DLBCL) Tumor Cells Reprogram Lymphatic Fibroblasts into Cancer-Associated Fibroblasts (CAFs) That Contribute to Tumor Microenvironment (TME)-Driven Immune Privilege. Blood. 2015;126(23):1474.
350. Ritter Z, Papp L, Zámbó K, Tóth Z, Dezső D, Veres DS, et al. Two-Year Event-Free Survival Prediction in DLBCL Patients Based on In Vivo Radiomics and Clinical Parameters. Front Oncol. 2022;12:820136.
351. Lu W, Chen W, Zhou Y, Yuan Y, Shu H, Deng H, et al. A model to predict the prognosis of diffuse large B-cell lymphoma based on ultrasound images. Scientific Reports. 2023;13(1):3346.
352. Kotlov N, Bagaev A, Revuelta MV, Phillip JM, Cacciapuoti MT, Antysheva Z, et al. Clinical and Biological Subtypes of B-cell Lymphoma Revealed by Microenvironmental Signatures. Cancer Discovery. 2021;11(6):1468-89.
353. Sangaletti S, Iannelli F, Zanardi F, Cancila V, Portararo P, Botti L, et al. Intra-tumour heterogeneity of diffuse large B-cell lymphoma involves the induction of diversified stroma-tumour interfaces. EBioMedicine. 2020;61:103055.
354. Sánchez-Beato M, Méndez M, Guirado M, Pedrosa L, Sequero S, Yanguas-Casás N, et al. A genetic profiling guideline to support diagnosis and clinical management of lymphomas. Clinical and Translational Oncology. 2024;26(5):1043-62.
355. Liu J, Chen Z, Li Y, Zhao W, Wu J, Zhang Z. PD-1/PD-L1 Checkpoint Inhibitors in Tumor Immunotherapy. Front Pharmacol. 2021;12:731798.
356. Brito MJ, Sequeira P, Quintas A, Silva I, Silva F, Martins C, et al. Programmed death-ligand 1 (PD-L1) expression in cervical intraepithelial neoplasia and cervical squamous cell carcinoma of HIV-infected and non-infected patients. Virchows Archiv. 2024;484(3):507-16.
357. Peligero C, Argilaguet J, Güerri-Fernandez R, Torres B, Ligero C, Colomer P, et al. PD-L1 Blockade Differentially Impacts Regulatory T Cells from HIV-Infected Individuals Depending on Plasma Viremia. PLoS Pathog. 2015;11(12):e1005270.
358. Opinto G, Vegliante MC, Negri A, Skrypets T, Loseto G, Pileri SA, et al. The Tumor Microenvironment of DLBCL in the Computational Era. Front Oncol. 2020;10:351.

Appendix A

Consent form used for patient recruitment

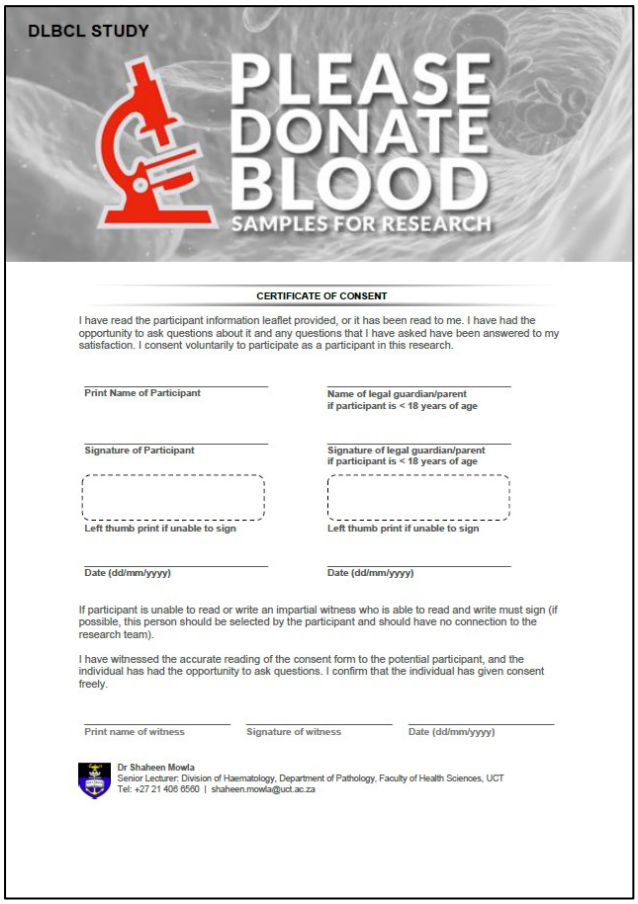

DLBCL STUDY

PLEASE DONATE BLOOD

SAMPLES FOR RESEARCH

CERTIFICATE OF CONSENT

I have read the participant information leaflet provided, or it has been read to me. I have had the opportunity to ask questions about it and any questions that I have asked have been answered to my satisfaction. I consent voluntarily to participate as a participant in this research.

Print Name of Participant	Name of legal guardian/parent if participant is < 18 years of age
Signature of Participant	Signature of legal guardian/parent if participant is < 18 years of age
Left thumb print if unable to sign	Left thumb print if unable to sign
Date (dd/mm/yyyy)	Date (dd/mm/yyyy)

If participant is unable to read or write an impartial witness who is able to read and write must sign (if possible, this person should be selected by the participant and should have no connection to the research team).

I have witnessed the accurate reading of the consent form to the potential participant, and the individual has had the opportunity to ask questions. I confirm that the individual has given consent freely.

Print name of witness	Signature of witness	Date (dd/mm/yyyy)

Dr Shaheen Mowla
Senior Lecturer: Division of Haematology, Department of Pathology, Faculty of Health Sciences, UCT
Tel: +27 21 406 6560 | shaheen.mowla@uct.ac.za

PARTICIPANT INFORMATION LEAFLET AND INFORMED CONSENT FORM (2020.03)

PROJECT TITLE: THE CHARACTERIZATION OF B-CELL SUBPOPULATIONS AND ACTIVATION MARKERS IN DIFFUSE LARGE B-CELL LYMPHOMA CASES AT GROOTE SCHUUR HOSPITAL

PART 1: INFORMATION
You are being invited to donate two tubes of blood (about 2 teaspoons) because you have recently been diagnosed with Diffuse Large B-cell lymphoma. Our goal is to understand this disease better and we hope that this research study will help us in doing that. Please take time to read the study information written below and ask the researcher/doctor any questions that you may have. Your participation is entirely voluntary, and you are also free to withdraw from the study at any point, even after you have already agreed to participate.

INTRODUCTION
We are studying diffuse large B-cell lymphoma (DLBCL) and how it affects the immune system. We wish to use your blood to study how cells of the immune system called lymphocytes (B-cells, T-cells, and Natural killer cells) work to fight viruses and cancer. We will also look at the expression of some genes/proteins when the immune system is actively fighting cancer and viral infections.

WHY IS THIS RESEARCH BEING DONE?
This study is being done because we want to learn more about the immune system of people with DLBCL, as well as how infection with viruses affects the immune response in some cases. The findings of this study will help improve our understanding of this disease, which may be beneficial to patients diagnosed with DLBCL in the future.

WHAT WILL HAPPEN IF YOU JOIN THIS STUDY?
If you agree to participate, you will be asked to donate two extra tubes (10 ml - about 2 teaspoons) of your blood once off. The medical staff in the lymphoma (E5) or the oncology (LE32) clinic will be responsible for drawing the blood. You will not need to visit the hospital any more than your regular visits.

POTENTIAL BENEFITS ASSOCIATED WITH THE RESEARCH
There is no benefit for you personally. Your participation will likely help us in understanding DLBCL better, which may assist in improving the testing or treatment in future.

POTENTIAL RISKS ASSOCIATED WITH THE RESEARCH
Blood is routinely drawn as we treat your disease and these two extra tubes will be taken concurrently. There is therefore very small risk associated with taking this extra blood.

STORAGE OF BLOOD FOR FUTURE TESTING
With your consent; part of your blood sample will be stored frozen for a maximum of 15 years, for future research in the field of lymphoma. This may include genetic tests on your DNA and may be analysed in a laboratory outside South Africa. All future research will be approved by the Human Research Ethics Committee. By participating in the study, you agree that your blood may be transported to other researchers, including to sites outside South Africa. During and after the study, you are the owner of the sample. This gives you the right to have the sample destroyed at any time by withdrawal of your consent. If you decide to have your sample destroyed, please contact the study doctor.

IS THERE ANYTHING ELSE THAT YOU SHOULD KNOW?
Other routine blood results and biopsy results will be collected for analysis. You will not be paid (money or gifts) for taking part in the study.

CONFIDENTIALITY
All the information that we will collect about you will be kept confidential. No one will see your personal information other than the researchers. A number will be assigned to your name, and that will be used for the information collected from your sample.

WHO TO CONTACT?
The research proposal has been reviewed and approved by University of Cape Town Human Research Ethics Committee, which is a committee whose task it is to make sure that research participants are protected from harm.

If you wish to ask questions later, you may contact the following:
UCT human research ethics committee: 021 406 6492
Dr Shaheen Mowla: 021 406 6560

STATEMENT BY RESEARCHER/PERSON TAKING CONSENT

I have accurately read out the information sheet to the potential participant, and to the best of my ability made sure that the participant understands that the following will be done:

Two extra 5ml Purple top (EDTA) tube of peripheral blood will be collected and:

1. Tested for lymphocyte (B-cells, T-cells, NK cells) cell surface markers
2. Tested for B-cell secreted activation markers

Other routine blood results including full blood count, HIV test (and CD4 count and viral load if available) will be collected. Information about ARV treatment, and diagnosis with other acute illnesses such as tuberculosis will be collected. All these results will be used for analysis

I confirm that the participant was given an opportunity to ask questions about the study, and all the questions asked by the participant have been answered correctly and to the best of my ability. I confirm that the individual has not been coerced into giving consent, and the consent has been given freely and voluntarily. A copy of the informed consent form has been provided/ offered to the participant.

Print name of researcher/person taking the consent	Signature of researcher/person taking taking the consent	Date (dd/mm/yyyy)

Appendix B

Recipes and Reagents

Flow cytometry:

1X FACS™ lysis solution (50 mL)

Perform a 1:10 dilution of the FACS™ lysis solution with dH_2O and store at room temperature.

10x PBS (1 L)

	Amount (g)
NaCl	80 g
KCl	2 g
Na_2HPO_4	14.4 g
KH_2PO_4	2.4 g

Weigh out the components as per the table above and dissolve in 800 mL dH_2O.

Adjust the pH to 7.4 with HCl and final volume to 1 L.

Autoclave the solution and store at 4°C.

1X PBS

Perform a 1:10 dilution of 10X PBS with dH_2O. Store at 4°C.

Immunohistochemistry:

TE buffer pH 8 (1 L)

	Amount/Volume
Tris Base	6.1 g
EDTA	0.37 g
Triton X-100	5 mL

Weigh out the components as per the table above and dissolve in 800 mL dH_2O.

Adjust the pH to 8 with HCl and final volume to 1 L.

Store at room temperature.

Proteinase K Stock Solution (400 µg/mL) (20 mL)

	Amount/Volume
Proteinase K (20mg/mL)	400 µL
TE buffer pH 8	9.8 mL
10% Glycerol	9.8 mL

Add proteinase K to TE buffer and mix until dissolved.

Add the glycerol and mix well.

Aliquot the solution and store at –20˚C.

Proteinase K Working Solution (20 µg/mL)

Perform a 1:20 dilution of 400 µg/mL Proteinase K Stock solution with TE Buffer pH 8 and mix well. Store at 4°C.

10X TBE (1 L)

	Amount
Tris	108 g
Boric acid	55 g
0.5 M EDTA (pH 8)	40 mL

Weigh out components as listed above and dissolve in 800 mL dH_20.

Add the EDTA and adjust the volume to 1 L.

Store at room temperature.

1X TBE

Perform a 1:10 dilution of 10X TBE and store at 4°C.

1% Copper sulphate (100 mL)

	Amount
Copper sulphate	1 g

Weight out copper sulphate as listed above and dissolve in 100 mL dH_20.

Store at room temperature.

10X TBS (1 L)

	Amount
Tris	60.6 g
NaCl	87.6 g

Dissolve the components above in 800 mL dH_2O.

Adjust the pH to 6.8 using HCl, and make the volume up to 1 L.

Autoclave and store at 4˚C.

1X TBS/0.1% Triton X-100 (1 L)

Perform a 1:10 dilution of 10X TBS with dH_2O.

Add 1 mL of Triton X-100 and mix well.

Store at 4˚C.

3% BSA in 1X TBS/0.1% Triton X-100

	Amount
BSA	1.5 g

Dissolve 1.5 g of BSA in 50 mL of 1X TBS/0.1% Triton X-100.

Store at room temperature.

<u>Tissue culture</u>

Supplemented growth media

Cell lines	P/S	FBS	Medium	Supplements
U2932; SU-DHL-4; HBL-1; WSU-DLCL2	1 mL (2%)	5 mL (10%)	44 mL (RPMI-1640)	
U2932-EBNA2-CL1; and -CLW	1 mL (2%)	5 mL (10%)	43.825 mL (RPMI-1640)	50 uL hypoxanthine, 100 uL xanthine, 25 uL mycophenolic acid
OCI-LY1; OCI-LY1-gMYC-1/2/3	1 mL (2%)	5 mL (10%)	44 mL (IMDM)	
HEK293T/FT; TZM-bl	1 mL (2%)	5 mL (10%)	44 mL (DMEM)	
HEK293T	1 mL (2%)	15 mL (30%)	34 mL (DMEM)	
OCI-LY1	1 mL (2%)	15 mL (30%)	34 mL (IMDM)	

Freezing media

Cell lines	FBS	Medium
U2932; U2932-EBNA2-CL1; and -CLW; SU-DHL-4; HBL-1; WSU-DLCL2	10%	RPMI-1640, as needed
OCI-LY1; OCI-LY1-gMYC-1/2/3	10%	IMDM, as needed
HEK293T/FT; TZM-bl	10%	DMEM as needed

Low serum media

Cell lines	P/S	FBS	Medium
U2932; U2932-EBNA2-CL1; and -CLW;	1 mL (2%)	0.2 mL (0.5%)	48.8 mL RPMI-1640

Protein isolation

RIPA buffer (50 mL)

	Amount/Volume
150 nM NaCl	1.5 mL
1% Triton X-100	0.5 mL
0.1% SDS	0.5 mL
10 mM tris, pH 7.5	0.5 mL
1% deoxycholate powder	0.5 g

Dissolve the deoxycholate powder in 40 mL dH_2O.

Add the remaining components, mix and make up to volume of 50 mL with dH_2O.

Store at 4˚C.

7X protease inhibitor

Dissolve one protease tablet in 1.5 mL of 1X PBS.

Aliquot and store at -20˚C.

RIPA solution (0.1% SDS)

Dilute the 7X protease inhibitor to 1X protease inhibitor using RIPA buffer.

RIPA buffer (5% SDS)

Dilute 10% SDS to a final concentration of 5% SDS using RIPA buffer.

SDS-PAGE and Western blot

1.5M Tris-HCl pH 8.8 or pH 6.8 (500 mL)

Dissolve 60.5g Tris base in 300 ml dH_2O.

Adjust pH with concentrated HCl and make up to a final volume of 500 mL with dH_2O.

Store at 4˚C.

10% SDS (100 mL)

Dissolve 10 g of SDS crystals in 80 mL dH_2O.

Adjust volume to 100 mL with dH_2O and store at room temperature.

30% acrylamide-bisacrylamide (100 mL)

	Amount/Volume
Acrylamide	29g
N.N'-methylenebisacrylamide	1g

Dissolve the components as listed above in 100 mL dH_2O.

Filter through a 0.45 µM membrane.

Cover with foil ad store at 4˚C.

10% Ammonium persulphate

Dissolve 0.1 g APS in 1 mL dH_2O.

Store at 4°C and prepare fresh every 2 weeks.

10X SDS-PAGE Running buffer (1 L)

	Amount
SDS	10 g
Tris	30.3 g
Glycine	144.1 g

Dissolve the above components in 800 mL dH_2O.

Adjust the volume to 1 L with dH_2O and store at room temperature.

1X SDS-PAGE Running buffer

Perform a 1:10 dilution of 10X SDS-PAGE running buffer with dH_2O.

10X SDS-PAGE Transfer buffer (1 L)

	Amount
Tris	38 g
Glycine	144 g

Dissolve the above components in 800 mL dH_2O.

Adjust the volume to 1 L and store at room temperature.

1X SDS-PAGE Transfer buffer

Perform a 1:10 dilution of 10X SDS-PAGE transfer buffer with dH_2O.

1x Ponceau S staining solution (0.1% (w/v) Ponceau S in 5% (v/v) acetic acid)

Dissolve 0.1g Ponceau S in 5 mL acetic acid and adjust volume to 100 mL with dH_2O.

Cover with foil and store at room temperature.

10 -12% resolving gel (7.5 mL)

	10% gel Volume	12% gel Volume
dH_2O	2.95 mL	2.4 mL
30% acryl-bisacrylamide mix	2.5 mL	3 mL
1.5m Tris pH 8.8	1.9 mL	1.95 mL
10% SDS	0.075 mL	0.075 mL
10% APS	0.075 mL	0.075 mL
Tetramethylethylenediamine (TEMED)	0.003 mL	0.003 mL

Prepare the gels as described above, mixing well between each component.

Add the TEMED last.

Pour into 1 mm glass plates, overlay with 0.1% SDS, and allow to set.

5% stacking gel (3 mL)

	Volume
dH_2O	2.1 mL
30% acryl-bisacrylamide mix	0.5 mL
1.5m Tris pH 6.8	0.35 mL
10% SDS	0.03 mL
10% APS	0.03 mL
Tetramethylethylenediamine (TEMED)	0.003 mL

Prepare the gel as described above, mixing well between each component.

Add the TEMED last.

Pour on top of the resolving gel, add the comb and allow to set.

5X Loading dye

	Volume
10% SDS	1 g
0.04% Bromophenol blue	0.004 g
2M Tris pH 6.8	1.25 mL
100% Glycerol	3 mL
β-mercaptoethanol	0.5 mL

Dissolve the SDS and Bromophenol Blue in 5.25 mL dH_2O.

Add the remaining components and mix.

Aliquot and store at room temperature.

1X TBS/0.1% Tween-20

Perform a 1:10 dilution of 10X TBS with dH_2O.

Add 1 mL of Tween-20 and mix well.

Store at 4˚C.

5% fat-free milk in 1x TBS-Tween 20 (0.1%) (50 mL)

Mix 41.7ml of fresh fat-free milk with 58.3 ml 1x TBS/Tween-20 (0.1%).

Store at 4˚C.

Stripping buffer

	Volume
β-mercaptoethanol	0.7 ml
10% SDS	20 ml
1.5m Tris-HCl pH 6.8	4.2 ml
dH2O	75.1 ml

Prepare as listed above, mix well and store at room temperature.

RNA isolation

0.1% (V/V) diethyl pyrocarbonate- (DEPC) treated water

Add1 mL of DEPC to 1 L of dH_2O.

Mix with a magnetic stirrer bar overnight in the fume hood, at room temperature.

Autoclave and store at room temperature.

Treating plasticware with DEPC

Place all plasticware (centrifuge tubes and pipette tips) to be used for RNA work in 0.1% DEPC-water.

Mix with a magnetic stirrer bar in a fume hood overnight.

Remove plasticware from the water and allow to airdry completely.

Place the centrifuge tubes in bags and the pipette tips in boxes and autoclave.

DNA/RNA gel electrophoresis

1.5% agarose gel

	Amount/Volume
Agarose	1.5 g
1X TBE	100 mL

Dissolve the agarose in 1X TBE by heating in the microwave.

Once cooled, add 5 uL Ethidium bromide (EtBr, 0.5 mg/mL).

Pour the gel onto a tray, add the comb and allow to set.

1% agarose gel

	Amount/Volume
Agarose	1 g
1X TBE	100 mL

Prepare as described above.

2X RNA loading dye

	Amount/Volume
Formamide	900 µL
Sucrose	99 µL
Bromophenol Blue	0.5 µL
Xylene Cyanol	0.5 µL

Mix components as listed above, aliquot and store at room temperature.

10X DNA loading dye

	Amount/Volume
Xylene Cyanol	0.025 g
Bromophenol Blue	0.025 g
10% SDS	1.25 mL
Glycerol	12.5 mL

Dissolve Xylene cyanol and Bromophenol Blue in 6.25 mL of dH_2O.

Add the 10% SDS and glycerol.

Mix well, aliquot and store at room temperature.

Bacterial Transformation

Lysogeny Broth (LB) (1 L)

Dissolve 10 g of LB powder media in 800 mL ddH2O and adjust the volume to 1 L

Sterilise by autoclaving and store at room temperature

LB agar

Mix 1.5 g Agar and 2 g LB powder media in 100 mL ddH2O

Sterilize by autoclaving and store at room temperature

Appendix C

Supplemental Tables and Figures:

Chapter 2

Supplemental Table 1: Distribution of cases with Breg percentages above or below the median, according to HIV status, DLBCL subtype, EBV status and biopsy site.

		HIV-negative DLBCL (median=57,5 %)			HIV-positive DLBCL (median=61,2)		
		n	**% of cases below 57,5%**	**% of cases above 57,5%**	**n**	**% of cases below 61,2%**	**% of cases above 61,2%**
COO subtype	Non-GCB	16	9 (56%)	7 (44%)	3	1 (33%)	2 (67%)
	GCB	5	2 (40%)	3 (60%)	7	4 (57%)	3 (34%)
	Other/unknown	1		1 (100%)	1		1 (100%)
EBV status	EBV+	2	1 (50%)	1 (50%)	3	2 (67%)	1 (33%)
	EBV-	19	10 (53%)	9 (47%)	8	3 (38%)	5 (62%)
	unknown	1		1 (100%)			
Biopsy site	Nodal	11	8 (73%)	3 (27%)	2	0	2 (100%)
	Extranodal	11	3 (27%)	8 (73%)	9	5 (56%)	4 (44%)

Supplemental Table 2: Distribution of cases with PD-L1^{+} Breg percentage above or below the median, according to HIV status, DLBCL subtype, EBV status and biopsy site.

		HIV-negative DLBCL (median=1,735%)			HIV-positive DLBCL (median=0,83%)		
		n	**% of cases below 1,735%**	**% of cases above 1,735%**	**n**	**% of cases below 0,83%**	**% of cases above 0,83%**
COO subtype	Non-GCB	16	8 (50%)	8 (50%)	3	2 (67%)	1 (33%)
	GCB	5	3 (60%)	2 (40%)	7	2 (29%)	5 (71%)
	Other/unknown	1		1 (100%)	1	1 (100%)	
EBV status	EBV+	2		2 (100%)	3	2 (67%)	1 (33%)
	EBV-	19	1(58%)	8 (42%)	8	3 (38%)	5 (62%)
	unknown	1		1			
Biopsy site	Nodal	11	7 (64%)	4 (36%)	2	1 (50%)	1 (50%)
	Extranodal	11	4 (36%)	7 (64%)	9	4 (44%)	5 (56%)

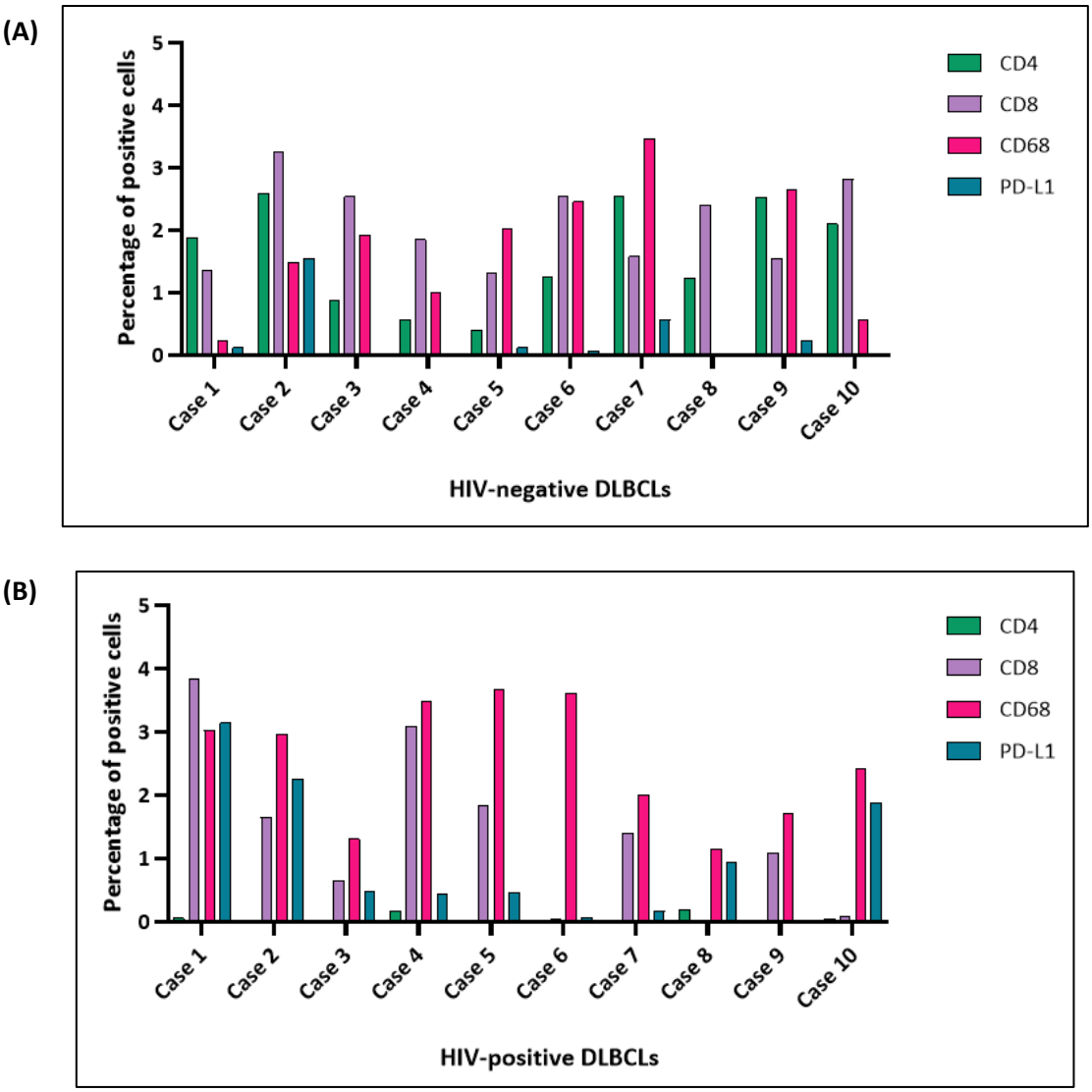

Supplemental Figure 1: Percentage of immune cells in the TME. Percentages of T cell and macrophage infiltration along with overall PD-L1-positivity in tumour tissues derived from DLBCL patients who were (A) HIV-negative and (B) HIV-negative.

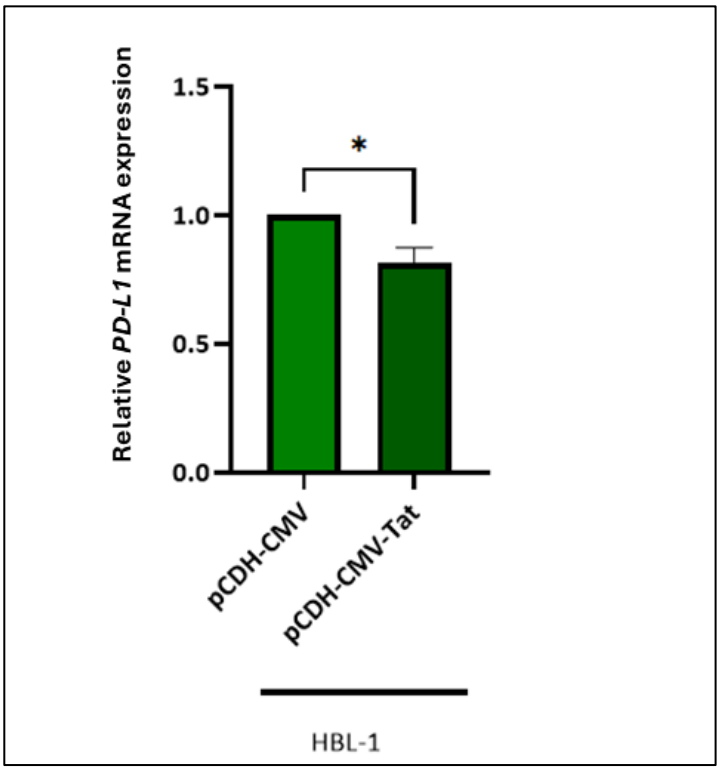

Supplemental Figure 2: qPCR analysis assessing the mRNA levels of *PD-L1* in the presence of Tat. after knockdown. Relative quantification qPCR was performed to assess the mRNA levels of *PD-L1* in HBL-1-Tat-transduced cells relative to the empty control. Statistical analysis was performed using GraphPad Prism 9 (Welchs t test, *p ≤ 0.05).

Appendix D

FACS Calibur instrument configuration:

The FACS Calibur had both red and blue lasers enabled. The flow rate was on high for all samples acquired on the FACS Calibur (60µl per minute), and the threshold was set at 100 on the parameter FCS-H. This allowed for exclusion of small events, such as debris, without excluding lymphocytes. In terms of quality control, the BD Calibrite beads were used to set the PMT voltages and check sensitivity as well as the fluidics and Lazer alignment. The voltages were saved and recorded so that stability could be monitored. Furthermore, an FMO control was included as a negative control and to distinguish between positive and negative events.